ABSTRACT

Title of Dissertation: PROTEIN ENGINEERING APPROACHES TO IMPROVING DIAGNOSIS AND TREATMENT OF *CANDIDA ALBICANS* INFECTIONS

Svetlana P. Ikonomova, Doctor of Philosophy, 2017

Dissertation directed by: Professor Amy J. Karlsson, Department of Chemical and Biomolecular Engineering

Candida albicans is an opportunistic pathogen that can cause infections that range from mild rashes to life-threatening bloodstream infections. The antifungal drug resistance of some *Candida* strains and the deficiencies in the current methods used to identify infection-causing species call for improvements in treatment and diagnosis of *Candida* infections.

Towards improving therapeutics, the antimicrobial peptide histatin 5 (Hst-5) was studied. Hst-5 is a salivary peptide with strong antifungal activity against *C. albicans.* However, the pathogen produces a family of secreted aspartic proteases (Saps), some of which can degrade and inactivate Hst-5. Of the family, Sap2 and Sap9 have been previously shown to degrade Hst-5. Variants of Hst-5 with one or two amino acid substitutions were designed and tested to evaluate the effect on the proteolysis of the peptide by the Saps. The results showed that even a single amino acid substitution results

in a significant reduction or enhancement of proteolysis by Saps. The K17R and K17L modifications led to significantly enhanced resistance to proteolysis to both Saps. The substitutions also had site-, residue-, and Sap-dependent effects and the proteases have preferences for certain amino acids at the substitution sites, such as leucine at the 13th residue by Sap9. The substitutions affect not only the cleavage at the substitution sites but also the degradation of the peptide as a whole. Some of the modifications (K11R, E16R, E16L) also led to enhanced antifungal activity. Furthermore, combination of two modifications (K11R-K17R) resulted in a peptide with both enhanced proteolytic resistance to Saps and enhanced antifungal activity, demonstrating its potential as an alternative therapeutic.

Towards improving diagnostics, a purification-free method to immobilize single-chain variable fragment (scFv) antibodies was developed. Two biotinylation tags—the biotin carboxyl carrier protein or the AviTag minimal sequence—were genetically fused to scFvs to allow for *in vivo,* site-specific biotinylation by endogenous *Escherichia coli* biotin ligases during protein expression. scFvs with different frameworks and antigens were all successfully immobilized directly from cell lysates onto streptavidin-coated plates, and the immobilized scFvs maintained their functionality for over 100 days at 4 °C. The simplicity and robustness of this method make it a suitable approach to create diagnostic arrays and could be used to capture and identify *Candida* infections.

PROTEIN ENGINEERING APPROACHES TO IMPROVING DIAGNOSIS AND TREATMENT OF *CANDIDA ALBICANS* INFECTIONS

by

Svetlana P. Ikonomova

Dissertation submitted to the Faculty of the Graduate School of the
University of Maryland, College Park, in partial fulfillment
of the requirements for the degree of
Doctor of Philosophy
2017

Advisory Committee:
Professor Amy J. Karlsson, Chair
Professor William E. Bentley
Professor Jeffery B. Klauda
Professor Ganesh Sriram
Professor Ian M. White

Dedication

I dedicate my PhD dissertation to my parents for all the encouragements and support they provided me throughout my PhD studies.

Acknowledgements

I thank my advisor Dr. Amy Karlsson for all the mentorship and support she provided during my PhD studies. She made research discussions enjoyable and taught me how to view a wide range of results from a more positive and useful perspective. Furthermore, she helped me grow not only academically but professionally as well, helping me become a better presenter and writer.

I also thank the fellow graduate students from the Karlsson lab—Dr. Zifan Gong, Parisa Moghaddam-Taaheri, and Sayanee Adhikari—for providing helpful discussions on various research topics and for creating an enjoyable and welcoming lab environment. Additionally, I had the great opportunity of mentoring undergraduate students Ziming "Vivi" He, Megan Le, and Neha Kalla in the lab, all of whom significantly contributed to the scFv immobilization work. I also acknowledge and thank Dr. Viviana Monje-Galvan for all of the help she provided in running and analyzing molecular dynamic simulations.

Outside of the lab and the department, Dr. Yan Wang from the Proteomics Core Facility on campus greatly helped me with running and analyzing mass spectrometry experiments. Dr. Mary Ann Jabra-Rizk (University of Maryland School of Dentistry) provided helpful discussions and mouse model data for the histatin project. Additionally, I thank the following people for providing enzymes and plasmids used in the dissertation: Dr. Bernhard Hube (Friedrich Schiller University, Germany) for the Sap enzymes, Dr. Dorothy Beckett (University of Maryland) for plasmid containing BirA enzyme, Dr. Joseph Bliss (Brown University) for plasmids containing scFv3, scFv5, and scFv12, Dr. Andreas Plückthun (University of Zurich, Switzerland) for plasmid containing scFvD10,

and Dr. Chatchai Tayapiwatana (Chiang Mai University, Thailand) for plasmid containing BCCP.

Finally, I want to acknowledge my friends and family who helped in numerous ways, from critiquing presentations to simply being available during the tough patches of PhD study.

Table of Contents

List of Tables

List of Figures

Chapter 5:

Chapter 6:

Appendix A:

Appendix B:

Appendix C:

List of Abbreviations

6XHis: hexahistidine

BCCP: biotin carboxyl carrier protein

CEMS: capillary electrophoresis-mass spectrometry

ELISA: enzyme-linked immunosorbent assay

gpD: bacteriophage lambda head protein D

HRP: horseradish peroxidase

Hst-5: histatin 5

IgG: immunoglobulin G

I-TASSAR: the Iterative Threading ASSEmbly Refinement

MD: molecular dynamics

NaPB: sodium phosphate buffer

OD_{600}: optical density at 600 nm

PBS: phosphate-buffered saline

PVDF: polyvinylidene difluoride

Sap: secreted aspartic protease

scFv: single-chain variable fragment

SDS-PAGE: sodium dodecyl sulfate polyacrylamide gel electrophoresis

TBS: tris-buffered saline

Chapter 1: Introduction

Candida species are fungal organisms that are part of the normal human flora, inhabiting areas such as skin and mucosal surfaces. They reside in the oral cavity of over 35% of healthy people [1]. While they are commensal organisms, they are also opportunistic pathogens that can cause infections that range from mild rashes to life-threatening systemic infections. Immunocompromised patients, such as those infected with human immunodeficiency virus (HIV) or those undergoing chemotherapy, are particularly susceptible to infection. In fact, *Candida* species are the fourth leading cause of hospital-acquired bloodstream infections [2]. Due to the prevalence and importance of *Candida* infections, new approaches to both therapeutics and diagnostics are needed.

Of the pathogenic *Candida* species, *C. albicans* is the most common species that causes infections. It is a diploid and polymorphic organism, able to grow as an oval-shaped yeast form as well as filamentous hyphae (Figure 1.1) [3]. Environmental factors such as temperature of 37 °C and pH above 7.0 can induce hyphal growth [4].

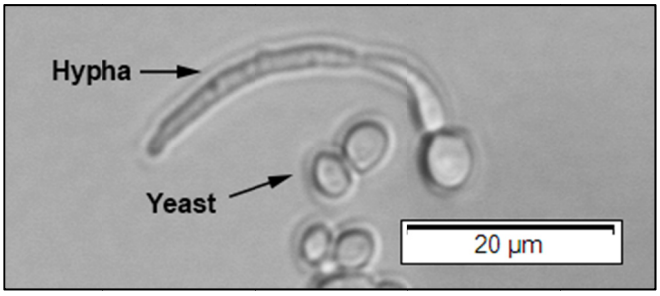

Figure 1.1. Morphologies of *C. albicans*: yeast and hypha.

As a fungal species, *C. albicans* has a multi-layered cell wall composed of an inner layer of polysaccharides, which include β-1,3-glucans, and an outer layer of mannoproteins [3, 5]. Cell wall proteins are non-covalently or covalently linked directly to β-1,3-glucans or indirectly through a glycosylphosphatidylinositol (GPI) remnant [5]. Expression of GPI-linked proteins such as Hwp1 is one of the virulence factors for *C. albicans*, and these virulence factors also include phenotypic switching opaque cells and secretion of hydrolytic enzymes [6].

1.1. Toward therapeutic improvements

Some treatments for *Candida* infections, such as the antifungal drugs amphotericin B and fluconazole, are available, but the options are few and they have limitations. For example, amphotericin B has toxicity to the kidneys and can cause kidney injuries in up to 50% of treated patients [7]. There is also an increasing prevalence of drug-resistance stains of *Candida* and, in fact, the Centers for Disease Control and Prevention listed fluconazole-resistant *Candida* infections as a serious threat to human health in its 2013 report on antibiotic resistance threats in the United States [8]. The limitations of the current treatments call for new therapeutic methods and one approach is to consider the role virulence factors of *Candida* infections.

1.1.1. Secreted aspartic proteases (Saps)

One of the key virulence factors of *C. albicans* is the secretion of hydrolytic enzymes, which are though to aid infection through degradation cell surfaces and host immune proteins [6]. Among these enzymes are the family of ten secreted aspartic proteases

(Saps) [9]. Sap1 to Sap8 are fully secreted to the extracellular environment, while Sap9 and Sap10 are GPI-anchored to cell wall [9, 10]. Saps play a role in a number of cellular processes and attributes, including cell adhesion, cell integrity, and virulence [9]. The expression levels of each Sap can depend on factors such as environmental conditions if tested *in vitro* and morphology of the cells. For example, the *SAP1* to *SAP3* genes are mainly expressed in yeast cells while the *SAP4* to *SAP6* genes are primarily expressed in the hyphal form of *C. albicans* [10]. Furthermore, the gene for Sap9 is the most highly expressed Sap in strains isolated from patients with both oral and vaginal *Candida* infections [11]. These Saps could interact with new potential treatment approaches and alter their effectivity.

1.1.2. Structure and properties of Saps

Saps are part of aspartic protease family, which catalyze the cleavage of peptide bonds using the aspartic acid residue found in each of the two lobes of the enzyme that form the highly negatively charged active site (Figure 1.2) [12-14]. Each Sap is initially

Figure 1.2. Structure of Sap2, showing the binding pocket. PDB ID: 1EAG [15]. Active-site aspartic acid residues are labeled in red.

produced as a larger preproenzyme and is ultimately transported by the secretory pathway [10] to be anchored on the cell wall or released to the extracellular space.

The Saps range in size from 36 to 52 kDa (Table 1.1). When samples of the purified recombinant Saps are run on sodium dodecyl sulfate polyacrylamide gel electrophoresis (SDS-PAGE) gels, Sap2, Sap4, and Sap7 – 9 show multiple distinct bands [9, 16, 17], likely due to internal cleavage or post-translational processing of the Saps. Some of the Saps have N-glycosylation sites, with Sap9 and Sap10 containing the most with five and eight sites, respectively [9]. In addition to size and N-glycosylation sites, the Saps differ in their active pH range; Sap1 – 3 and Sap8 prefer lower pH while Sap4 – 7, and Sap 9 – 10 prefer higher pH [16-18]. In particular, Sap7, Sap9, and Sap10, have higher activity closer to physiological pH. Consideration of the roles of Saps that are most active at physiological pH will be important as new treatments need to be active at that pH.

Table 1.1. Properties of the ten secreted aspartic proteases.

Protease	Molecular Mass (kDa)	pH Range	N-linked glycosylation	Pepstatin A inhibition	Ref.
Sap1	39-40[a]	3.5 - 6.0	-	+	[10, 16, 17]
Sap2	38-49[a.b]	2.5 - 5.5	-	+	[10, 16, 17]
Sap3	37-42[a]	2.0 - 5.0	-	+	[10, 16, 17]
Sap4	39[b]	4.0 -7.0	+	+	[16, 17]
Sap5	36	3.0 - 7.0	-	+	[16, 17]
Sap6	38	3.0 - 7.0	+	+	[16, 17]
Sap7	52, 15[b]	3.5 - 7.5	+	-	[17]
Sap8	36[b]	2.0 - 5.0	+	+	[17]
Sap9	44, 11[b]	3.5 - 8.0	+	Partial	[17, 18]
Sap10	42	4.0 - 8.0	+	Partial	[17, 18]

[a] Range in size due to molecular mass estimated from gels.
[b] Although multiple bands were observed for these Saps, estimated size of other band were only reported for Sap7 and Sap9.

1.1.3. Substrate specificity and proteolytic preferences of Saps

Knowledge of proteolytic activity of Saps will be valuable as it is desirable that new treatment method is not susceptible to the Saps and inactivated by them. The Saps are able to cleave various human proteins, and studies on the substrate specificity of the Saps have focused most extensively on Sap2. Sap2 has a broad specificity that includes immune host proteins, such as immunoglobulin A, lactoferrin, and antimicrobial peptides [10, 19-21]. The rest of the Saps also cleave antimicrobial peptides [19-21], and Sap9 – 10 additionally cleave covalently bound cell wall proteins [18].

To gain a more detailed understanding of how the Saps cleave their substrates, studies have analyzed various libraries of peptides to elucidate the amino acid preferences for each Sap. The library studies agree that, in general, the Saps have a preference for basic amino acids or large hydrophobic amino acids at the cut sites [17, 18, 22]. More explicitly, Sap1 – 6 and Sap8 appear to prefer residues such as phenylalanine, leucine, and tyrosine [17, 22] while Sap7, Sap9, and Sap10 have a more specific preference for methionine, arginine, or histidine, respectively [17]. However, these peptide library studies are limited to varying the residue that is either immediately N-terminal or immediately C-terminal to the cleavage site, while leaving the other residue fixed [17, 22]. Thus, they do not account for the potential roles of residues further way from the cut site. Furthermore, the peptides typically consist of random amino acid sequences with no apparent function, and the studies do not relate the cleavages to the functionality of the peptide.

1.1.4. Histatin 5

One of the common mucosal surfaces for *C. albicans* to colonize is inside the oral cavity. The oral cavity contains various salivary proteins that help keep *C. albicans* at commensal levels by clearing the cells or killing them. Immunoglobulin A and mucins help clear *C. albicans* through swallowing by binding to the cells and aggregating them [23]. Others proteins like antimicrobial peptides, which include the histatin peptides, eliminate the pathogen through their antifungal properties [23, 24]. However, the histatins, particularly histatin 5 (Hst-5), are cleaved by some of the Saps and lose their activity [20, 25].

Histatins are a family of histidine-rich peptides that have antifungal activity against *C. albicans* [26]. Histatin 1, histatin 3, and histatin 5 (Hst-5) are the major histatins secreted by parotid and submandibular glands [27]. The 24-amino acid Hst-5 (Figure 1.3) is a proteolytic fragment of histatin 3 [28] and has the strongest antifungal activity against *C. albicans* [27]. Whole saliva contains 15 – 30 μM of Hst-5 [29], however, reduced levels of Hst-5 have been reported in HIV-positive patients [30] and may contribute to their high susceptibility to oral candidiasis.

Figure 1.3. The amino acid sequence of Hst-5. The antifungal fragments of the sequence are underlined.

Unlike some other common antimicrobial peptides, Hst-5 does not act on *C. albicans* cells by forming pores on the cell membrane [31], and, instead, it acts intracellularly. Hst-

5 binds to the cell wall heat shock protein Ssa2 [32] and is translocated into the cell in a separate, energy-dependent manner through the fungal polyamine transporters Dur3 and Dur31 [29]. The exact mechanism of action is still being studied, but the uptake of Hst-5 results in ion imbalance (especially of K^+) and volume loss that eventually causes cell death [3, 29].

To determine the section of the peptide sequence that contributes to the antifungal activity, the activities of truncated Hst-5 peptides (Table 1.2) have been previously tested. The N-terminal fragments had no activity, and, initially, the C14 fragment (residues 11 – 24) was identified as the minimal sequence required for antifungal activity against *C. albicans* [33]. However, a later study found that the P-113 fragment (residues 4 – 15) has antifungal activity even greater than Hst-5 [34]. These findings show that while the whole peptide sequence is not required for the antifungal activity, the active fragment of the peptide appears to depend on what section of the peptide is truncated and may be influenced by surrounding amino acids.

Table 1.2. Truncated fragments of Hst-5 and their antifungal activity compared to Hst-5.

Name	**Sequence** 1	4	8	12	16	20	24	**Antifungal activity**	**Ref.**
Hst-5	D S H A K R H H G Y K R K F H E K H H S H R G Y								[33]
N16	D S H A K R H H G Y K R K F H E							Less than Hst-5	[33]
C16			G Y K R K F H E K H H S H R G Y					Same as Hst-5	[33]
M10		H H G Y K R K F H E						Very weak	[33]
C14/dh-5			K R K F H E K H H S H R G Y					Similar to Hst-5	[33, 35]
C12			K F H E K H H S H R G Y					Less than Hst-5	[33]
C10			H E K H H S H R G Y					Weak	[33]
P-123	D S H A K R H H G Y K R K F							Not active	[34]
P-103	K R H H G Y K R K F H E K H H S H R							Less than Hst-5	[34]
P-112	D S H A K R H H G Y K R							Not active	[34]
P-113	A K R H H G Y K R K F H							More than Hst-5	[34]
P-114	H H G Y K R K F H E K H							Not active	[34]
P-115	Y K R K F H E K H H S H							Not active	[34]
P-116	K F H E K H H S H R G Y							Not active	[34]
P-117	K R H H G Y K R K F H							Less than Hst-5	[34]
P-118	A K R H H G Y K R K F							Less than Hst-5	[34]
P-119	A K R H H G Y K R K							Not active	[34]
P-120	A K R H H G Y K R							Not active	[34]

1.1.5. Amino acid substitutions and antifungal activity

Once the antifungal fragments were identified, the amino acids within the fragments were modified to gain a better understanding of how the residues within the sequences contribute to the antifungal activity. The amino acid substitutions were done to the full Hst-5 sequence or truncated fragments. For the full-length Hst-5, the importance of the charge, hydrophobicity, and the imidazole rings of the amino-acid side chains and the potential for the peptide to form an α-helical structure were tested (Table 1.3). Mutation of one or four charged amino acids to glycine [36] or alanine [37] within the active fragment 11 –24 led to a significant decrease in antifungal activity, which suggests that the charged side groups of some, if not all, of the modified residues—R12, K13, H15, E16, K17, H18, H19, H21, R22—play a role in the antifungal activity. Specifically, the reduced activity from the single E16G substitution in pHst5ΔGlu shows that the glutamic acid at that site is important for the antifungal activity [36]. K13 is another crucial site, as the K13T (m21) and K13E (m71) modifications led to a decrease in activity [38]. On the other hand, the imidazole side chains at H19 and H21 do not a play significant role in the antifungal activity (m12 and m70), though the positive charge at H21 may be vital as the substitution of both histidine residues to proline (2P) leads to reduced antifungal activity [39]. Additionally, the α-helical structure of the peptide in non-aqueous conditions [40, 41] does not appear to be important for the antifungal activity. Situ et al. inserted one to three prolines into the sequence to disrupt the α-helical structure, and the peptide with the most proline insertions (3P) still had activity comparable to original Hst-5, which suggests the α-helical structure does not play a significant role. Overall, the residue substitutions suggest that the tendency to form α-helical structure and the presence of

imidazole rings are not vital for the antifungal activity of the intact peptide, but the charge of the residue is important.

Table 1.3. One to four amino acid substituted Hst-5 and antifungal activity compared to Hst-5.

Name	Sequence																								Antifungal activity	Ref.
	1			4				8				12				16				20				24		
Hst-5	D	S	H	A	K	R	H	H	G	Y	K	R	K	F	H	E	K	H	H	S	H	R	G	Y		
pHst5ΔHis	-	-	-	-	-	-	-	-	-	-	-	-	-	-	G	-	-	G	G	-	G	-	-	-	Not active	[36]
pHst5ΔGlu	-	-	-	-	-	-	-	-	-	-	-	-	-	-	-	G	-	-	-	-	-	-	-	-	Less than Hst-5	[36]
pHst5ΔLys/Arg	-	-	-	-	-	-	-	-	-	-	-	G	G	-	-	-	G	-	-	-	-	G	-	-	Less than Hst-5	[36]
reHsn-5	G	-	-	-	-	-	-	-	-	-	-	-	-	-	-	-	-	-	-	-	-	-	-	-	Similar to Hst-5	[38]
m1	-	-	-	-	-	-	-	-	-	-	-	I	-	-	-	-	-	-	-	-	-	-	-	-	Similar to Hst-5	[38]
m2	-	-	-	-	-	-	-	-	-	-	-	I	-	-	-	-	N	-	-	-	-	-	-	-	Similar to Hst-5	[38]
m12	-	-	-	-	-	-	-	-	-	-	-	I	-	-	-	-	-	-	-	-	L	-	-	-	Similar to Hst-5	[38]
m21	-	-	-	-	-	-	-	-	-	-	-	-	T	-	-	-	-	-	-	-	-	-	-	-	Less than Hst-5	[38]
m68	-	-	-	-	-	-	-	-	-	-	-	-	E	-	-	-	-	-	-	-	-	G	-	-	Less than Hst-5	[38]
m70	-	-	-	-	-	-	-	-	-	-	-	-	-	-	-	-	-	-	P	-	R	-	-	-	Similar to Hst-5	[38]
m71	-	-	-	-	-	-	-	-	-	-	-	-	E	-	-	-	-	-	-	-	-	-	-	-	Less than Hst-5	[38]
F14A/H15A	-	-	-	-	-	-	-	-	-	-	-	-	-	A	A	-	-	-	-	-	-	-	-	-	Less than Hst-5	[37]
F18A/H19A	-	-	-	-	-	-	-	-	-	-	-	-	-	-	-	-	-	A	A	-	-	-	-	-	Less than Hst-5	[37]
1P	-	-	-	-	-	-	-	-	-	-	-	-	-	-	-	-	-	-	-	-	P	-	-	-	Less than Hst-5	[39]
2P	-	-	-	-	-	-	-	-	-	-	-	-	-	-	-	-	-	-	P	-	P	-	-	-	Less than Hst-5	[39]
3P	-	-	-	-	-	-	-	-	-	-	-	-	-	-	-	P	-	-	P	-	P	-	-	-	Similar to Hst-5	[39]

As was done for the intact peptide, the contribution of amphipathicity, positive charge, and hydrophobicity of the antifungal fragments to the antifungal activity was studied through amino acid modifications (Table 1.4). The enhancement of the lateral amphipathicity of the dh-5 fragment (residues 11 – 24 of Hst-5) by substitution of single lysine, leucine, or phenylalanine—based on position in helical-wheel—had no effect, but multiple substitutions (dhvar1 and dhvar2) led to enhanced activity [35]. Further modification of glutamic acid to lysine increased the overall charge of dhvar1 and dhvar2 and led to some improvement in the antifungal activity, as well [42]. Another peptide, dhvar5, was designed to have a hydrophobic N-terminus and a hydrophilic C-terminus

when it forms an α-helix[42]. Surprisingly, dhvar5 showed improved antifungal activity not only in the low ionic buffer used for the other fragments, but also in highly ionic phosphate buffered saline (PBS) [42]. For the dh-5 fragment, multiple modifications that significantly change the sequence of the fragment were required for amino acid substitutions to have an effect on the antifungal activity.

Table 1.4. Amino acid substitution of dh-5 and P-113 Hst-5 fragments and antifungal activity compared to unmodified fragment.

Name	Sequence																							Antifungal activity	Ref.
	1			4				8				12				16				20				24		
Hst-5	D	S	H	A	K	R	H	H	G	Y	K	R	K	F	H	E	K	H	H	S	H	R	G	Y		
dh-5											K	R	K	F	H	E	K	H	H	S	H	R	G	Y		
dh13L											-	-	L	-	-	-	-	-	-	-	-	-	-	-	Similar to dh-5	[35]
dh15K											-	-	-	-	K	-	-	-	-	-	-	-	-	-	Similar to dh-5	[35]
dh17L											-	-	-	-	-	-	L	-	-	-	-	-	-	-	Similar to dh-5	[35]
dh18L											-	-	-	-	-	-	-	L	-	-	-	-	-	-	Similar to dh-5	[35]
dh18K											-	-	-	-	-	-	-	K	-	-	-	-	-	-	Similar to dh-5	[35]
dh19K											-	-	-	-	-	-	-	-	K	-	-	-	-	-	Similar to dh-5	[35]
dh21F											-	-	-	-	-	-	-	-	-	-	F	-	-	-	Similar to dh-5	[35]
dh23K											-	-	-	-	-	-	-	-	-	-	-	-	K	-	Similar to dh-5	[35]
dhvar1											-	-	L	-	K	-	L	K	F	-	L	-	K	-	More than dh-5	[35]
dhvar2											-	-	L	-	K	-	L	L	F	-	L	-	K	-	More than dh-5	[35]
dhvar3											-	-	L	-	K	K	L	K	F	-	L	-	K	-	More than dh-5	[42]
dhvar4											-	-	L	-	K	K	L	L	F	-	L	-	K	-	More than dh-5	[42]
dhvar5											L	L	L	-	L	L	-	K	R	K	K	-	K	-	More than dh-5	[42]
P-113				A	K	R	H	H	G	Y	K	R	K	F	H											
113-F4.5.12				-	-	-	F	F	-	-	-	-	-	-	F										Similar to P-113	[34]
113-Y4.5.12				-	-	-	Y	Y	-	-	-	-	-	-	Y										Similar to P-113	[34]
113-L4.5.12				-	-	-	L	L	-	-	-	-	-	-	L										Less than P-113	[34]
113-Q2.10				-	Q	-	-	-	-	-	-	-	Q	-	-										Not active	[34]
113-Q3.9				-	-	Q	-	-	-	-	-	Q	-	-	-										Less than P-113	[34]
113-Q2.3.9.10				-	Q	Q	-	-	-	-	-	Q	Q	-	-										Not active	[34]
113-K6				-	-	-	-	-	K	-	-	-	-	-	-										Less than P-113	[34]
113-H8				-	-	-	-	-	-	-	H	-	-	-	-										Similar to P-113	[34]
113-K6H8				-	-	-	-	-	K	-	H	-	-	-	-										Similar to P-113	[34]

Similar overall effects from modifications were observed with the peptide fragment P-113 (residues 4 – 15 of Hst-5). Substitution of positively charged lysine (113-Q2.10) or arginine (113-Q3.9) residues or both (113-Q2.3.9.10) led to a significant reduction or complete loss of antifungal activity [34], indicating that the cationic nature of the peptide fragment is crucial for the antifungal activity. On the other hand, modifications that led to increased hydrophobicity (113-F4.5.12, 113-Y4.5.12, 113-L4.5.12) or amphipathicity (113-K6, K113-H8, K113-K6H8) had little to no effect on the antifungal activity. These modifications on the fragments show that while the charges of the residues play role in the antifungal activity, as observed with the full-length Hst-5, the amphipathicity and hydrophobicity do not significantly contribute to the activity.

1.1.6. Proteolytic susceptibility to Saps

The antifungal properties of Hst-5 show its promise as a tool to fight *C. albicans* infection in the human mouth. However, the peptide can be cleaved and inactivated by the Saps produced by *C. albicans*. Meiller et al. showed that at physiological pH Hst-5 is vulnerable to proteolysis by Sap2, Sap9, and, to a lesser extent, Sap10 (Table 1.5) [20]. Furthermore, Bochenska et al. showed Hst-5 can also be cleaved by Sap1, Sap3 – 4, and Sap7 – 8 when tested at the optimal pH condition for each Sap [25]. The susceptibility of Hst-5 to proteolysis by the Saps motivates further study to explore whether reduction of proteolytic susceptibility to Saps can improve the therapeutic potential of the peptide.

Table 1.5. Fragments detected from cleavage by Sap1 – 4 and Sap7 – 10.

Sequence																								Sap	Ref.
1			4				8				12				16				20				24		
D	S	H	A	K	R	H	H	G	Y	K	R	K	F	H	E	K	H	H	S	H	R	G	Y		
D	S	H	A	K	R	H	H	G	Y	K	R	K	F	H	E	K								1, 2, 3, 4, 9, 10	[20, 25]
																	H	H	S	H	R	G	Y	1, 2, 3, 4, 8, 9	[20, 25]
D	S	H	A	K	R	H	H	G	Y	K	R	K												2, 3, 9	[20, 25]
													F	H	E	K	H	H	S	H	R	G	Y	2, 3, 7, 8, 9, 10	[20, 25]
D	S	H	A	K	R	H	H	G	Y	K	R													2, 4, 7, 9	[20, 25]
D	S	H	A	K	R	H	H	G	Y															2, 4, 8, 9	[20, 25]
											R	K	F	H	E	K	H	H	S	H	R	G	Y	10	[20]
D	S	H	A	K																				2	[20]
					R	H	H	G	Y															2	[20]
										K	R	K	F	H	E	K								1, 2	[20, 25]
																	H	H	S	H	R	G	Y	1, 2	[20, 25]
												K	F	H	E	K								2	[20]
					R	H	H	G	Y	K	R	K													2	[20]
													F	H	E	K								1, 2, 3, 9	[20, 25]
			A	K	R	H	H	G	Y	K	R	K	F	H	E	K									1	[25]
			A	K	R	H	H	G	Y																1	[25]
										K	R	K	F	H	E	K								1	[25]
										K	R	K	F	H	E	K	H	H	S	H	R	G	Y	4	[25]
D	S	H	A	K	R	H	H	G	Y	K	R	K	F	H	E	K	H	H	S	H				7	[25]
																					R	G	Y	7	[25]

1.2. Toward diagnostic improvements

Early detection of a fungal infection is strongly desirable to enable the identification and the start of appropriate treatments. For *Candida* infections, determination of the species causing the infection is important as some of the drugs are less effective in treating certain species than others [7] and the occurrence of drug-resistant strains is increasing [8]. The current gold standard for diagnosis of *Candida* infection is culturing of a clinical sample. However, this method is time-consuming, requiring 24 – 72 hours or even longer for a result [7]. Furthermore, despite requiring days to complete, only 50% of

infections are identified [43]. These current limitations in diagnostics show the need for and motivate further study into improving diagnostic methods.

1.2.1. Antibody array and single-chain variable fragments (scFvs)

A potential alternative approach to diagnosis is to use an array of antibodies that will bind to the *Candida* cells and, based on the binding pattern, identify the species. There are various types of antibodies used in biological applications, with the Y-shaped immunoglobulin G (IgG) antibody being one of the most commonly used isotypes (Figure 1.4) [44]. However, the multiple disulfide-bonds present in the full-size antibody limit the methods of its production.

Instead of the full-size IgG, small antibody fragments have seen increasing use due to their ease of production in *Escherichia coli* [44]. The single-chain variable fragment (scFv) is one such fragment, composed of the variable light chain (V_L) and variable heavy chain (V_H) domains of the antigen-binding site of an IgG antibody connected by a flexible linker (Figure 1.4). scFvs are one of the smallest IgG fragments that retain an antigen-binding capability similar to the full-length antibody [45]. Typical scFvs are 26-28 kDa in size, considerably smaller than the 150 kDa of IgGs [44]. The small size of scFvs allows for easy insertion of their encoding DNA sequences into plasmids and fast replication in *E. coli* [46]. The ease of production while maintaining antigen-specificity makes scFvs great tools for developing antibody arrays. These antibody arrays could be used as part of a diagnostic device to detect pathogens such as *Candida*.

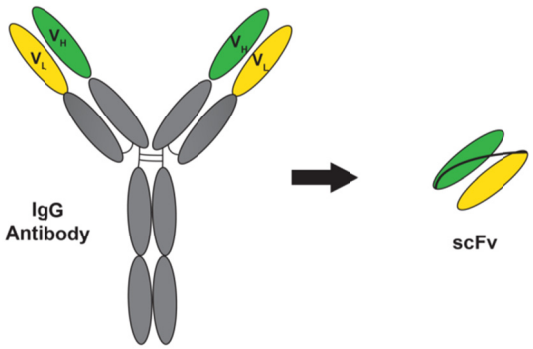

Figure 1.4. Schematic of IgG vs. scFv. scFv is composed of the V_H and V_L domains of the antigen-binding site fused with a linker.

1.2.2. Immobilization methods

To use scFvs in a diagnostic array, they must first be immobilized onto a surface. Multiple protein immobilization methods have been explored for antibodies and antibody fragments thus far, including physical adsorption, covalent immobilization, and bioaffinity immobilization. Proteins, including antibody fragments can adsorb onto a surface through electrostatic, ionic, or hydrophobic interactions [47]. This enables easy immobilization through physical adsorption. However, the antibodies are randomly oriented and weakly attached [48]. Antibodies can attach in an orientation where the antigen binding site is obstructed, reducing its functionality. Stronger, irreversible immobilization can be achieved through a covalent bond. For example, the coupling reagents *N*-hydroxysuccinimide (NHS) and 1-ethyl-3-(3-dimethylaminopropyl)-carbodiimide (EDC) and are commonly used to form covalent bonds between amine and carboxyl groups [49]. However, because several lysine residues are normally present within an antibody or antibody fragment, the bond formation is not site-specific and results in non-oriented immobilization [48, 49]. Some of the covalent bonds also require harsh chemicals to form the bond, which can have a detrimental effect on a protein.

Oriented immobilization without harsh chemicals can be achieved by taking advantage of the affinity of different biological components through bioaffinity immobilization. The interaction of Protein A and the Fc region of full-length antibodies is one of the common bioaffinity interactions used for immobilization [50, 51]. This approach, however, is not applicable to scFvs since they lack the Fc region. Fusion tags such as the hexahistidine (6XHis) tag can also be used for oriented immobilization onto surfaces modified with nickel-nitriloacetic acid (Ni-NTA) [52, 53]. Unfortunately, the affinity of the 6XHis tag to Ni-NTA is weak and reversible, with a dissociation constant of $K_d = 10^{-7}$ M [54].

As an alternative to the weak interaction of the 6XHis tag with Ni-NTA, the biotin-streptavidin interaction, which is one of nature's strongest non-covalent bonds ($K_d = 10^{-14}$ M) [55], can be used. This interaction has been previously used to successfully immobilize IgG antibodies and fragments, typically by attaching biotin *in vitro* to lysine residues through sulfo-NHS/EDC chemistry and immobilizing onto a streptavidin-functionalized surface [56]. As with the covalent immobilization with NHS/EDC, the addition of biotin through chemical modification does not lead to site-specific, oriented immobilization.

E. coli cells produce biotin holoenzyme synthetases, also known as biotin ligases, which covalently attach biotin *in vivo* to a specific lysine residue of a native *E. coli* protein called the biotin carboxyl carrier protein (BCCP) (Figure 1.5A) [57]. Fusion of the 87-residue BCCP to other proteins allows biotinylation of the fusion proteins [57, 58], and the biotinylated proteins can then bind to streptavidin to immobilize proteins from a cell lysate [59, 60]. In addition to the full-length BCCP biotinylation sequence, a 15-amino acid minimal peptide substrate for biotinylation was reported by Schatz et al.

(Figure 1.5B) [61, 62]. The biotinylation of this peptide, called the AviTag, is catalyzed by one of the biotin holoenzyme synthetases, BirA [62]. The site-specific *in vivo* biotinylation of a protein with BCCP or AviTag combined with the biotin-streptavidin affinity interaction can be used to develop a method to immobilize a variety of antibody fragments and create an antibody array for diagnostics. By immobilizing antibody fragments that are specific to various *Candida* species, an alternative diagnostic method of *Candida* infection could be developed.

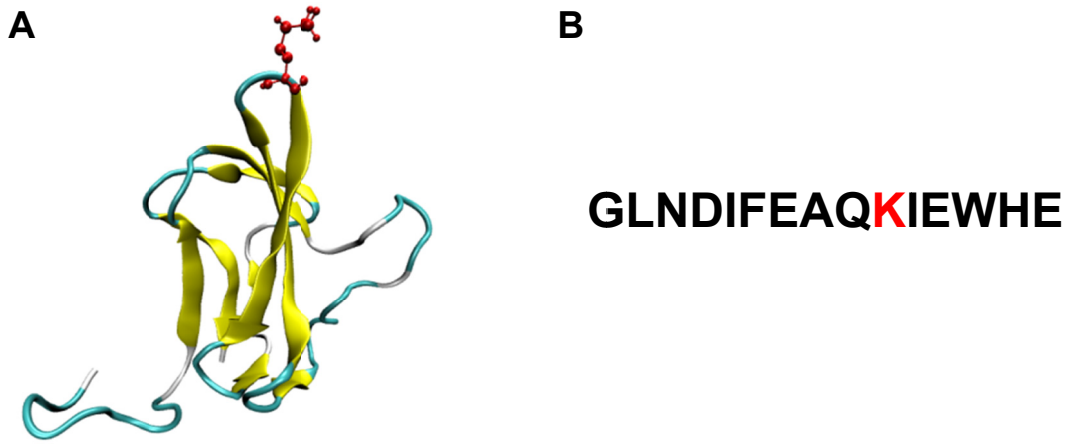

Figure 1.5. Structure of (A) apo-BCCP and (B) sequence of AviTag minimal substrate. The lysine residue that binds to biotin is highlighted in red. PDB ID: 1A6X [63].

1.3. Overview of dissertation

This dissertation explores improvement in treatment of *Candida* infections through study of the antifungal peptide Hst-5 and progress towards improvement in diagnosis by development of immobilization method for scFvs. The first part (Chapters 2 – 3) describes work to enhance the resistance of Hst-5 against proteolysis by Saps produced by *C. albicans* and improve its antifungal activity. Chapter 2 describes the effects of substituting lysine residues in the peptide sequence to arginine or leucine. Chapter 3

expands on the Chapter 2 work to test effects of additional amino acid modifications and also gain insight into the kinetics of the degradation by Sap9. The second part of this dissertation (Chapter 4 – 5) describes a purification-free method to immobilize scFvs onto a surface as a potential method to produce antibody arrays. Chapter 4 describes the method and its capabilities and Chapter 5 looks to improve the method through use of peptide linkers. Finally, Chapter 6 describes summarizes the contributions of this thesis and provides recommendations for future work with Hst-5 work.

Chapter 2: Designing histatin 5 variants for reduced susceptibility to secreted aspartic proteases

2.1. Introduction

Candida albicans is a fungal species that is part of the normal human flora. It commonly colonizes mucosal surfaces, including the oral cavity in over 35% of healthy people [1]. However, *C. albicans* is also an opportunistic pathogen, and, under conditions of immune system disruption, such as infection with the human immunodeficiency virus (HIV), it causes an array of infections, most notably oral candidiasis, which is also called oral thrush.

To help prevent infections by *C. albicans* and other organisms, the human oral saliva contains an arsenal of proteins and peptides [24]. One such peptide that fights against *C. albicans* is the antimicrobial peptide histatin 5 (Hst-5). It is one of twelve members of the histatin family of histidine-rich peptides secreted by salivary glands in the human mouth [26], with the 24-amino-acid Hst-5 having the strongest activity [26, 27]. As part of host innate immunity, Hst-5 has been proposed to play a crucial role in maintaining *C. albicans* at commensal levels in the oral cavity [20]. Reduced levels of Hst-5 have been reported in HIV-positive patients [30] and may contribute to their high susceptibility to oral thrush. Unlike some other common antimicrobial peptides, Hst-5 does not act on *C. albicans* cells by forming pores on the cell membrane [31]; instead, the peptide acts intracellularly, ultimately leading to ion imbalance and volume loss that causes cell death [29].

Although Hst-5 has potent activity against *C. albicans,* the fungal pathogen produces a family of ten secreted aspartic acids (Saps), some of which can degrade and inactivate Hst-5. The Saps play a role in a number of cellular processes and attributes, including cell adhesion, cell integrity, and virulence [9]. While Sap1 to Sap8 are fully secreted to the extracellular environment, Sap9 and Sap10 remain attached to the cell wall via a glycosylphosphatidylinositol (GPI) anchor [9, 10]. Each Sap contains the two conserved aspartic acids characteristic of aspartic proteases, along with four conserved cysteine residues [14].

Although Sap9 is the most highly expressed Sap in strains isolated from patients with both oral and vaginal *Candida* infections [11], studies on the substrate specificity of the Saps have focused most extensively on Sap2. Sap2 has a broad specificity that includes immune host proteins, such as immunoglobulin A and lactoferrin, and antimicrobial peptides like Hst-5 [10, 19-21]. Recently, the interaction of Sap2 and other Saps with antimicrobial peptides, including Hst-5, has been more carefully studied [19-21]. Meiller et al. showed that at physiological pH Hst-5 is vulnerable to proteolysis by Sap2, Sap9, and, to a lesser extent, Sap10 [20]. Furthermore, Bochenska et al. showed Hst-5 can also be cleaved by Sap1, Sap3 – 4, and Sap7 – 8 when tested at the optimal pH condition for each Sap [25]. In both studies, a lysine residue was typically present on at least one side of the sites cleaved by the Saps. These results suggest Saps may target the lysine residues in the Hst-5 sequence, which is supported by previous sequence-specific studies that indicate Saps prefer hydrophobic residues or basic residues [17, 18, 22, 64].

To improve the understanding of the interaction between Hst-5 and Saps, we designed Hst-5 variants with substitutions made at the lysine residues. While earlier

investigations have elucidated how modifications to the sequence of Hst-5 modulate antifungal activity [34, 36, 38, 39, 42, 65], the effect of modifications on degradation specifically by aspartic proteases has not yet been explored. The designed variants were evaluated for susceptibility to proteolysis by *C. albicans* Saps and for antifungal activity against *C. albicans*. Our results demonstrate that even a single amino acid modification is sufficient to significantly modulate the degradation of Hst-5 by the proteases or *C. albicans* cells, while maintaining antifungal potency. Based on these findings, designing peptides for reduced proteolysis could be a viable approach for engineering antimicrobial peptides with increased resistance to proteolysis and, thus, longer-lived antimicrobial potency.

2.2. Materials and methods

2.2.1. Peptides and enzymes

The parent Hst-5 peptide and the variants in Table 2.1 were synthesized by GenScript with a purity ≥95% and trifluoroacetic acid salt removal to hydrochloride. Purified Sap2 and Sap9 were gifted by Dr. Bernhard Hube from Friedrich Schiller University, Germany. The Saps were produced in *Pichia pastoris*, as previously described [16], and Sap9 was produced without its GPI anchor [18]. The proteolytic activities of the Saps were confirmed using the EnzChek Protease Assay Kit (ThermoFisher Scientific).

2.2.2. Proteolytic degradation of the peptides

To determine the extent of degradation of the peptides by the Saps, Hst-5 and the Hst-5 variants were each mixed with Sap9 or Sap2 at final concentrations of 150 μg/mL

peptide and 3.13 μg/mL or 6.25 μg/mL protease for Sap9 or Sap2, respectively. Experiments were done in 1 mM NaPB. The mixtures were incubated at 37 °C for 2 h, and NaPB with no Sap was used as a control. After the incubation, the samples were mixed with tricine sample buffer (without Coomassie Blue G-250, except in control samples) containing β-mercaptoethanol and boiled for 5 min at 100 °C to inactivate the proteases. The degraded and non-degraded peptides were separated by gel electrophoresis in 10 – 20% Tris-tricine gels (Bio-Rad), and the gels were then fixed in a 10% acetic acid/40% methanol/50% water mixture for 30 min. The fixed gels were stained with Bio-Safe Coomassie stain (Bio-Rad) for 1 h and washed with fresh water three times, once overnight and then twice for at least 2 h each time. The gels were imaged on a Chemidoc imager (Bio-Rad), and densitometric analysis was done with Image Lab software (Bio-Rad). In the analysis, the upper band was taken as intact peptide and the lower band was taken as degraded products. Three replicates of the assay were done.

For degradation with *C. albicans*, a single colony of the ATCC 90028 strain (American Type Culture Collection) was used to inoculate YPD. The culture was grown overnight, subcultured, and grown to an optical density of 1 – 1.2 at OD_{600}. All incubations were done at 30 °C. The cells were washed three times in 100 mM NaPB and diluted to 2×10^9 cells/mL. Equal volumes of cells and peptides were mixed and incubated for 2 h at 37 °C. The cells were removed by centrifugation, and the supernatants were mixed with tricine sample buffer and boiled for 10 min. The samples were then run on gels and analyzed as described above for degradation by the Saps. Three biological replicates were performed.

For statistical analysis, we performed one-way ANOVA tests with $p < 0.05$ and Dunett's multiple comparison tests with the Hst-5 sample as the control. The number of asterisks indicates the level of statistical significance: * for $p < 0.05$, ** for $p < 0.01$, *** for $p < 0.001$, and **** for $p < 0.0001$.

2.2.3. Antifungal activity assay

The anti-*Candida* activities of the intact peptides were assessed by an antifungal activity assay. As described above for the degradation assay, an overnight culture of *C. albicans* was subcultured and grown in YPD media. Cells were washed three times in 2 mM NaPB and diluted to 5×10^5 cells/mL or 5×10^7 cells/mL. Serial dilutions (0 – 100 μM for the lower cell density and 0 – 400 μM for the higher cell density) of parent Hst-5 and the Hst-5 variants were prepared in water, and 20 μL of the peptides and 20 μL of the cells were mixed and incubated in round-bottom 96-well culture plates for 30 min at 30 °C. After incubation, 320 μL of 1 mM NaPB was loaded into each well to stop additional killing of the cells by the peptides [66]. Mixtures were further diluted and approximately 250 cells were inoculated into round-bottom culture plates with equal volumes of YPD media and 1 mM NaPB at a total volume of 200 μL. Wells containing only YPD and NaPB were served as a sterility control and provided measurements for the background signal. The OD_{600} was measured after overnight incubation on a microplate shaker at 30 °C. The reduction in viability was calculated as

$$\%\ \text{reduction in viability} = \left[1 - \frac{\left(\mathrm{OD}_{\text{with peptide}} - \mathrm{OD}_{background}\right)}{\left(\mathrm{OD}_{\text{no peptide}} - \mathrm{OD}_{background}\right)}\right] \times 100$$

Three biological replicates were performed on separate days, with two replicates on each day.

To measure the antifungal activity of the peptides following degradation by the Saps, the antifungal activity assay was performed as described above, except the peptides were first exposed to Saps. The peptide fragments were prepared by incubating each peptide (150 μg/mL) with 6.25 μg/mL Sap9 or 18 μg/mL Sap2 for 2 h at 37 °C. The enzymes were then inactivated by heating at 100 °C for 5 min. As controls, each peptide was also incubated with only NaPB buffer. Samples were then stored at –20 °C until use in the antifungal activity assay.

2.2.4. MS/MS analysis

The cleavage sites of the Saps and the abundance of the fragments produced by cleavage were determined using mass spectrometry. After incubation with 3.13 μg/mL Sap9 or 6.25 μg/mL Sap2 and heat inactivation of the Saps, 25 μL of each sample was desalted using a C-18 TopTip micro-spin column (Glygen Corp.) following the manufacturer's protocol. The binding solution was 0.1% formic acid, and the releasing solution was 0.1% formic acid/60% acetonitrile (ACN). To ensure equal flow-through volume of each sample, 18 μL of desalted sample was aliquoted and 1 μL of the four-amino acid peptide MRFA at 0.1 mg/mL was added. Samples were manually loaded through loop injection at 25 μL/min with 40% ACN/0.1% formic acid. Mass spectra were acquired with a Thermo Scientific Orbitrap Fusion Lumos Tribrid mass spectrometer with data-dependent analysis at a 5 s cycle time. Manufacturer recommended source parameters for a flow rate of 25 μL/min were applied. Full scan mass spectra of m/z 350 – 1550 were acquired in the orbitrap at R=120000 (m/z 200) with fluoranthene ion as the internal calibrant. CID and ETD fragments of the most intense ions ($z > 1$) were recorded with the orbitrap at R=60000 (m/z 200). Dynamic exclusion was set at 30 s.

The molecular weights of the peptides and their fragments were calculated from full scan MS spectra using the XTract program in the XCalibur software (Thermo Scientific). MS/MS spectra from electron-transfer dissociation (ETD) and collision-induced dissociation (CID) fragmentation were processed using Proteome Discoverer (V2.1) with Prosight PD node to identify peptides and their degradation products (Figure A.1). The database was the collection of Hst-5 and its analogs used in this study. Intensities of identified peptides and their degradation products relative to the internal standard MRFA were obtained from the deconvoluted full scan mass spectra (Figure A.2).

2.3. Results and discussion

To study the interaction of Hst-5 with *C. albicans* Saps, we evaluated the proteolysis of Hst-5 and eight variants by Sap2 and Sap9, which substantially cleaved Hst-5 in previous work from Meiller et al. [20]. Our design of the Hst-5 variants focused on the four lysine residues in the peptide, as we observed that lysine residues are prominent at the reported cleavage sites of Hst-5 with Saps or *C. albicans* cells [20, 25]. We hypothesized that these lysine residues are important for the recognition or cleavage of Hst-5 and replaced each of the lysine residues with either an arginine or a leucine (Table 2.1). The arginine substitutions were selected to preserve the positive charge, as the cationic nature of antimicrobial peptides often plays a role in their function [67, 68]. The leucine substitutions were selected to remove the positive charge, which could affect the interaction of the peptides with the aspartic acid residues in the active site of the Saps.

Table 2.1. Variants of Hst-5 with arginine or leucine substitutions at lysine residues.

Peptide	Sequence[a]																							
	1	2	3	4	5	6	7	8	9	10	11	12	13	14	15	16	17	18	19	20	21	22	23	24
Hst-5	D	S	H	A	K	R	H	H	G	Y	K	R	K	F	H	E	K	H	H	S	H	R	G	Y
K5R	-	-	-	-	R	-	-	-	-	-	-	-	-	-	-	-	-	-	-	-	-	-	-	-
K5L	-	-	-	-	L	-	-	-	-	-	-	-	-	-	-	-	-	-	-	-	-	-	-	-
K11R	-	-	-	-	-	-	-	-	-	-	R	-	-	-	-	-	-	-	-	-	-	-	-	-
K11L	-	-	-	-	-	-	-	-	-	-	L	-	-	-	-	-	-	-	-	-	-	-	-	-
K13R	-	-	-	-	-	-	-	-	-	-	-	-	R	-	-	-	-	-	-	-	-	-	-	-
K13L	-	-	-	-	-	-	-	-	-	-	-	-	L	-	-	-	-	-	-	-	-	-	-	-
K17R	-	-	-	-	-	-	-	-	-	-	-	-	-	-	-	-	R	-	-	-	-	-	-	-
K17L	-	-	-	-	-	-	-	-	-	-	-	-	-	-	-	-	L	-	-	-	-	-	-	-

[a] Dash indicates residue was unchanged from the parent Hst-5.

2.3.1. Lysine substitutions modulate susceptibility to proteolysis by purified Saps

To determine whether the single-residue substitutions have an effect on the overall degradation of Hst-5, we incubated Hst-5 and each modified peptide with purified recombinant Sap9 and Sap2. Hst-5 and each variant in Table 2.1 were incubated with or without 3.13 μg/mL Sap9 or 6.25 μg/mL Sap2 for 2 h at 37 °C in 1 mM sodium phosphate buffer (NaPB). We then separated the intact peptide from the degradation products using gel electrophoresis and quantified the level of degradation using densitometric analysis of Coomassie-stained gels (Figure 2.1). Both arginine and leucine substitutions at the K17 site led to a dramatic decrease in degradation by Sap9 and Sap2. Following incubation with Sap9, 82% and 77% of K17R and K17L, respectively, remained intact compared to 47% of Hst-5 (Figure 2.1A). No detectable degradation of the K17R and K17L variants was visible after incubation with Sap2, while only 61% of the parent Hst-5 peptide remained intact (Figure 2.1B).

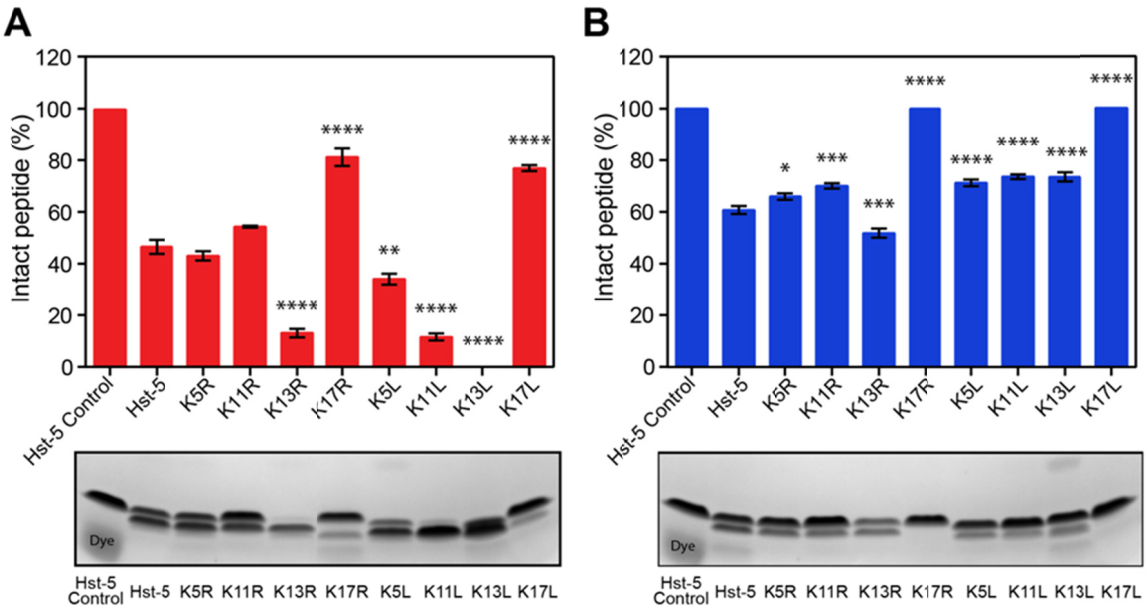

Figure 2.1. Degradation of parent Hst-5 and Hst-5 variants by purified (A) Sap9 and (B) Sap2. The peptides (150 μg/mL) and Saps (3.13 μg/mL Sap9 and 6.25 μg/mL Sap2) were incubated for 2 h at 37 °C. Samples were run on a gel, and the amount of intact peptide was quantified by densitometry to compare the amount of intact peptide (upper band) to the peptide fragments. Error bars represent standard error of the mean (n = 3). The number of asterisks indicates the level of statistical significance against parent Hst-5 incubated with Sap: * for $p < 0.05$, ** for $p < 0.01$, *** for $p < 0.001$, and **** for $p < 0.0001$. The lower band in the Hst-5 control lanes is due to Coomassie dye.

With the exception of the K17 residue, modification of lysine residues to leucine made the Hst-5 variants more susceptible to degradation by Sap9. The K5L, K11L, and K13L peptides all showed greater degradation than their arginine-substituted counterparts or parent Hst-5 (Figure 2.1A). In fact, the K13L peptide was degraded to the extent that no intact peptide could be detected on the gel.

While leucine substitutions resulted in more proteolysis of the modified peptides by Sap9, they led to a decrease in proteolysis by Sap2 (Figure 2.1B). With the exception of K13R, all of the Hst-5 variants exhibited a decrease in degradation compared to the parent Hst-5 after incubation with Sap2.

These results demonstrate the ability to easily detect changes in a peptide's susceptibility to proteolysis by gel electrophoresis and indicate that this approach is feasible for exploring how aspartic proteases interact with antimicrobial peptides. Additionally, they demonstrate that single-residue changes can have a major impact on the susceptibility of a peptide to degradation by Saps.

2.3.2. Proteolysis by *C. albicans* cells is comparable to proteolysis by purified Saps

After observing the effect of residue modifications on the cleavage of Hst-5 by the purified recombinant Saps, we evaluated whether incubation of the peptides with whole *C. albicans* cells natively expressing Saps (rather than with Saps produced recombinantly) would yield similar results. Hst-5 and the variants were incubated with *C. albicans* cells for 2 h at 37 °C in 100 mM NaPB. The high ionic strength of this buffer prevents internalization of the peptides by *C. albicans* [69], allowing analysis of degradation of the peptides without the confounding effects of peptide internalization, which would reduce the amount of peptide available for degradation by the Saps in the buffer. Following incubation with the cells, the peptide samples were run on a gel and stained, and densitometric analysis revealed a pattern that exhibits characteristics of the results observed with the individual Saps (Figure 2.2). As seen with the results for purified Sap9 and Sap2, both K17 modifications resulted in an increase in the amount of intact peptide remaining. The results for the K13L peptide followed the Sap9 proteolysis pattern, with an increase in degradation compared to the parent Hst-5. The peptides with modifications at K5 showed a mixed pattern, with a decrease in proteolysis for K5L emulating the Sap2 result and no significant effect for K5R emulating the Sap9 result. These outcomes demonstrate that both the cell-wall anchored Sap9 and the fully secreted

Sap2 play a role in proteolysis by *C. albicans* cell. It is important to note that additional Saps are likely to be present in the cell-based degradation assay and could contribute to the observed degradation. However, the overall results with the purified Saps are consistent with the results observed with the fungal cells, indicating that using purified Saps is a reasonable approach for studying biologically relevant effects of peptide sequence on susceptibility to Saps produced by cells.

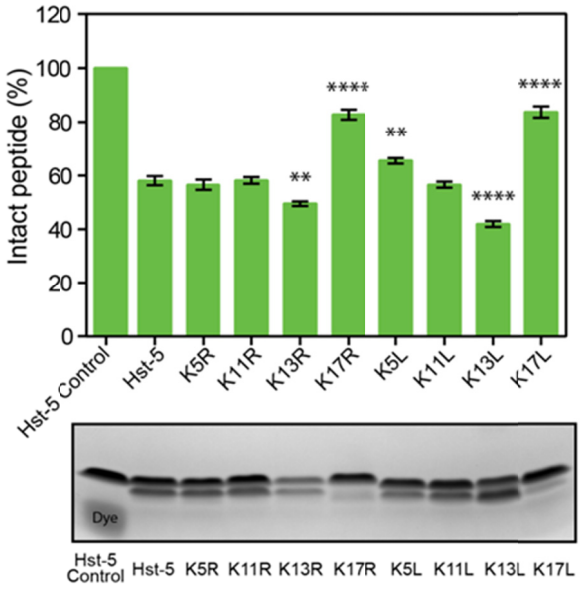

Figure 2.2. Degradation of parent Hst-5 and Hst-5 variants by *C. albicans*. The peptides (150 μg/mL) and *C. albicans* (1×10^9 cells/mL) were incubated for 2 h at 37 °C. Samples were run on a gel, and the amount of intact peptide was quantified by densitometry to compare the amount of intact peptide (upper band) to the peptide fragments. Error bars represent standard error of the mean ($n = 3$). The number of asterisks indicates the level of statistical significance against parent Hst-5 incubated with cells: ** for $p< 0.01$ and **** for $p< 0.0001$.The lower band in Hst-5 control lane is due to Coomassie dye.

2.3.3. Mass spectrometry confirms the effects of lysine modifications

To gain a more in-depth understanding of how the modifications to the peptide sequence affect the cleavage of Hst-5 by Saps, we used mass spectrometry to determine the cleavage sites and the relative abundance of peptide fragments. After incubation of

the peptides with each Sap, the four-amino-acid peptide MRFA was added as an internal standard, and samples were directly injected into the mass spectrometer.

Mass spectrometry of the parent Hst-5 peptide incubated with Sap9 showed that the signal for the degradation fragment containing amino acids 1 – 17 of Hst-5 was higher than the intact peptide (Figure 2.3). We observed cleavage on both sides of K13 and on the C-terminal side of K17, which are cleavage sites that have been previously reported for Sap9 and Sap2 [20, 25]. No cleavage was seen on either side of the K11 residue, consistent with the work of Bochenska et al. [25], though Meiller et al. did report cleavage at the N-terminal side of this residue [20]. We also detected cleavage between the H18 and H19 residues of the parent Hst-5, which has previously been observed after incubation with *C. albicans* cells [70] but not specifically associated with Sap9.

In general, the degradation of the Hst-5 variants with Sap9 produced results in agreement with the gel electrophoresis data. For K17R and K17L, the most intense signal came from the intact peptide, as expected from the large percentage of intact peptide seen in the gel electrophoresis results (Figure 2.1A). Furthermore, while the parent Hst-5 was cleaved on the C-terminal side of K17, neither K17R nor K17L showed significant cleavage at this site. K11R also shows the intact peptide to be the species with the highest signal. With the exception of the peptides with K17 substitutions, the variants with leucine substitutions showed relatively lower levels of intact peptide than the corresponding arginine-substituted peptides. Furthermore, K13L showed an apparent shift in cleavage site preference compared to the parent Hst-5. The fragments containing amino acids 1 – 12 and 13 – 24 had higher signals for K13L than the fragments containing amino acids 1 – 17 and 18 – 24, while the latter fragments had higher signals

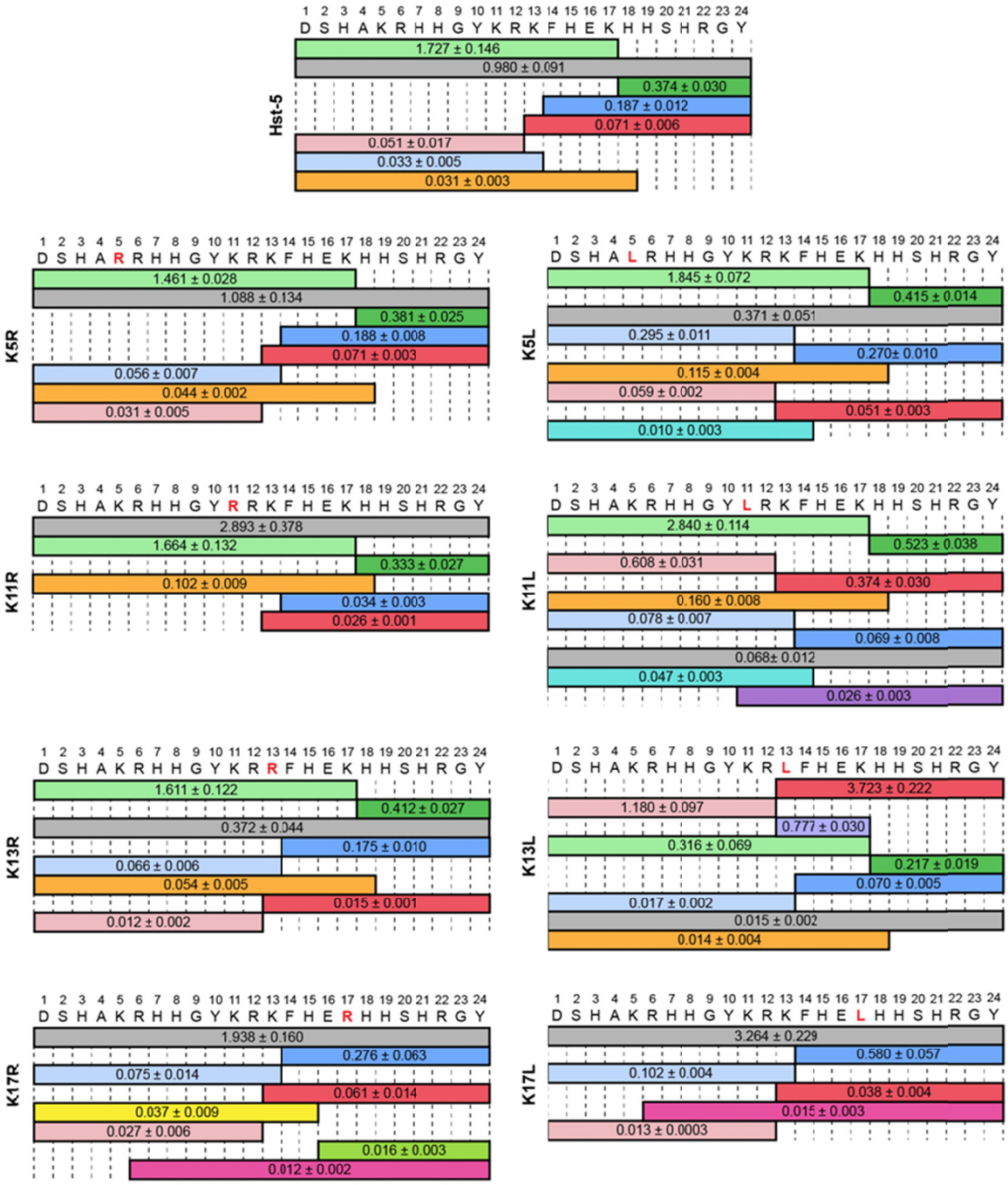

Figure 2.3. Relative mass spectrometry signal intensity of intact peptide (gray) and peptide fragments produced by incubation of parent Hst-5 and Hst-5 variants (modified residue in red) with 3.13 μg/mL Sap9. The values on each fragment indicate the signal for the fragment relative to the signal for an internal standard. Fragments with signals greater than 0.01 relative to the standard are shown. The relative signal is the mean with standard error (n = 3).

for the other modified peptides and parent Hst-5. The loss of cleavage site for the K17-modified peptides and the shift in cleavage site preference for K13L show that the substitutions affect cleavage around the modified residues. In addition, the presence of more intact peptide for K11R indicates that substitutions can also affect the peptides as a whole.

In contrast to incubation with Sap9, incubation of the parent Hst-5 peptide with Sap2 resulted in the intact peptide having the highest signal under the conditions tested (Figure 2.4). A lower number of distinct fragments was detected for Hst-5 degradation by Sap2 compared to Sap9. For example, the fragments containing amino acids 1 – 12 and 13 – 24 were not significantly detected in incubation with Sap2 but were detected with Sap9. The cleavage sites that did occur with Sap2 were also observed with Sap9 and are in agreement with previously reported results [20, 25], except that cleavage between H18 and H19 was not previously specifically attributed to Sap2. Meiller et al. also reported a cleavage site at the C-terminal side of K5 [20], which neither we nor Bochenska et al. observed [25].

As with incubation of the parent Hst-5, incubation of all the Hst-5 variants with Sap2 resulted in higher signals for intact peptides than for proteolytic fragments. The outcome was in line with the gel electrophoresis result, which showed that, overall, the Hst-5 variants incubated with Sap2 had more intact peptide remaining than when incubated with Sap9 (Figure 2.1). Substitutions at K17 did lead to a significant decrease in signals from fragments formed by cleavage at the C-terminal side of K17; however, unlike Sap9, Sap2 still cleaved K17L and K17R at this site.

The trends seen with the gel electrophoresis (Figure 2.1) and mass spectrometry results (Figure 2.3 and Figure 2.4) generally corroborate each other. Enhanced resistance to proteolysis was observed around the K17 residue for substitutions to both arginine and leucine with both Saps. The similar increase in resistance to degradation at K17, independent of the charge of the substituted residue, indicates that Sap9 and Sap2 have a preference for lysine at the K17 site and not simply a preference for a basic residue.

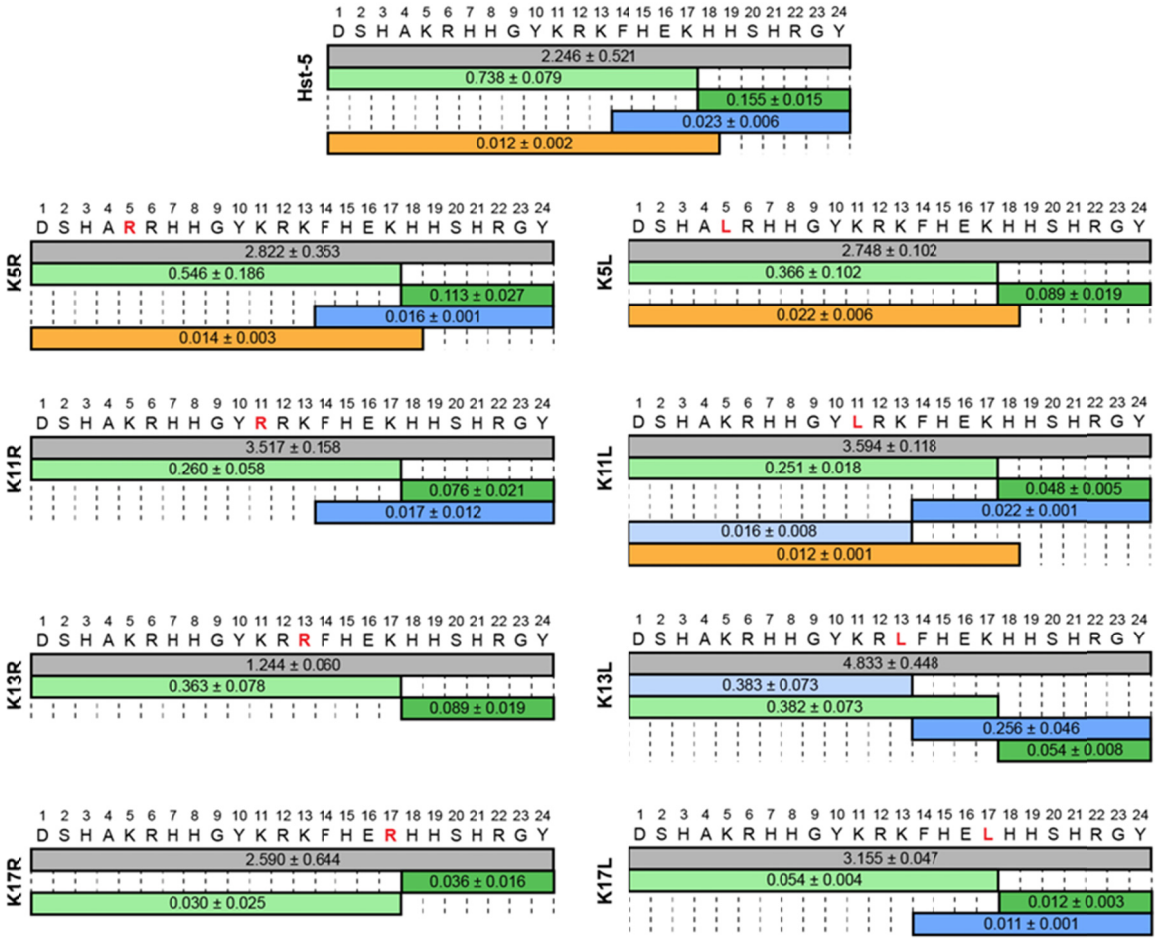

Figure 2.4. Relative mass spectrometry signal intensity of intact peptide (gray) and peptide fragments produced by incubation of parent Hst-5 and Hst-5 variants (modified residue in red) with 6.25 μg/mL Sap2. The values on each fragment indicate the signal for the fragment relative to the signal for an internal standard. Fragments with signals greater than 0.01 relative to the standard are shown. The relative signal is the mean with standard error (n = 3).

Unlike Sap9, Sap2 still cleaved at the C-terminal side of K17, suggesting the preference is more stringent for Sap9 than Sap2. At the other locations where lysine residues were modified, Sap9 appears to favor an uncharged leucine over a positively charged arginine or lysine. The leucine residues at these sites are N- or C-terminal to an arginine in the peptide sequence, and their preference by Sap9 agrees with previous work indicating Sap9 favors cleavage of peptides that contain leucine at the N-terminal side of an arginine [18]. Sap2, on the other hand, appears to favor lysine at the residues of Hst-5 that we studied. The preference is residue-dependent rather than charge-dependent, as Sap2 preferred lysine over both arginine and leucine. The one exception was at the K13 site, where Sap2 appears to prefer an arginine. Collectively, these results confirm our gel electrophoresis results and indicate single amino-acid modifications can affect overall susceptibility to cleavage and significantly reduce cleavage at the modification site.

2.3.4. Most residue substitutions do not diminish antifungal activity

Some previously reported modifications to Hst-5 had a negative impact on the peptide's antifungal activity [36, 38, 39]. To ensure that modification of lysine residues does not adversely affect the antifungal activity, we performed an antifungal activity assay to determine the reduction in the viability of *C. albicans* cells after exposure to the parent Hst-5 peptide and the Hst-5 variants (Figure 2.5). Serially diluted peptides were incubated with *C. albicans* cells at 2.5×10^5 cells/mL or 2.5×10^7 cells/mL *C. albicans* for 30 min at 30 °C in 1 mM NaPB. The mixtures were then diluted, transferred to YPD media, and incubated overnight to determine the reduction in cell viability due to incubation with the peptides.

When incubated with *C. albicans* at 2.5×10^5 cells/mL, Hst-5 variants behaved similarly to parent Hst-5, with an increasing reduction in viability with increasing peptide concentration (Figure 2.5A). Hst-5 had a minimum inhibitory concentration for 50% inhibition of growth (MIC_{50}) of 9.49 µg/mL, and the MIC_{50} values for the Hst-5 variants were within one dilution factor of Hst-5 (Figure 2.5A). The similar growth inhibition curves and MIC_{50} values show that the antifungal activity of Hst-5 is tolerant to substitutions of its lysine residues.

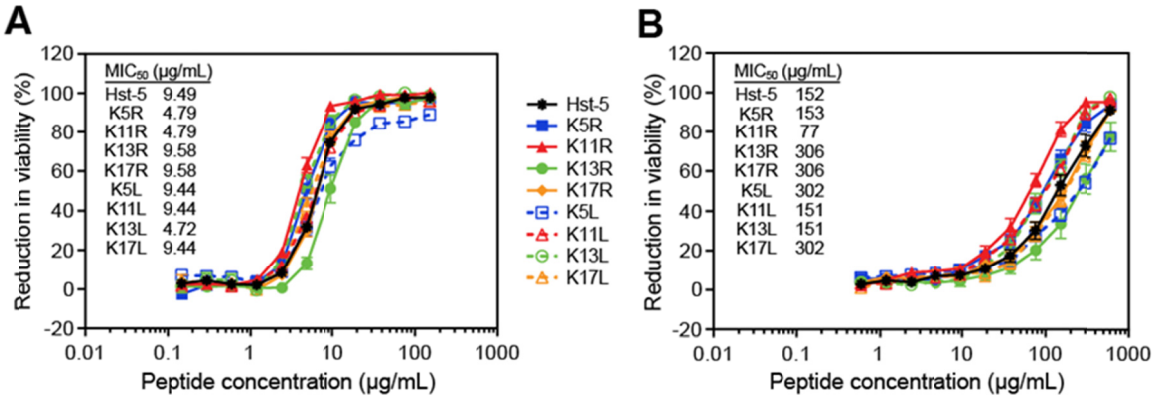

Figure 2.5. Antifungal activity of parent Hst-5 and the Hst-5 variants. Serially diluted peptides were incubated with (A) 2.5×10^5 cells/mL or (B) 2.5×10^7 cells/mL *C. albicans* for 30 min at 30 °C. Error bars represent standard error of the mean (n = 6). MIC_{50} values for the peptides are provided.

Increasing the cell concentration to 2.5×10^7 cells/mL resulted in a shift of the MIC_{50} value for Hst-5 to 152 µg/mL (Figure 2.5B), which is expected with the hundred-fold increase in cell density. With this higher cell density, the growth inhibition curves for each peptide were more widely separated, allowing differences between the antifungal activities of the peptides to be more apparent (Figure 2.5B). The K11R curve showed enhanced antifungal activity that was not apparent at the lower cell concentration. The K11 residue is present in both truncated peptides that were previously identified as active

fragments for antifungal activity—fragment C14 (residues 11 – 24) [33] and fragment P-113 (residues 4 – 15) [34]. Therefore, the K11R modification is at a critical location in the peptide and altering the interaction of the peptide with the Saps at this residue could have a larger effect on the antimicrobial activity of the peptide and its degradation fragments than most other lysine residues. Interestingly, neither K17R nor K17L showed improvement in antifungal activity despite the gel and mass spectrometry results that demonstrated more intact peptide. This may be a function of the incubation time in the assay. The antifungal assay we used (based on the assay used by several other groups [34, 39, 66]) incorporates a short contact time for the peptides and *C. albicans* to minimize the effect of cell division on assay results. Since the kinetics of proteolysis of the *in vivo* Saps may be slow enough that their effect on Hst-5 is not easily observed under these conditions, improvements of the K17 modifications on antifungal activity may not be observed at the conditions tested. Overall, the antifungal activity assay demonstrates that replacement of a lysine with an arginine or a leucine does not abolish the antifungal activity of the Hst-5 and may lead to improvements. While there have been no previous studies evaluating the effect of lysine to arginine modifications on the antifungal activity of Hst-5, Helmerhorst et al. reported that a lysine to leucine substitution in a fragment of Hst-5 called dh-5 showed similar activity to the peptide containing lysine [35], further supporting the tolerance of Hst-5 to lysine-to-leucine modifications.

2.3.5. Several Hst-5 variants retain antifungal activity after treatment with Saps

After confirming that substitutions to the lysine residues did not eliminate antifungal activity, we investigated whether the peptides retained their antifungal activity after exposure to purified Saps. To amplify differences in antifungal activity due to

degradation by the Saps, we increased the concentrations of the Saps by at least two-fold compared to the concentrations used for the gel electrophoresis data in Figure 2.1 (to 6.25 µg/mL for Sap9 and 18 µg/mL for Sap2). Incubation with Sap9 led Hst-5 to lose over 60% of its antifungal activity, while incubation with Sap2 almost completely eliminated its activity (Figure 2.6). In contrast, both K17 variants retained much of their antifungal

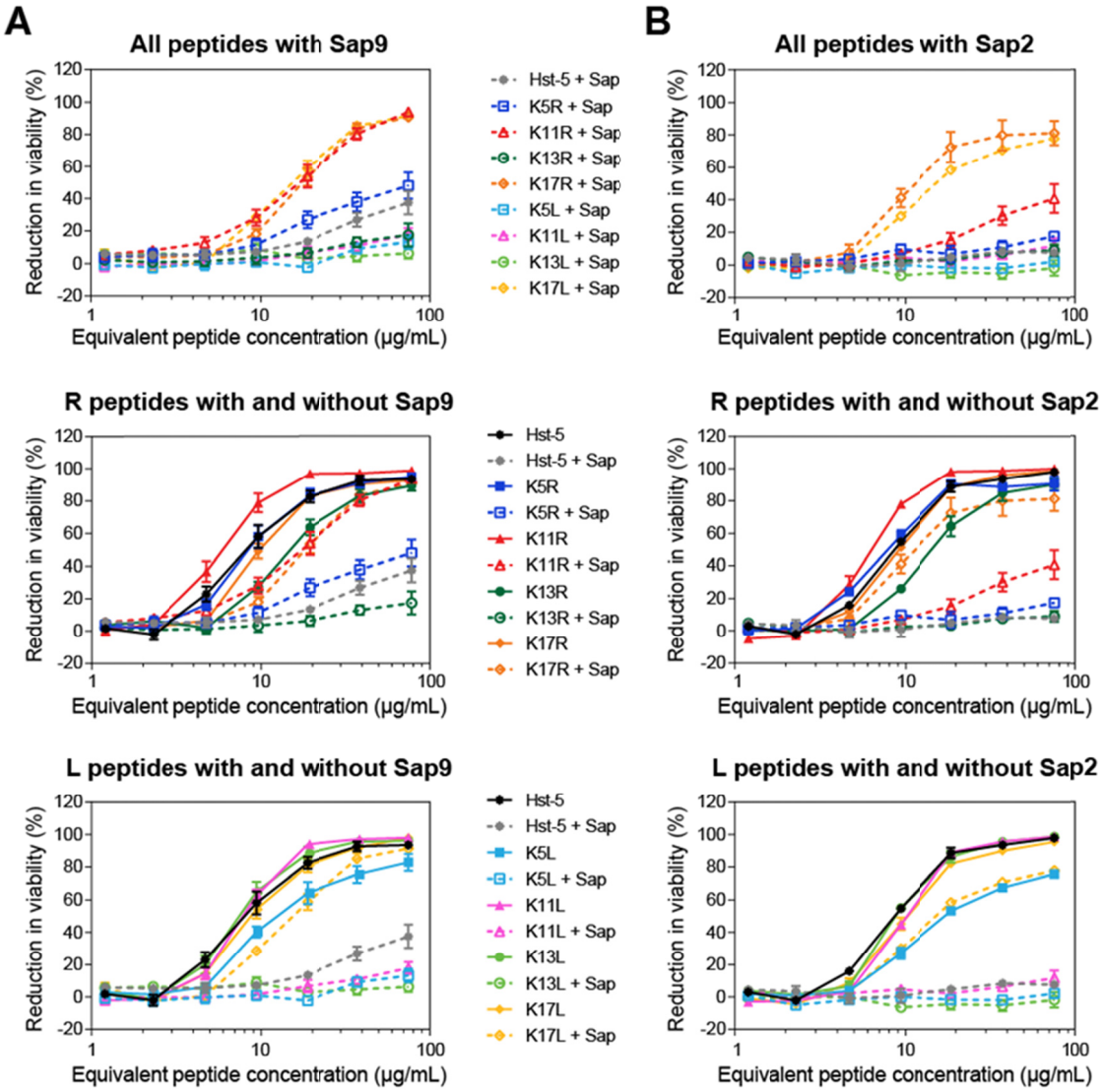

Figure 2.6. Antifungal activity of parent Hst-5 and the Hst-5 variants following incubation with Sap 9 and Sap2. The peptides (150 µg/mL) with (A) Sap9 (6.25 µg/mL) and (B) Sap2 (18 µg/mL) were incubated for 2 h at 37 °C. Samples were serially diluted and incubated with 2.5×10^5 cells/mL *C. albicans* for 30 min at 30 °C. Error bars represent standard error of the mean ($n = 6$).

activity after exposure to each Sap, which is consistent with the high level of intact peptide that remained following incubation with both Sap9 (over 60% remaining for each peptide) and Sap2 (over 90% remaining for K17R and over 70% remaining for K17L) (Figure 2.7). The K11R peptide also had a strong performance in the antifungal activity assay following exposure to Sap9, with a level of activity similar to that of the K17 variants. The improved activity following incubation indicates that resistance to proteolysis could prolong the antimicrobial potency in the presence of the Saps produced by *C. albicans*.

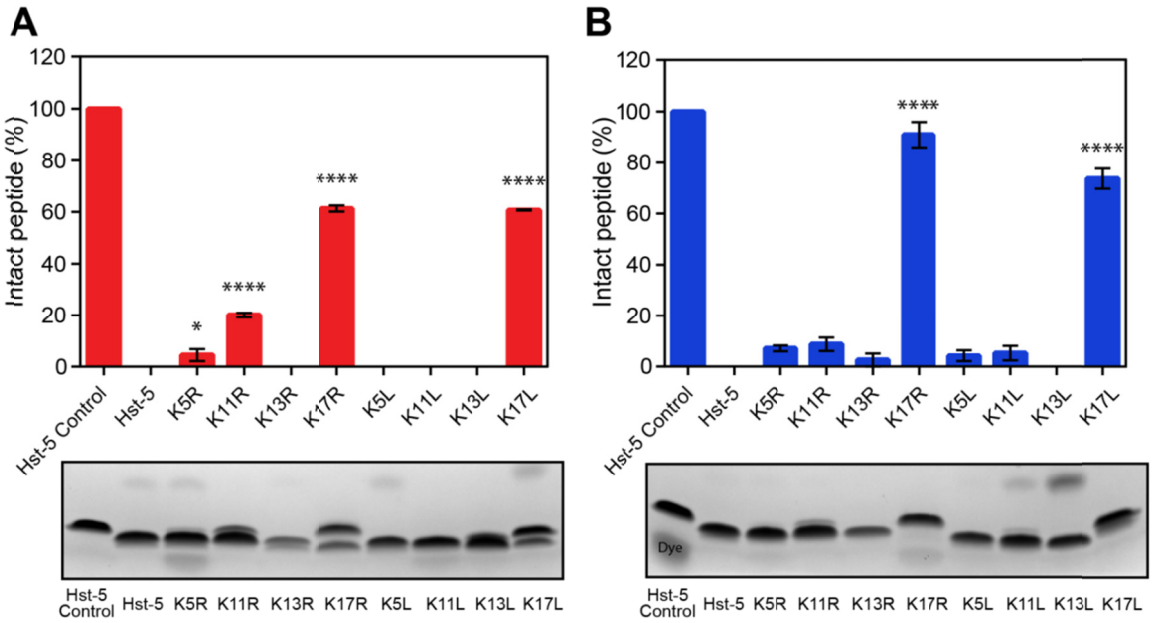

Figure 2.7. Degradation of parent Hst-5 and Hst-5 variants by purified (A) Sap9 and (B) Sap2. The peptides (150 µg/mL) and Saps (6.25 µg/mL Sap9 and 18 µg/mL Sap2) were incubated for 2 h at 37 °C in 1 mM NaPB. Samples were run on a gel to separate the intact peptide and peptide fragments. The amount of intact peptide was quantified by densitometry to compare the amount of intact peptide (upper band) to the peptide fragments. Error bars represent standard error of the mean (n = 3). The number of asterisks indicates the level of statistical significance against parent Hst-5 incubated with the Saps: * for $p < 0.05$ and **** for $p < 0.0001$. The lower band in the Hst-5 control lane in (B) is due to Coomassie dye.

Overall, following degradation by each of the Saps, the arginine-substituted peptides retained more antifungal activity compared to the analogous leucine-substituted peptides. For example, the Sap9- and Sap2-degraded K5R and K11R variants still displayed some antifungal activity, while the degraded K5L and K11L variants showed almost none. The K5R and K11R peptide also retained some intact peptide after Sap9 incubation (4.5% and 20% of peptide, respectively), while no statistically significant amount of these peptides remained after Sap2 incubation (Figure 2.7B). The presence of intact K5R and K11R but not intact K5L and K11L after incubation with Sap9 further supports a preference for leucine at these sites by Sap9 and also shows a preference for lysine over arginine, since the parent Hst-5 is completely degraded under these conditions.

Although the variants with the largest amount of intact peptide remaining had the strongest antifungal activity, intact peptide was not required for antifungal activity. The parent Hst-5 peptide had no intact peptide remaining after incubation with Sap9, but it did show a measurable level of antifungal activity. Moreover, while less intact K11R peptide remained after incubation with Sap9 compared to K17R or K17L (Figure 2.7A), the antifungal activity was at the same level as the K17 modified peptides. This suggests that the antifungal activity comes not only from the intact K11R peptide, but also from its proteolytic fragments. This is consistent with previous studies with Hst-5 that found varying levels of antifungal activity from Hst-5 truncation peptides [33-35].

Our results indicate that, while some peptide modifications make the intact peptide more robust (e.g., K17R, K17L), others can lead to degradation fragments with improved antifungal activity compared to the degradation fragments of parent Hst-5 (e.g., K11R). Consequently, even if the intact versions of Hst-5 variants do not have improved

antifungal activity themselves, a longer half-life of intact peptide or a higher activity of degradation fragments leads to improved therapeutic potential of K11R, K17R, and K17L compared to Hst-5. We recently showed that Hst-5 delivered in a bioadhesive hydrogel could effectively prevent the development of an oral *C. albicans* infection in mice [71]. The modified peptides could be delivered directly to mucosal surfaces in the same manner, or they could be incorporated into coatings on implantable devices or prosthetics using thin films, which have been used previously to successfully create antimicrobial surfaces using other antimicrobial peptides [72-74].

2.4. Conclusion

We have demonstrated that changing a single lysine residue in the Hst-5 sequence can significantly alter its proteolysis by purified Sap9 and Sap2, as well as by whole *C. albicans* cells. Further, we show that the effects of the modifications are site-, residue-, or Sap-dependent, and the substitutions affect not only cleavage at the substitution sites but also the degradation of the peptide as a whole. These findings can be used to design and test additional modifications to study the interaction between Hst-5 and both Saps and *C. albicans* cells. Additionally, our work provides peptide engineering approaches that can be used to design more robust peptides in the presence of aspartic proteases, which could have applications as potential therapeutics to treat or prevent *C. albicans* infections.

Chapter 3: Effects of histatin 5 residue modifications on kinetics of its proteolysis and antifungal activity

3.1. Introduction

Chapter 2 demonstrated that substitutions of single lysine in histatin 5 (Hst-5) to arginine or leucine have site-, residue-, and protease-specific effects on the antifungal peptide's susceptibility to proteolysis by secreted aspartic proteases (Saps), produced by *Candida albicans*. Furthermore, the substitutions do not diminish the antifungal activity of the peptide. The study found modifications that enhanced the resistance to degradation by Sap9, Sap2, and *C. albicans* cells (K17R and K17L), as well as a modification that enhanced the antifungal activity (K11R). The K17R and K17L peptides also retained significantly higher antifungal activity than Hst-5 after exposure to Saps. However, not all of the tested lysine substitutions led to enhanced properties. In fact, the K13 site modifications led to an increase in susceptibility to proteolysis by Sap9 and *C. albicans* cells. Interestingly, while the K13L modified peptide was particularly susceptible to Sap9, it maintained antifungal activity similar to Hst-5.

To gain further insight into interactions between Hst-5 and *C. albicans*, this chapter expands on the study in Chapter 2 by investigating additional amino acid modifications at the K13 and E16 residues and combining two previously tested lysine modifications. The effects of the substitutions on the susceptibility to proteolysis by Saps and *C. albicans* and on the antifungal activity were tested. A time course study on the proteolysis of Hst-5 and its variants by Sap9 was also conducted to study influences of the modifications on

kinetics. The study revealed that residue substitution significantly affected the kinetics of proteolysis and modifications that make the overall peptide more susceptible to degradation could lead to fragments with enhanced antifungal activity. It also demonstrated the effects from single amino acid modifications can be combined into one peptide, which expands the possibilities of future designs of antimicrobial peptides.

3.2. Materials and methods

3.2.1. Peptides and enzymes

Hst-5 and its variants were synthesized by Genscript (purity ≥95% with trifluoroacetic acid salt removal to hydrochloride). Dr. Bernhard Hube from Friedrich Schiller University, Germany provided the recombinant Sap2 and Sap9. The Saps were expressed in *Pichia pastoris* [16], and Sap9 was expressed sans its GPI anchor [18].

3.2.2. Degradation of peptides by Saps and *C. albicans*

The overall extent of proteolysis of the peptides by purified Saps was evaluated through gel electrophoresis. Hst-5 and its variants (20 μL) were mixed with Saps (20 μL) in 0.5 mL microcentrifuge tubes to final concentrations of 50 μM peptide and 3 μg/mL Sap9 or 0.05 μg/mL Sap2. As controls, the peptides were mixed with sodium phosphate buffer (NaPB). The incubations were done in 1 mM NaPB for 2 h at 37 °C. The samples were then mixed with tricine sample buffer (200 mM Tris-HCl, pH 6.8, 40% glycerol, 2% SDS, no Coomassie Blue G-250) containing 2% β-mercaptoethanol and heated at 100 °C for 5 min to inactivate the Saps. To separate the intact peptide and its degradation

products, the samples were run on 16.5% Tris-tricine gels (Bio-Rad) at 60 V. After separation, the gels were fixed for 30 min in a 10% acetic acid/40% methanol/50% water fixing solution and stained with Bio-Safe Coomassie stain (Bio-Rad) for 1 h. The stained gels were washed with fresh water four times: once overnight and at least 1.5 h each for the rest of the washes. The stained gels were imaged on a Chemidoc imager (Bio-Rad). Image Lab software (Bio-rad) was used for densitometric analysis, where the upper band in each lane was analyzed as non-degraded peptide and the lower band was analyzed as degraded products. Degradation reactions were performed on three different days with two replicates with in each day for total of $n = 6$.

For the study of proteolysis by *C. albicans*, an overnight culture of the ATCC 90028 strain (American Type Culture Collection) was subcultured and grown in YPD media (10 g/L yeast extract, 20 g/L peptone, 20 g/L dextrose) at 30 °C to an optical density (OD_{600}) of 1 – 1.2. Cells were harvested and washed three times in 100 mM NaPB. Washed cells were resuspended in the buffer and mixed with an equal volume of each peptide to final concentrations of 1×10^9 cells/mL *C. albicans* and 50 μM peptide. As controls, the peptides were mixed with NaPB. After incubation for 2 h at 37 °C, cells were removed by centrifugation and heated at 100 °C for 10 min after addition of tricine sample buffer. Afterwards, following the protocol described above for degradation by Saps, samples were run on Tris-tricine gels, stained, and analyzed. Degradation reactions were performed on three different days with two replicates with in each day for total of $n = 6$.

One-way ANOVA tests with $p< 0.05$ and Dunett's multiple comparison tests (Hst-5 sample as the control) were performed for statistical analysis. The level of statistical

significance in figures is indicated by the number of asterisks: * for $p < 0.05$, ** for $p < 0.01$, *** for $p < 0.001$, and **** for $p < 0.0001$.

3.2.3. Capillary electrophoresis-mass spectrometry

Capillary electrophoresis-mass spectrometry (CEMS) was used to determine and quantify the fragments formed from cleavage by Saps. Once Saps (3 μg/mL Sap9 or 0.05 μg/mL Sap2) were heat inactivated after incubation with 50 μM peptides, 25 μL of each sample was desalted with a C-18 TopTip micro-spin column (Glygen Corp.) following the manufacturer's protocol. Solutions of 0.1% formic acid and 0.1% formic acid/60% acetonitrile (ACN) were used for binding and eluting, respectively. To each elution, 1 μL of the peptide MRFA (0.1 mg/mL) was added as an internal standard. The samples were further diluted with 0.1% formic acid before CEMS analysis.

The separation was done at 30 kV with a CMP Scientific ECE-001 capillary electrophoresis system with a CMP Scientific EMASS-II ion source. An etched capillary with PS1 neutral coating was used with the system.

A Thermo Scientific Orbitrap Fusion Lumos Tribrid mass spectrometer was used to acquire full mass spectra in the range of 200 – 1450 m/z with resolution R=120000 (200 m/z). EthcD spectra at R=120000 (200 m/z) with a 3 s cycle time were recorded to identify peptide fragments from degradation by Saps. The EthcD spectra of each sample were processed with Proteome Discoverer (V2.1) with the Prosight PD node to identify the degradation products. Full scan mass spectra were deconvoluted, and the intensities of the intact peptide, fragments, and the internal standard MRFA were analyzed with Thermo Xcalibur 3.0 software (Figure B.1).

3.2.4. Kinetics of proteolysis

To gain an understanding of the kinetics of the interaction between the peptides and Saps, a time-course study on the proteolysis of Hst-5 and its variants by Sap9 was performed. As described for the proteolytic study with gel electrophoresis, a series of peptide and Sap9 mixtures with final concentrations of 50 μM peptide and 3 μg/mL Sap9 were prepared. Samples were incubated for 5 min, 30 min, or 120 min at 37 °C and then heated at 100 °C for 5 min to inactivate Sap9. For the 0 min time point, Sap9 was first heat inactivated and then added to the peptides. The samples were desalted with a C-18 TopTip micro-spin column and analyzed by CEMS as described above.

3.2.5. Antifungal activity assay with intact peptide and fragments

The antifungal activity of intact parent Hst-5 and its variants was evaluated using an optical density-based candidacidal assay. An overnight culture *C. albicans* was subcultured and grown at 30 °C in YPD media to an OD_{600} of 1 – 1.2. Cells were harvested, washed three times with 2 mM NaPB, and diluted to 5×10^7 cells/mL. Meanwhile, each of the peptides was serially diluted (0 – 400 μM) in water. Equal volumes (20 μL) of diluted cells and diluted peptide were then mixed in a round-bottom 96-well culture plate. As a control, an equal volume of water was mixed with the diluted cells. After 30 min of incubation at 30 °C, 320 μL of 1 mM NaPB was added to stop additional interaction of peptides and cells [66]. Samples were further diluted and approximately 250 cells were inoculated into an equal mixture of YPD (100 μL) and 1 mM NaPB (100 μL) in round-bottom culture plates, and the cells were grown overnight at 30 °C on a microplate shaker at 350 rpm. Wells with only YPD and NaPB provided the

background signal. After overnight incubation, cells in each well were resuspended, and the OD_{600} was measured. The reduction in viability was calculated as

$$\%\ \text{reduction in viability} = \left[1 - \frac{\left(\text{OD}_{\text{with peptide}} - \text{OD}_{background}\right)}{\left(\text{OD}_{\text{no peptide}} - \text{OD}_{background}\right)}\right] \times 100$$

The activity assays were performed on three different days with two replicates with in each day for total of $n = 6$.

For determining the antifungal activity of the peptides after exposure to Saps, 50 μM peptide was first incubated with 6 μg/mL Sap9 or 0.2 μg/mL Sap2 for 2 h at 37 °C. After the incubation, the Saps were inactivated by heating the samples at 100 °C for 5 min. As controls, the peptides were mixed with NaPB. The antifungal activity of Sap-incubated samples was assessed following the described protocol for intact peptide, with the modification of using a lower *C. albicans* concentration of 5×10^5 cells/mL. Degraded peptide samples were prepared on two different days for each of the Saps. The antifungal activity assays were performed on two different days for each Sap samples with two replicates within the same day for total of $n = 4$.

3.3. Results

To further characterize the interaction between Hst-5 and *C. albicans*, new residue modifications to the Hst-5 sequence were designed and tested (Table 3.1). The investigation of the K13 site was continued as at it is part of both antifungal fragments of Hst-5 (residues 4 – 15 [33] and 11 – 24 [34]). Histidine was substituted at the K13 site to form an arginine-histidine pair with the R12 site since no prior cleavage between arginine-histidine pair by Sap2, Sap9, or *C. albicans* within the Hst-5 sequence had been

reported [20]. Bocheska et al. did report cleavage with Sap7, but it was in buffer and pH conditions optimal for Sap7. The K13E modified peptide was also designed to test the potential role of negative charge in proteolysis at the site. Although the K13E substitution has been previously tested for its impact on antifungal activity [38], its effect on proteolysis has not been explored.

Table 3.1. Hst-5 and variants with one or two amino acid substitutions.

Peptide	**Sequence**[a]																							
	1	2	3	4	5	6	7	8	9	10	11	12	13	14	15	16	17	18	19	20	21	22	23	24
Hst-5	D	S	H	A	K	R	H	H	G	Y	K	R	K	F	H	E	K	H	H	S	H	R	G	Y
K13H	-	-	-	-	-	-	-	-	-	-	-	-	H	-	-	-	-	-	-	-	-	-	-	-
K13E	-	-	-	-	-	-	-	-	-	-	-	-	E	-	-	-	-	-	-	-	-	-	-	-
E16R	-	-	-	-	-	-	-	-	-	-	-	-	-	-	-	R	-	-	-	-	-	-	-	-
E16L	-	-	-	-	-	-	-	-	-	-	-	-	-	-	-	L	-	-	-	-	-	-	-	-
K11R-K17R	-	-	-	-	-	-	-	-	-	-	R	-	-	-	-	-	R	-	-	-	-	-	-	-

[a] Dash indicates residue was unchanged from the parent Hst-5.

A new substitution at the E16 site was investigated since the glutamic acid at the site is the only negative-charged residue in the active fragments of the peptide. It is also next to the K17 site where the modifications to arginine and leucine enhanced the peptide's resistance to Saps. To test the role of the negative charge on the robustness and the activity of Hst-5, it was modified to a positively charged arginine or an uncharged leucine.

Finally, to determine whether the enhancements seen with single amino acid modifications (Chapter 2) can be combined to achieve further enhancement, both K11 and K17 were substituted to arginine. Since the K11R modification led to enhanced

antifungal activity and the K17R modification led to enhanced resistance to proteolysis, the new peptide was hypothesized to have both of the enhanced properties.

3.3.1. Modified peptides are more susceptible to Sap9

The effect of the amino acid modifications on the overall proteolytic susceptibility of Hst-5 was evaluated by incubating Hst-5 and its variants with purified, recombinant Sap9 and Sap2. After 2 h of incubation at 37 °C in 1 mM NaPB, the intact peptide and degradation products were separated via gel electrophoresis. The level of degradation was quantified through densitometric analysis of Coomassie-stained gels (Figure 3.1). The double substituted peptide K11R-K17R showed significantly enhanced resistance to both Saps. Compared to 37% of parent Hst-5, over 88% of intact K11R-K17R peptide remained after incubation with Sap9 (Figure 3.1A). The modified peptide's resistance to proteolysis was even greater for Sap2; no detectable level of the K11R-K17R degradation was observed whereas only 37% of intact Hst-5 remained (Figure 3.1B).

Overall, the modified peptides were more susceptible to degradation by Sap9 than Sap2. The E16R modification enhanced resistance to Sap2, with 60% of intact peptide remaining (Figure 3.1B). However, there was significantly more degradation when exposed to Sap9 (Figure 3.1A). A similar pattern was also observed at the K13 site. After exposure to Sap2, the K13H and K13E peptides retained an amount of intact peptide comparable to Hst-5, but they were completely degraded by Sap9. It should be noted that the source of the additional band in the K13H lane that is at a molecular weight higher than intact peptide is currently unknown and was not considered in the analysis (Figure 3.1A).

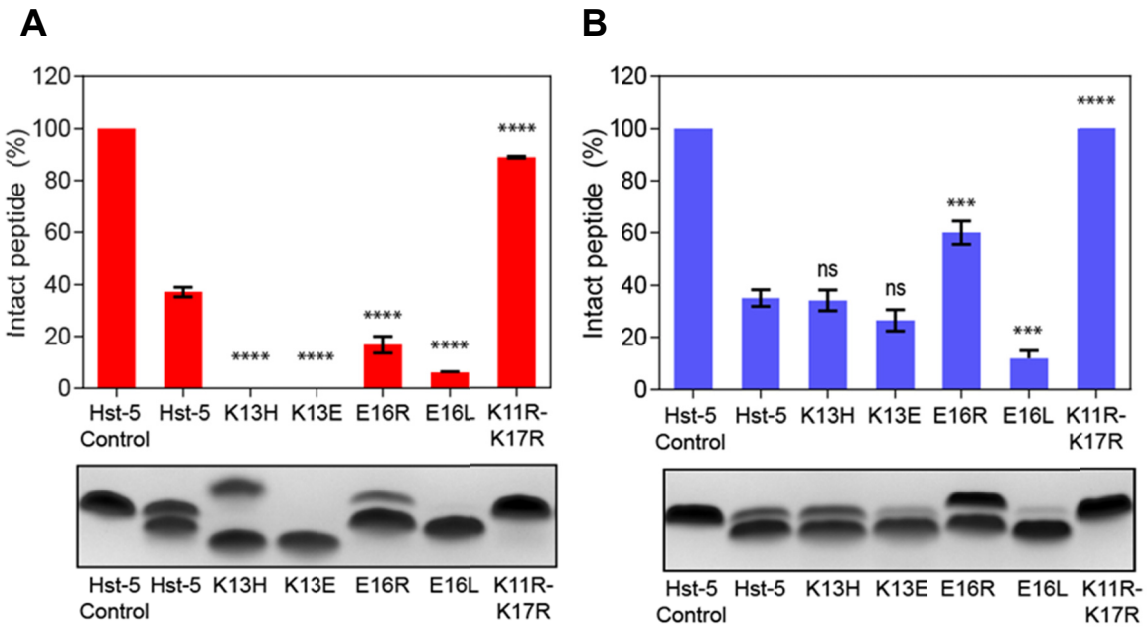

Figure 3.1. Extent of proteolysis of parent Hst-5 and Hst-5 variants by purified (A) Sap9 and (B) Sap2. After the peptides (50 μM) and the Saps (3 μg/mL Sap9 or 0.05 μg/mL Sap2, respectively) were incubated for 2 h at 37 °C, samples were run on a gel and stained with Coomassie. The amount of intact peptide remaining was quantified by comparing the intensity of the intact peptide (upper band) to the fragments (lower band) through densitometric analysis. The source of the additional band in the K13H lane of Sap9 is unknown and not included in the analysis. Error bars indicate standard error of the mean (n = 6). The level of statistical significance relative to parent Hst-5 is indicated by the number of asterisks: ns for no significance, *** for $p < 0.001$, and **** for $p < 0.0001$.

The preference by Sap9 for proteolysis of leucine-substituted peptide over arginine-substituted peptide, observed in Chapter 2, was also seen with the modifications at the E16 site. Leucine-substituted E16L showed more degradation than the arginine-substituted E16R. Interestingly, the preference appeared to be not limited to Sap9. Incubation with Sap2 also showed greater degradation of the E16L-modified peptide compared to the E16R-modified peptide. The variances in the extent of degradation among the modified peptides and between the Saps bolster the concept that the Saps have different preferences for the same residue.

3.3.2. Proteolysis by *C. albicans* follows the degradation pattern for Sap9 and Sap2

To determine the proteolytic effect when the peptides are exposed to natively expressed Saps, the peptides were incubated with *C. albicans*. The parent Hst-5 and the modified peptides were incubated with *C. albicans* for 2 h at 37 °C in 100 mM NaPB (the high ionic buffer was used to prevent internalization of the peptides into the cells [69]). The cells were removed by centrifugation and the peptides were run on a gel. The extent of degradation was quantified via densitometric analysis of the stained gels (Figure 3.2). As expected from the recombinant Sap results, the K11R-K17R modified peptide showed a significant increase in resistance to proteolysis by *C. albicans*, with over 81% of intact peptide remaining compared to 54% of Hst-5. The degradation of the K13-modified peptides mimicked the results with recombinant Sap2 more closely than the results with recombinant Sap9. The amount of intact K13H peptide remaining was comparable to Hst-5, and, although the K13E peptide had less intact peptide, it still retained more full-length peptide than the E16L peptide, as observed after incubation with Sap2. On the other hand, the proteolysis of the E16R peptide more closely resembled the Sap9 result; less intact E16R remained than intact Hst-5. However, despite the higher degradation of the E16R, the pattern of higher susceptibility of leucine-substituted peptides over arginine-substituted peptides for proteolysis was maintained (13% vs. 27% intact E16L and E16R, respectively). Other Saps are present when testing with whole *C. albicans* cells, and, therefore, some of the degradation may be due to Saps other than Sap2 or Sap9. This could account for the fact that the difference in intact peptide between Hst-5 and the K11R-K17R modified peptide is smaller than when tested with Sap9 and Sap2 individually. Regardless, the influences of amino acid modification were successfully

detected, and, for the case of the K11R-K17R peptide, its enhanced proteolytic resistance was confirmed even when exposed to all Saps produced by *C. albicans*.

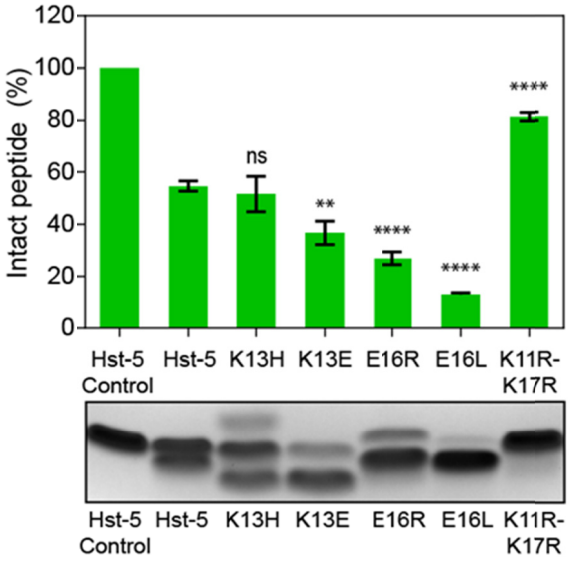

Figure 3.2. Extent of degradation for Hst-5 and its variants after exposure to *C. albicans* cells. After the peptides (50 μM) and the *C. albicans* cells (1×10^9 cells/mL) were incubated for 2 h at 37 °C, samples were run on a gel and stained with Coomassie. The amount of intact peptide remaining was quantified by comparing the intensity of the intact peptide (upper band) to the fragments (lower band) through densitometric analysis. The source of the additional band in the K13H lane is unknown and not included in the analysis. Error bars indicate standard error of the mean (n = 6). The level of statistical significance relative to parent Hst-5 is indicated by the number of asterisks: ns for no significance, ** for $p< 0.01$, and **** for $p< 0.0001$.

3.3.3. Amino acid substitutions shift cleavage sites

The gel electrophoresis analysis presented the overall changes to the susceptibility of Hst-5 to proteolysis due to the amino acid substitutions. To discern the impact on the cleavage sites and relative amount of the fragments produced, the peptides were analyzed with CEMS after incubation with the Saps. The peptide MRFA was added to each sample as an internal standard prior to CEMS. The abundance of each intact peptide or its fragments was quantified by looking at the area of the peak for each peptide in the chromatogram relative to the peak area for the internal standard in the chromatogram

(Figure B.1). However, below a peak area of 1×10^6, the signal to concentration relationship was found to be non-linear; therefore these values were not considered in the analysis.

For the relative abundance of intact peptide, the mass spectrometry results are consistent with the gel electrophoresis results for both Saps. The most abundant peptide in the E16R incubation with Sap2 and the K11R-K17R incubation with Sap9 and Sap2 was the intact peptide (Figure 3.3). The same samples showed enhanced resistance to proteolysis in analysis by gel electrophoresis. For the rest of the peptide and Sap combinations, the fragment containing residues 1 – 17 was more prevalent than the intact peptide. The high abundance of the same fragment was also previously observed with single a lysine substitution at the K5 or K11 sites [75].

Incubation with Sap9 led to significant degradation of E16R and E16L. While multiple different fragments were detected in the Hst-5 sample, only a few fragments remained in E16R and E16L samples, with little to no intact peptide (Figure 3.3A). The substantially lower amount of E16R peptide was surprising, as its presence was expected from the gel electrophoresis analysis (Figure 3.1A). The CEMS may not get a high signal from the intact E16R. Even in the sample incubated with Sap2, the signal of the intact E16R is lower than or comparable to the degradation fragments of other peptides

The mass spectra of the K11R-K17R peptide were quite different from Hst-5 or the other variants. First, no significant amount of the amino acids 1 – 17 fragment was detected after incubation with either Sap. This indicates that no cleavage occurred at the R17 site, as predicted during the peptide design, since the K17R substitution previously reduced degradation at this site. Furthermore, new fragments were detected and the

majority of them were due to cleavage in the N-terminal half of the peptide. In Hst-5 and

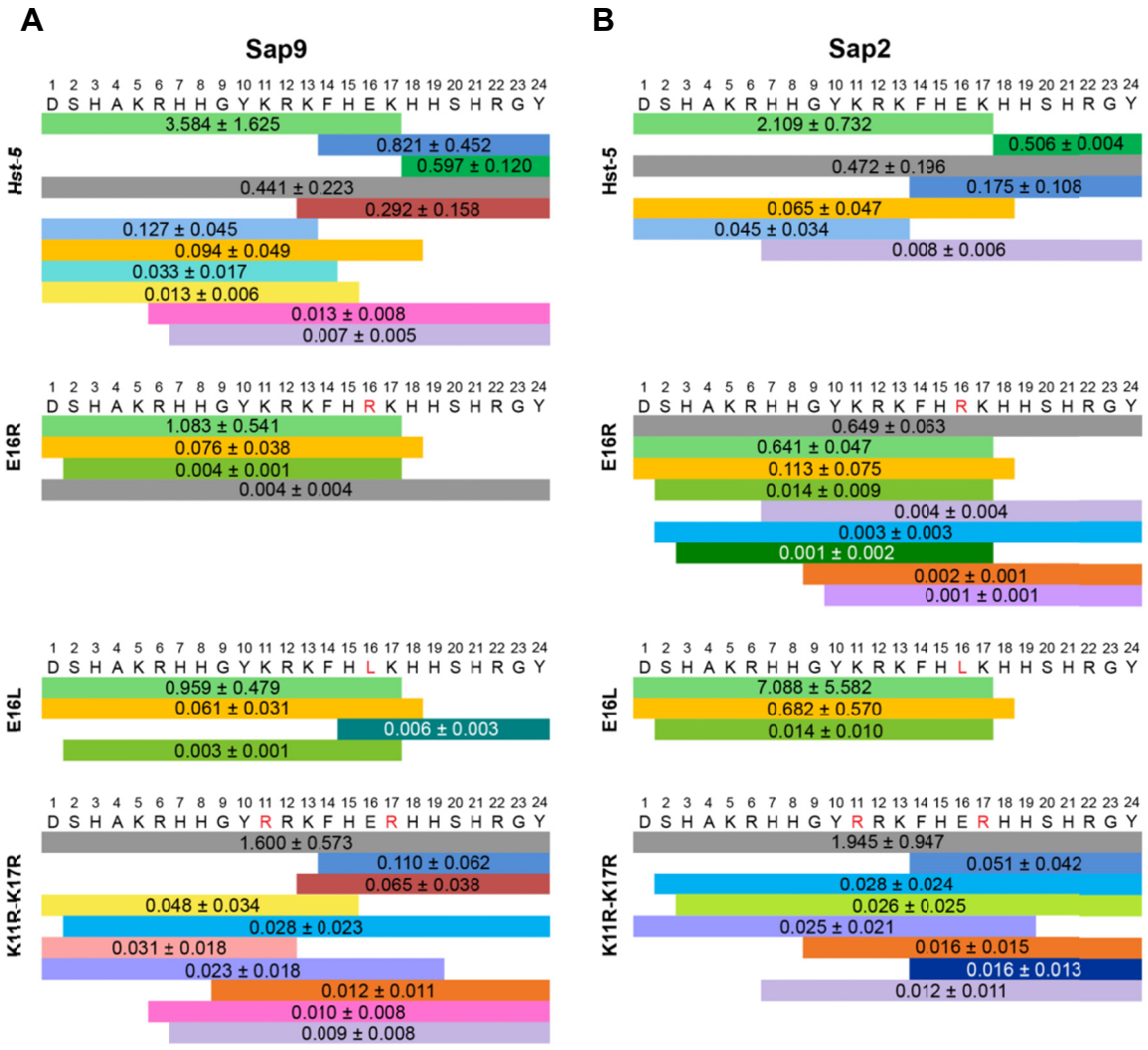

Figure 3.3. Average of peak area obtained from chromatogram of the data, relative to internal standard, of intact peptide (gray) and degradation fragments of Hst-5 and its analogs from mass spectrometry of peptides after incubation 50 µM peptide with (A) 3 µg/mL Sap9 and (B) 0.05 µg/mL Sap2. Errors are the standard error of the mean (n = 3). Fragments with a peak area above 1×10^6 in at least one of three replicates are displayed.

the other variants, the majority of the fragments were due to cleavage in the C-terminal half of the peptides. Therefore, the residues substitutions alter not only the abundance of degradation fragments but also shift the location of the cleavage sites.

3.3.4. Modifications modulate the rate of proteolysis by Sap9

The mass spectrometry analysis showed that residue substitutions change the type and abundance of the peptide fragments that remain after incubation for 2 h with Sap9, so a time-course study was conducted to characterize the kinetics of proteolysis by Sap9. The peptides Hst-5, E16L, and K11R-K17R were incubated with Sap9 for 5 min, 30 min, and 120 min and analyzed with CEMS. For controls at 0 min, Sap9 that was first heat inactivated was added to the peptide samples.

Each of the tested peptides showed a unique degradation pattern (Figure 3.4). For the intact peptides, Hst-5 and E13L were degraded at faster rate than K11R-K17R in the first 5 min of incubation. The degradation rates of all the peptides slowed after 30 min of incubation and while some intact Hst-5 and K11R-K17R remained after 120 min, K13L was completely degraded. The formation and the degradation of the peptide fragments also showed variability among the peptides. For Hst-5, with the exception of the amino acids 3 – 17 and 7 – 24 fragments, the proteolytic fragments accumulated at increased rates after 30 min. On the other hand, most of the fragments of the E13L peptide, particularly the amino acids 1 – 17 fragment, accumulated during the first 30 min of incubation, but were subsequently degraded. This could explain why only few fragments were detected in the data for the 120 min incubation (Figure 3.3). The presence of the residues 13 – 24 fragment, which has been seen with proteolysis by Sap9 but not Sap2 (Figure 3.3), was also detected in middle of the time-course for K13L. Lastly, some of the fragments of the K11R-K17R peptide showed an interesting trend. The smaller fragments (amino acids 14 – 24 and 13 – 24), and N-terminus fragments (amino acids 1 – 12 and 1 – 15) accumulated at an increased rate after 30 min, as did most of the

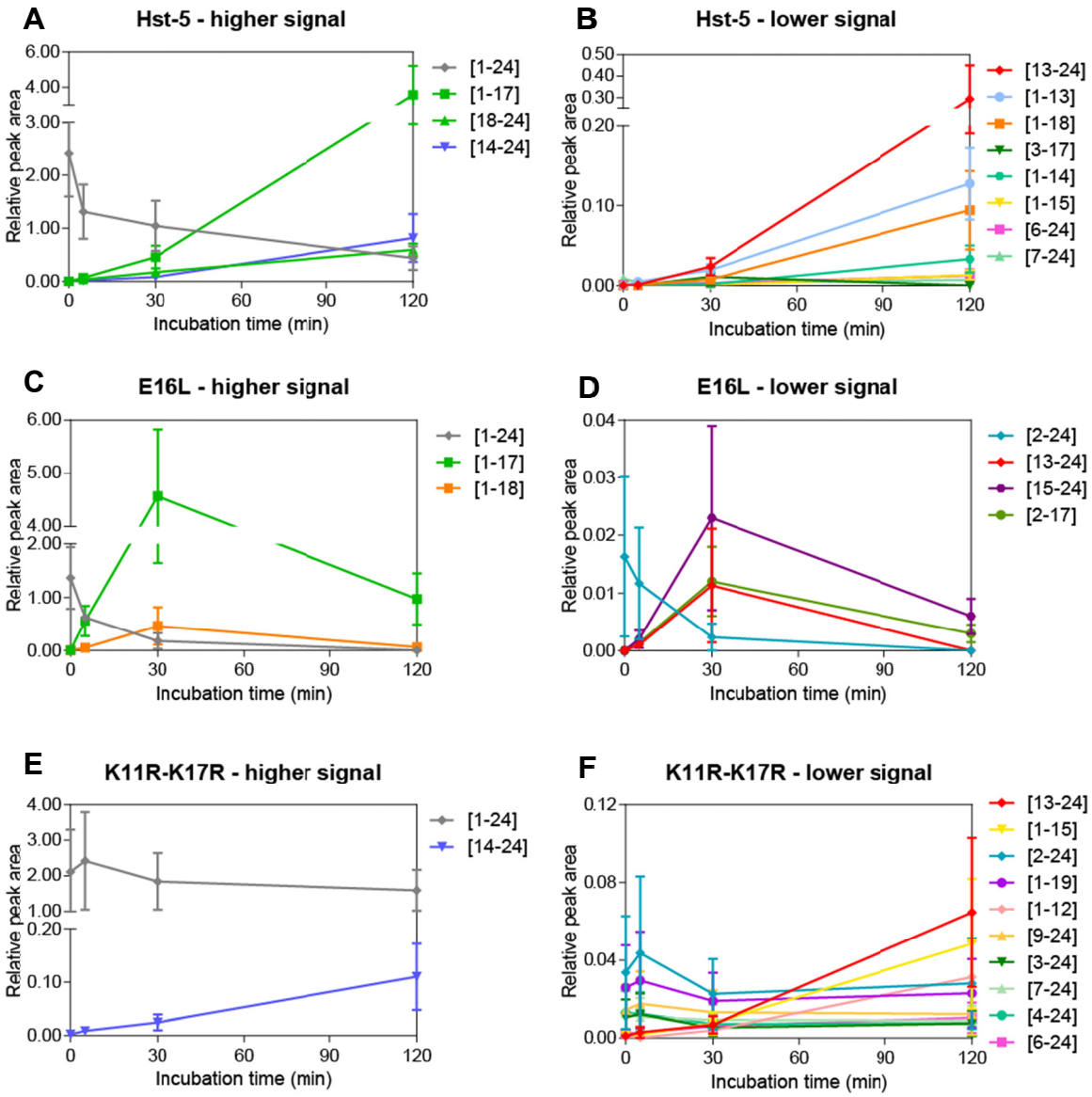

Figure 3.4. Kinetics of degradation of 50 µM (A & B) Hst-5, (C & D) E16L, and (E & F) K11R-K17 peptides incubated with 3 µg/mL Sap9. The peptides were incubated for 0 min, 5 min, 30 min, or 120 min. For the 0 min samples, heat-inactivated Sap9 was added. Average of the peak area obtained from chromatogram of the sample mass spectra, relative to internal standard, are shown. Fragments that did not reach a raw peak area signal of at least 1×10^6 during the time course were omitted from the figure. Below a raw peak area signal of 1×10^6, the relationship between the peak area to concentration is non-linear.

fragments in the Hst-5 sample. However, larger fragments, such as the amino acids 2 – 24 and 1 – 19 fragments, were rapidly degraded in the first 30 min and then approached a

nearly steady-state level. This suggests that these fragments are less preferred by Sap9 once other fragments are formed in the first 30 min. The time-course study shows that the modifications to the peptides not only affected the rate of degradation of the intact peptide, but also the fragments formed from the degradation.

3.3.5. Some amino acid substitutions lead to enhanced antifungal activity

Previous work demonstrated that substitution of a single lysine residue to arginine or leucine at the K5, K11, K13, or K17 sites in Hst-5 does not diminish the antifungal activity of the peptide, even if the modifications lead to an increase in proteolysis by Saps (Chapter 2). Therefore, all of the current Hst-5 variants were tested for their antifungal activity, even if the substitution led to an increase in the susceptibility to proteolysis. To determine the antifungal activity of Hst-5 and the modified peptides, the peptides were serially diluted and incubated with *C. albicans* cells at 2.5×10^7 cells/mL for 30 min at 30 °C in 1 mM NaPB. The mixtures were then diluted, inoculated into YPD media, and grown overnight to determine the reduction in cell viability due to exposure to the peptides.

As hypothesized during the peptide design, the K11R-K17R modification led to enhanced antifungal activity (Figure 3.5) with a minimum inhibitory concentration for 50% inhibition of growth (MIC_{50}) of 25 μM. This improvement is comparable to the enhanced activity of the K11R modified peptide previously observed (Figure 2.5). Therefore, the enhanced antifungal activity of the K11R modification is preserved in the double-mutated K11R-K17R peptide, while gaining proteolytic resistance from the K17R substitution.

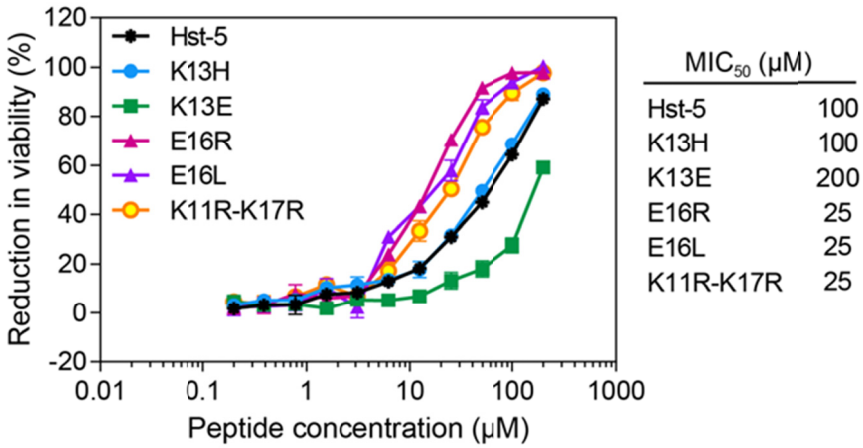

Figure 3.5. Antifungal activities of Hst-5 and the modified peptides. The peptides (50 μM) were serially diluted and incubated with 2.5×10^7 cells/mL *C. albicans* for 30 min at 30 °C in 1 mM NaPB. The error bars indicate the standard error of the mean (n = 6), though many are too small to be visible. MIC_{50} (minimum inhibitory concentration for 50% inhibition of growth) values for the peptides are listed.

Surprisingly, both of the modifications at the E16 site led to enhanced antifungal activity despite showing increased susceptibility to degradation by *C. albicans* (Figure 3.2). The proteolysis may not have affected the antifungal fragment of the peptides and the antifungal fragments of the E16 modified peptides are likely to include the 16th residue, as all of the fragments of E16R and E16L detected after incubation with Saps included the 16th residue (Figure 3.3). This result suggests that at the E16 site, a positively charged or non-charged residue is preferred over a negatively charged residue for the antifungal activity. Lower antifungal activity due to a negatively charged glutamic acid was also observed at the K13 site. While the K13H modification showed similar antifungal activity to the parent Hst-5, the K13E modification led to a significant reduction in the activity. Even at 200 μM peptide, the peptide was toxic to only about 50% of cells. Overall, removal of a negatively charged glutamic acid residue within the

active fragment of the peptide improves its antifungal activity, while addition of it reduces the activity.

3.3.6. Some modified peptides retain antifungal activity after exposure to Saps

After observing that the E16-modified peptides had enhanced antifungal activity despite their susceptibility to proteolysis by Saps, the antifungal activity of the proteolytic fragments was tested. The peptides were first incubated with Saps that were two or four times concentrated (6 μg/mL Sap9 or 0.2 μg/mL Sap2) than the concentration used for the gel electrophoresis assay to ensure more proteolytic fragments are formed and no intact E16 modified peptides remained (Figure 3.6). As expected from the antifungal

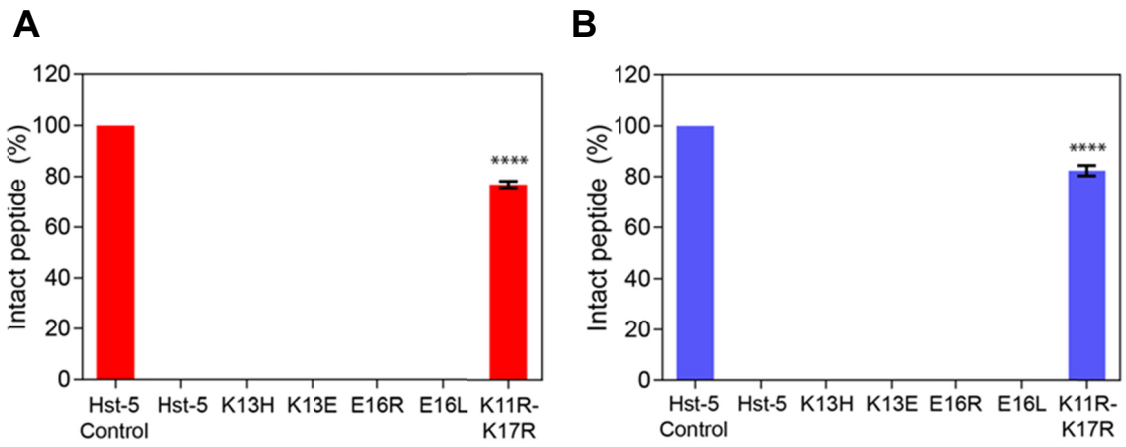

Figure 3.6. Extent of proteolysis of parent Hst-5 and Hst-5 variants by higher concentrations of purified (A) Sap9 and (B) Sap2. After the peptides (50 μM) and the Saps (6 μg/mL Sap9 and 0.2 μg/mL Sap2, respectively) were incubated for 2h at 37 °C, samples were run on a gel and stained with Coomassie. The amount of intact peptide remaining was quantified by comparing the intensity of the intact peptide (upper band) to the fragments (lower band) compared through densitometry. Error bars indicate standard error of the mean (n = 4). The level of statistical significance relative to parent Hst-5 is indicated by the number of asterisks: **** for $p < 0.0001$.

activity assay with the intact peptides, the K11R-K17R, E16R, and E16L peptides retained the most antifungal activity after exposure to either Sap (Figure 3.7), while the K13H and K13E modified peptides completely lost their activity. The Sap-treated K11R-

K17R peptide retained antifungal activity at a level similar to the untreated peptide, demonstrating its robustness. The gel electrophoresis analysis of the same samples showed that an ample amount of the intact K11R-K17R remained (76 % with Sap9 and 82% with Sap2) even after incubation with the higher Sap concentrations (Figure 3.6). Therefore, the antifungal activity is likely primarily from the intact peptide rather than degradation fragments.

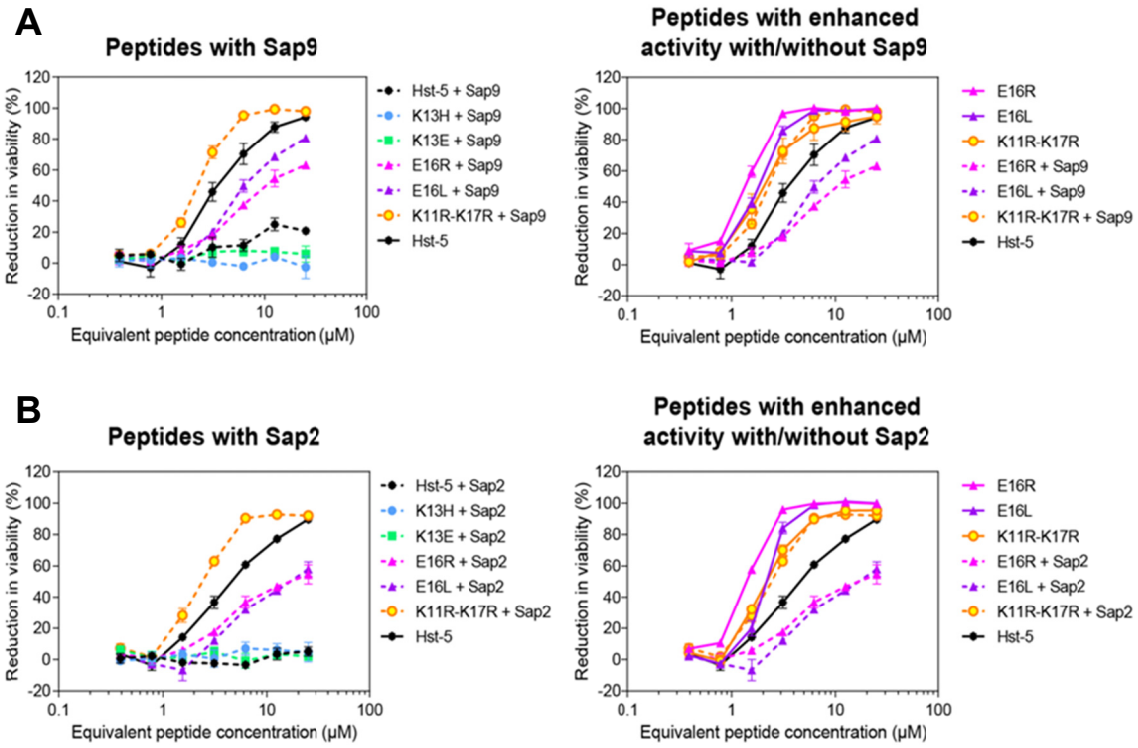

Figure 3.7. Antifungal activity of the peptides after incubation with or without (A) Sap9 or (B) Sap2. The peptides (50 μM) were incubated with Sap9 (6 μg/mL), Sap2 (0.2 μg/mL), or 1 mM NaPB buffer for 2 h at 37 °C. The peptides were then serially diluted and incubated with 2.5×10^5 cells/mL *C. albicans* for 30 min at 30 °C in 1 mM NaPB. The error bars indicate the standard error of the mean (n = 4).

Unlike the K11R-K17R peptide, the antifungal activity of the E16R and E16L peptides are from the proteolytic fragments. The E16-substituted peptides were completely degraded by the higher concentrations of the Saps (Figure 3.6) and yet still

retained a high amount of antifungal activity. Interestingly, for the peptides that were incubated with Sap9, the fragments of the E16L peptide have greater antifungal activity than the fragments of the E16R peptide at higher equivalent peptide concentrations (Figure 3.7A). This could indicate that the E16L sample had more active fragments remaining than the E16R sample after exposure to Sap9. The perseverance of the fragments is particularly noticeable in the Sap2 incubated samples. After incubation with Sap2, essentially all of the antifungal activity of Hst-5 has been eliminated, but the E16-modified peptides still retain a significant amount of activity. The antifungal activity assay further supports the notion that the substitution of glutamic acid with arginine and leucine enhances the antifungal activity of the degradation fragments of the modified peptides.

3.4. Discussion

This work explored effects of single amino acid substitutions and combination of previously studied lysine substitutions on Hst-5's susceptibility to proteolysis by Saps and *C. albicans* and the impact on the antifungal activity of the peptide. The role of the E16 and the K13 residues of the Hst-5 sequence were investigated by single amino acid substitutions at these sites. The gel electrophoresis and mass spectrometry analysis demonstrated that some of the modifications led to a Sap-dependent response while others showed similar responses to both Sap9 and Sap2 (Figure 3.1 and Figure 3.3). The arginine substitution at the E16 site displayed a Sap-dependent response, with the E16R modification leading to enhanced resistance to proteolysis by Sap2 but decreased resistance to proteolysis by Sap9. The increased degradation of E16R is in agreement

with the previously identified preference of Sap9 for arginine [17]. On the other hand, the leucine substitution at the same site indicated no Sap-dependent response, with the modified peptide being more degraded than Hst-5 by both of the Saps. Sap2's preference for leucine [22] could play a role in the modified peptide's susceptibility to Sap2. Similarly to the E16R peptide, the K13H and K13E modifications resulted in more proteolysis by Sap9 than Sap2. The increased degradation of K13E may be due to the presence of the negatively charged glutamic acid residue on the C-terminal side of the R12 residue. Schild et al. previously reported enrichment of cleavage in peptides with an acidic amino acid C-terminal to an arginine or lysine [18]. Overall, with the exception of the E16L, the tested modifications were more susceptible to degradation by Sap9, even though Hst-5 showed a similar level of degradation between the two Saps at the tested concentrations (Figure 3.1).

The single residue modifications had a profound impact on the antifungal activity of the intact peptides (Figure 3.5) and the degradation fragments (Figure 3.7). While substitution of K13 with a histidine had no impact on the antifungal activity, introduction of a glutamic acid at this site led to a decrease in antifungal activity. This corroborates the decrease in antifungal activity observed by Tsai et al. for the same modification [38]. The preservation of the antifungal activity by the K13H modification at a comparable level to Hst-5 further supports the importance of the positive charge at this site, as previously suggestion by Tsai et al. [38], and demonstrates that the positive charge is more important than the specific residue at the K13 site.

Both of the E16 site modifications led to an increase in the antifungal activity, despite an increase in proteolysis by *C. albicans* cells (Figure 3.2). This effect is different from

the previously tested substitution of glycine at the site, which led to significantly less antifungal activity [36]. Helmerhorst et al. also improved antifungal activity of modified Hst-5 fragments dhvar1 and dhvar2 by further substituting the glutamic acid with lysine [42]. The improved activity with arginine, leucine, and lysine substitutions but worsened activity with a glycine substitution suggests that identity of the residue at the site plays an important role for the antifungal activity. Residues with a positively charged or neutral side chain (larger than hydrogen) lead to better antifungal activity than residues with negatively charged side chains. It is also possible that by removing the negative charge, the antifungal activity of the N-terminal end of the peptide improved. The mass spectrometry analysis showed more N-terminal fragments for both E16R and E16L (Figure 3.3), which would contain the residues 4 – 15 fragment identified as the antifungal fragment [34] but not most of the residues in the amino acids 11 – 24 antifungal fragment [33]. Even after incubation with higher concentration of Saps than used for samples in mass spectrometry analysis, the modified peptides retained a significant amount of antifungal activity. Therefore, the proteolysis by Saps likely did not cleave the active fragments of the each modified peptides.

In addition to single amino acid substitutions, this study also investigated whether individual modifications that lead to more resistance to Saps (K17R) and enhanced antifungal activity (K11R) can be combined into one peptide that has both of the enhanced properties. Previous studies have combined amino acid modifications to study the effect on antifungal activity of Hst-5 or Hst-5 fragments [34, 38], but no other work has attempted to combine positive improvements in two different properties. This goal was successfully achieved with the K11R-K17R peptide. The double arginine-modified

peptide had significantly enhanced resistance to proteolysis by both Saps and *C. albicans* and showed no degradation around the R17 modified residue, as expected from the K17R modification. The antifungal activity of the intact peptide was at a level similar to that of the previously tested K11R peptide, demonstrating the positive effect on antifungal activity from that modification. Interestingly, the mass spectrometry analysis showed a shift in the cleavage sites of K11R-K17R compared to Hst-5, with more distinct cleavage sites in the N-terminal portion of the peptide, which was not previously observed in the individual modifications. The improvements observed with the K11R-K17R peptide show that it is possible to combine enhancements from individual modifications into one peptide.

The kinetic study with Sap9 on Hst-5, E16L, and K11R-K17R revealed that the residue substitutions do indeed affect the kinetics of proteolysis (Figure 3.4). While a kinetic degradation study on Hst-5 has been previously done with Saps [25] and with whole saliva [76], no previous study explored the effect of amino acid substitutions on the kinetics. The initial degradation of the Hst-5 and E16L peptides led to rapid accumulation of the amino acids 1 – 17 fragment, suggesting that the first cleavage of the peptides occurs C-terminal to the K17 site. Bochenska et al. observed a similar initial rapid accumulation of the same Hst-5 fragment during incubation with Sap9 [25]. However, after 30 min, they recorded a decrease of the fragment [25], whereas in this study it accumulated throughout the study period. It is important to note, however, that the enzyme:substrate ratio, buffer, and pH used are different between the studies and the differences are likely to affect the results. Meanwhile, the amino acids 1 – 17 fragment was not detected in degradation of the K11R-K17R peptide. Compared to the Hst-5 and

E16L peptides, the proteolysis of K11R-K17R was at a slower rate and slowed down further over course of the study. The slowed kinetics may contribute to the increased resistance of the peptide to proteolysis.

In addition to showing the degradation of the intact peptides, the kinetic study also revealed interesting trends for degradation of the peptide fragments. The continued accumulation of the fragments or the steady state level of the fragments seen in Hst-5 and K11R-K17R samples suggest that these degradation fragments are robust and less targeted by Sap9. On the other hand, the fragments of E16L showed a decrease in abundance after an initial increase. All of the detected fragments contain the E16L modified site, which suggests that the residue modifications made the proteolytic fragments that contain the modified site more susceptible to Sap9. Therefore, the residue substitutions modify not only the degradation kinetics of the intact peptide but also the degradation kinetics of the cleavage fragments.

3.5. Conclusion

The work in this chapter revealed that modifications to one or two amino acids of Hst-5 can significantly affect the kinetics of the proteolysis by Sap9. They can also impact the antifungal activity of both the intact peptide and its degradation fragments. Substitutions can increase the rate of degradation of the intact peptide, but simultaneously create fragments that are more robust with enhanced antifungal activity compared to the same fragments of the parent peptide, as demonstrated by the enhanced antifungal activity of the fragments of the E16L peptide. The K11R-K17R peptide also shows that characteristics observed from single amino-acid modifications can be combined together

into one peptide. Based on these findings, other modifications that lead to enhanced properties should be explored in combination to design a peptide that is even more robust and improve its potential as an alternative therapeutic to treat *C. albicans* infections.

Chapter 4: A simple and robust approach to immobilization of antibody fragments

(This chapter is published in Ikonomova, S. P., He, Z. & Karlsson, A. J. (2016) A simple and robust approach to immobilization of antibody fragments, *J Immunol Methods.* **435**, 7-16)

4.1. Introduction

With increasing prevalence of drug-resistant strains, early detection of *Candida* infections is strongly desirable to enable the identification of the causative species and the start of appropriate treatment. However, the current gold standard for identifying *Candida* infections is through culturing of samples from infected patients, which can take two to three days to obtain a result [7]. This calls for a more rapid approach to identify *Candida* infections.

One alternative approach is use of an antibody array to capture and identify different species of *Candida*. Rather than full-sized antibody, small antibody fragments are seeing increasing use due to their ease of production in *Escherichia coli*. The single-chain variable fragment (scFv) is one such fragment, and it contains only the variable light chain and variable heavy chain domains of an IgG antibody connected by a flexible peptide linker. scFvs are one of the smallest IgG fragments that retain an antigen-binding capability similar to the full-length antibody [45], and their small size allows for easy insertion of their encoding DNA sequences into plasmids and fast replication in *E. coli* [46].

To create an array using antibody fragments, the fragments must first be immobilized onto a surface with a method that will be versatile to multiple antibody fragments. Previous studies of immobilization of antibody fragments have typically focused on

optimizing the immobilization of only one or two antibody fragments at a time and use methods to detect the immobilization that are specific to the antibody fragment, diminishing the adaptability of the procedure to other antibodies [77]. The immobilization process also often first requires purification of the antibody fragments [78-81]. Purification of antibodies and other proteins can be time-consuming and costly, and the commonly used affinity purification methods may result in poor purities or yields. For example, affinity purification using a FLAG tag fusion gives high purity but the method is expensive and results in low yield of the desired protein; using a hexahistidine (6XHis) tag is far less expensive and gives a higher yield, but the product is plagued by low purity [82]. Elimination of the purification step would reduce cost and save time in immobilization protocols.

A robust and purification-free method for immobilizing antibody fragments was developed using the biotin-streptavidin interaction. It takes advantage of the ability of *E. coli* to attach biotin *in vivo* to a specific lysine residue of a native *E. coli* protein biotin carboxyl carrier protein (BCCP) [57] or a 15-amino acid minimal peptide substrate AviTag [61, 62]. Multiple scFvs from *E. coli* cell lysate were immobilized using the high-affinity biotin-streptavidin interaction and the capabilities of the BCCP and AviTag biotinylation sequences were evaluated under endogenous levels of biotin ligases and with overexpression of BirA. The results show that this approach leads to functional scFvs with a high level of stability under different storage conditions.

4.2. Materials and Methods

4.2.1. Plasmid construction

Table 4.1. Plasmids used to express scFvs and other proteins in this study.

scFv/protein	Source plasmid ref.	Binding target	Plasmid backbone	Construct
scFv13R4 [83]	Lab stock	β-Galactosidase	pSPI01B pSPI01A	scFv13R4-BCCP scFv13R4-AviTag
scFvD10 [84]	[84-87]	Bacteriophage lambda head protein D	pSPI01B pSPI01A	scFvD10-BCCP scFvD10-AviTag
scFv3 [88]	[88, 89]	*C. albicans*	pSPI02B pSPI02A	scFv3-BCCP scFv3-AviTag
scFv5 [89]	[89]	*C. albicans*, *C. dubliniensis*	pSPI02B pSPI02A	scFv5-BCCP scFv5-AviTag
scFv12 [89]	[89]	*C. albicans*	pSPI02B pSPI02A	scFv12-BCCP scFv12-AviTag
scFv26-10 [90]	Lab stock	Digoxin	pSPI02B pSPI02A	scFv26-10-BCCP scFv26-10-AviTag
gpD	[91, 92]	N/A	pET21a(+)	pET21-gpD-His
BirA	Dorothy Beckett	N/A	pSPI03	pSPI03-BirA-His

The plasmids containing the scFvs and a C-terminal BCCP or AviTag (Table 4.1) were constructed by modifying the pAK400cb-SVV [59] plasmid. The plasmid backbone pSPI01B was created by digesting pAK400cb-SVV with *Nde*I and *Eco*RI to remove the gene encoding for the SVV protein. The pSPI01A backbone is analogous to pSPI01B, except the gene encoding for the BCCP tag was replaced with a sequence encoding for the AviTag [62] by using a pair of complementary primers. A *Sal*I site was added to pSPI01B and pSPI01A to construct plasmids pSPI02B and pSPI02A, respectively, which allow for insertion of scFv genes containing an *Eco*RI site. The DNA encoding the scFvs in Table 1 was amplified by polymerase chain reaction (PCR) with a C-terminal FLAG tag, except for scFv3, scFv5, and scFv12, which were amplified with the N-terminal FLAG tag present in their source plasmids. The genes encoding scFv13R4 and scFvD10

were amplified from source plasmids and inserted into both pSPI01B and pSPI01A between the *Nde*I and *Eco*RI sites. The DNA encoding scFv3, scFv5, and scFv12 was inserted into pSPI02B and pSPI02A between the *Nde*I and *Sal*I sites. The scFv26-10 gene was inserted between *Nde*I and *Eco*RI of pSPI02B and pSPI02A.

Bacteriophage lambda head protein D (gpD), the binding target of scFvD-10, was expressed from the pET21a(+) plasmid (Novagen). The gpD gene was amplified from pAT222 [91, 92] and ligated between the *Nde*I and *Hin*dIII sites of pET21a(+), which contains a C-terminal 6XHis tag. The plasmid was transformed into BL21(DE3) cells for expression.

A plasmid containing BirA was used to increase the level of the enzyme present in cells producing biotinylated scFvs. The sequence encoding for the tac promoter, lac operator, and BirA enzyme with a C-terminal 6XHis tag was amplified from a plasmid gifted by Dorothy Beckett and inserted between the *Eco*RI and *Hin*dIII sites of the pMS421 plasmid to construct pSPI03-BirA-His. pSPI03-BirA-His was co-transformed into cells already containing the scFv plasmids in Table 1. The empty pMS421 plasmid was also co-transformed into cells expressing each scFv to serve as controls for the experiments with overexpressed BirA.

4.2.2. scFv expression and Western blot analysis

The scFv fusions to biotinylation sequences were produced in *E.coli* MC4100 cells, except in experiments involving co-expression of BirA. For experiments involving co-expression of BirA BL21 cells were used, because MC4100 cells have resistance to the streptomycin antibiotic required for maintenance of pMS421-based plasmids. Cultures were grown to mid-log phase at 37 °C with appropriate antibiotic(s) (20 μg/mL

chloramphenicol and 25 μg/mL streptomycin). Isopropyl β-D-1-thiogalactopyranoside (IPTG) to 100 μM and biotin to 5 μM were then added [59, 62], and protein expression was induced overnight at 20 °C. After expression, the cultures were harvested at 4 °C, and cell pellets were stored at -20 °C until use. To obtain cell lysates containing biotinylated scFvs, thawed cell pellets were lysed with BugBuster Master Mix (EMD Millipore) following the manufacturer's protocol. A 5 kDa molecular weight cut-off column (GE) was used to remove excess biotin and exchange the buffer to phosphate-buffered saline (PBS). The total protein concentration of the cell lysates was determined by measuring absorbance at 280 nm using a Nanodrop 2000 (Thermo Scientific), which assumes 1 absorbance unit = 1 mg total protein/mL.

For Western blot analysis, proteins in cell lysates were separated by SDS-PAGE on Any kD Mini-PROTEAN TGX gels (Bio-Rad) and detected using standard Western blotting protocols. The separated proteins were transferred onto polyvinyl difluoride (PVDF) membranes and stained with a horseradish peroxidase (HRP)-conjugated anti-FLAG antibody (Sigma) to compare expression level or with an HRP-conjugated anti-biotin antibody (Abcam) to detect biotinylation. Stained membranes were incubated with Clarity Western ECL substrate (Bio-Rad), and chemiluminescence was imaged on a ChemiDoc MP imaging system (Bio-Rad).

4.2.3. Streptavidin gel-retardation assay

To get an estimate of biotinylation efficiency, a method was adapted from Predonzani et al. [93]. Boiled samples of scFv13R4 and scFvD10 lysates mixed with SDS-PAGE loading buffer were incubated with or without streptavidin (NEB) for 1 hour at 4 °C. Samples were separated by SDS-PAGE on 10% Mini-PROTEAN TGX gels (Bio-Rad).

The proteins were transferred to a PVDF membrane and detected with an HRP-conjugated anti-FLAG antibody. Biotinylated scFvs bind to streptavidin and travel more slowly [93], appearing at a higher molecular weight than the scFvs alone. Densitometry analysis was done on the blots to estimate the biotinylation efficiency based on the decrease in the band volume at the unbound scFv molecular weight due to binding to streptavidin. Biotinylation experiments were performed in triplicate for three biological replicates.

4.2.4. gpD expression and preparation

The gpD protein was expressed in *E. coli* BL21(DE3) cells. Cultures were grown to mid-log phase at 37 °C with 100 μg/mL ampicillin. IPTG was then added at 100 μM, and protein expression was induced overnight at 20 °C. Cells were harvested and lysed using protocols analogous to those for harvesting scFvs (Section 2.2). Desalting columns (Thermo Fisher Scientific) were used to exchange the buffer to PBS. Lysates were then filtered through 100 kDa molecular weight cut-off columns (GE) to clear the lysate of large components and concentrated with 3 kDa molecular weight cut-off columns (GE).

4.2.5. Purification of scFvs

For evaluating immobilization of purified scFvs, the BCCP and AviTag constructs of scFv13R4 and scFvD10 were purified using the FLAG Immunoprecipitation Kit (Sigma) following the manufacturer's protocol. The concentration of each purified product was calculated by measuring absorbance at 280 nm, assuming all protein within the sample was the purified scFv construct. Extinction coefficients for the constructs were calculated using the ProtParam tool on the ExPASy website [94] and are as follows: 46090 M^{-1} cm^{-1}

for scFv13R4-BCCP, 50100 M^{-1} cm^{-1} for scFv13R4-AviTag, 47580 M^{-1} cm^{-1} for scFvD10-BCCP, and 51590 M^{-1} cm^{-1} for scFvD10-AviTag. The purity of the samples was confirmed by running SDS-PAGE on the samples and staining the proteins with Bio-Safe Coomassie stain (Bio-Rad).

4.2.6. Enzyme-linked immunosorbent assay

The immobilization and the antigen-binding capabilities of the scFvs were assessed using an enzyme-linked immunosorbent assay (ELISA) done in triplicate. The scFvs were immobilized onto 96-well high-binding polystyrene plates (Corning) coated with streptavidin. Streptavidin-coated plates were prepared based on the method described by Winkler et al. [60] In each well of 96-well plates, 50 µL of 0.1 µg/µL streptavidin (NEB) was loaded, and the water was evaporated overnight in a 37 °C incubator. The dried plates were covered and stored at 4 °C until use, typically within one week. Plates were washed with PBS containing 0.1% Tween 20 (PBST) immediately prior to use in assays.

For immobilization assays, cell lysates or purified scFvs were serially diluted two-fold with PBST containing 0.5% milk. The diluted scFvs (50 µL/well) were loaded onto washed streptavidin-coated plates, and the plates were incubated for 45 minutes at room temperature. The immobilized scFvs were then incubated with an HRP-conjugated anti-FLAG antibody for 1 hour at room temperature. After each incubation step, the plates were washed with PBST four times to remove any unbound components. Plates were then incubated in the dark for 30 minutes with *o*-phenylenediamine dihydrochloride HRP substrate (Sigma), and the enzyme-substrate reaction was quenched with 3 M H_2SO_4. The absorbance in each well was measured at 492 nm on a plate reader (Epoch, Bio-Tek).

The ability of the immobilized scFv13R4-BCCP, scFv13R4-AviTag, and scFvD10-BCCP to bind to their targets (β-galactosidase for scFv13R4 and gpD for scFvD10) was evaluated using a procedure similar to the process for detecting immobilization. Constant concentrations of lysate (1 μg/μL of total protein) and purified scFvs (0.0125 μg/μL) were incubated on streptavidin-coated plates to obtain a surface saturated with scFv. After incubating for 45 minutes and washing with PBST, serial dilutions (0 – 50 μg/mL) of commercial β-galactosidase (Sigma) and serial dilutions (0 – 8 μg/μL total protein) of lysate containing 6XHis-tagged gpD in PBST with 0.5% milk were loaded in the wells (50 μL/well) with scFv13R4 and scFvD10 constructs, respectively. The plates were incubated for 1 hour. The bound β-galactosidase was detected with an HRP-conjugated anti-β-galactosidase antibody (Abcam), and the bound gpD was detected with an HRP-conjugated rabbit anti-6XHis antibody (Abcam) using protocols analogous to those for detecting immobilization of the scFv constructs. scFvD10-AviTag was not tested, because we found that the anti-6XHis antibody used to detect bound gpD cross-reacts with the AviTag constructs of scFvD10, scFv13R4, and scFv26-10.

4.2.7. Stability assay

To determine the length of time that immobilized scFvs can be stored while maintaining functionality, 0.1 μg/μL of scFv13R4-BCCP and scFv13R4-AviTag cell lysates and 1 μg/μL of scFvD10-BCCP cell lysates were incubated in each well as described in Section 2.6 and washed with PBST. PBST containing 0.5% milk or 50% glycerol in water was then added to the wells. Plates were covered with a lid, wrapped in Parafilm, and stored at 4 °C or -20 °C. Over a 100-day period, plates were removed from storage periodically, and the scFvs were tested for binding to β-galactosidase or gpD.

4.3. Results

4.3.1. scFvs are expressed and biotinylated in vivo by *E. coli* cells

In this work, we aimed to find a simple immobilization method that would be widely applicable to multiple scFvs without requiring purification. Immobilization via the high-affinity biotin-streptavidin interaction fit our criteria (Figure 4.1). To study the versatility of the immobilization method, six different scFvs were inserted into plasmid constructs with either a BCCP biotinylation fusion tag or the smaller AviTag biotinylation fusion tag. We tested the AviTag to determine whether its smaller size (15 amino acids vs. 87 amino acids of BCCP) may lead to less steric hindrance and allow better immobilization and scFv function. For both biotinylation tags, biotin was covalently attached *in vivo* to a lysine residue within the tags during expression of the scFv fusions in *E. coli* [61].

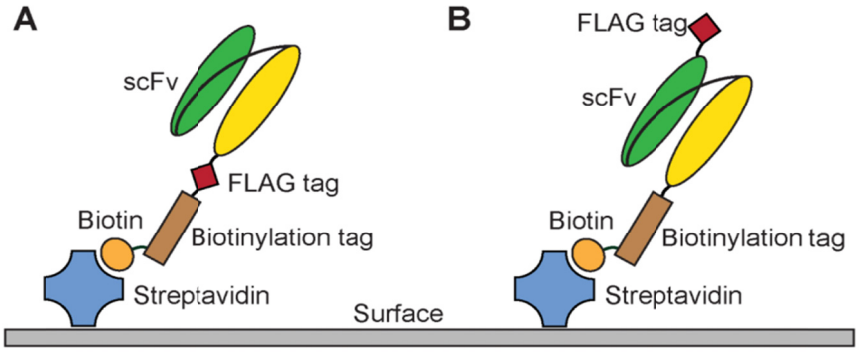

Figure 4.1. Immobilization scheme. scFvs with either (A) C-terminal or (B) N-terminal FLAG tags were produced in *E. coli* cells as fusions to a C-terminal biotinylation tag. The biotinylation tag was biotinylated *in vivo*, and the scFv constructs were immobilized from a cell lysate through binding of biotin to streptavidin coated on a surface.

Although previous work has shown that overexpression of the biotin holoenzyme synthetase BirA increases the biotinylation efficiency of the AviTag [61] and BCCP [58], we initially chose to keep our system as simple as possible and did not overexpress BirA

during expression and biotinylation of our scFv fusions.

We tested the immobilization of six scFvs: scFv13R4, scFvD10, scFv26-10, scFv3, scFv5, and scFv12. These scFvs were selected because they have different scFv frameworks and different antigens, allowing an analysis of the applicability of our immobilization method to a variety of scFvs. The expression and the biotinylation of the scFv constructs were confirmed by Western blotting of scFv cell lysates with an anti-FLAG antibody and an anti-biotin antibody, respectively (Figure 4.2). For scFv13R4,

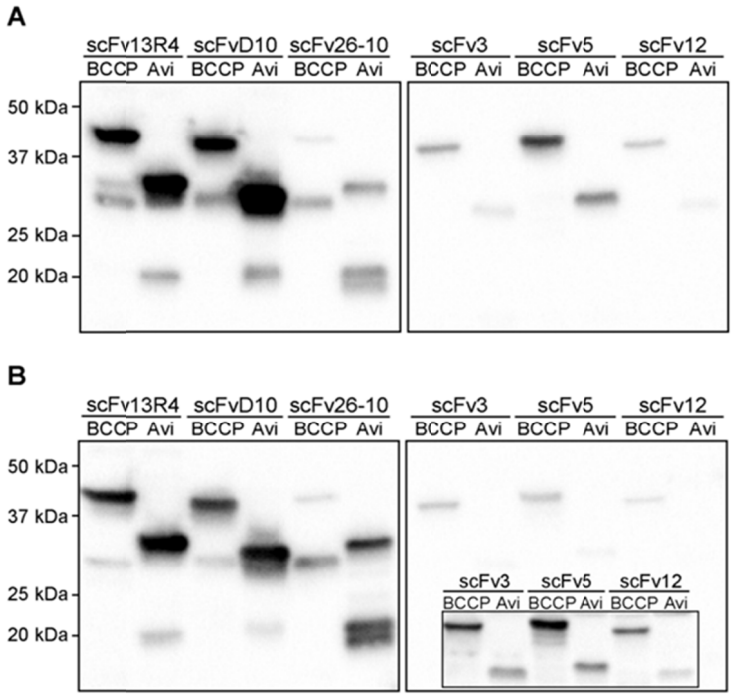

Figure 4.2. Expression and biotinylation of scFv constructs. Expression of scFv constructs containing BCCP or the AviTag (Avi) was induced overnight in *E. coli* MC4100 cells in the presence of 5 μM biotin, and Western blot analysis was performed on the soluble cell lysate. (A) The FLAG tag on the scFv constructs was detected with an anti-FLAG antibody to evaluate total scFv expression. (B) Biotinylated protein was detected using an anti-biotin antibody. Samples were normalized by total protein concentration. The inset in (B) shows results with twice as much protein loaded to more clearly demonstrate the presence of biotinylated scFvs.

scFvD10, and scFv26-10, the overall expression level in the soluble fraction of the cell lysate was higher for the AviTag constructs than for the BCCP constructs. For scFv3,

scFv5, and scFv12, however, the BCCP constructs were more highly expressed and higher levels of the biotinylated BCCP constructs were present than for the AviTag constructs. The relatively low expression of these scFvs compared to scFv13R4 and scFvD10 was expected, since scFv13R4 and scFvD10 have been engineered for high levels of cytoplasmic solubility [83, 84], whereas scFv3, scFv5, and scFv12 have not been engineered for solubility [88, 89]. The lower molecular weight bands seen in both blots appear to be degradation products containing the biotinylation fusion tags and the FLAG tag. Although the degradation products were present, in all but one case (scFv26-10) the scFvs were the most abundant biotinylated protein in the sample. The successful expression and biotinylation of various scFvs shows the potential for wide applicability of *in vivo* biotinylation of scFvs for protocols that take advantage of the biotin-streptavidin interaction.

4.3.2. scFvs are immobilized directly from cell lysate

After establishing that the scFvs were expressed and biotinylated *in vivo*, we evaluated their immobilization onto streptavidin-coated 96-well plates. The immobilization of the scFvs on the plates was quantified through an ELISA to detect the FLAG tag at the C-terminal (scFv13R4, scFvD10, scFv26-10) or N-terminal (scFv3, scFv5, scFv12) end of the scFv (Figure 4.1). As the data in Figure 4.3 show, all scFvs were successfully immobilized, though the level of immobilization varied. scFv constructs with BCCP exhibited a higher level of immobilization than scFv constructs with the AviTag at lower total protein concentrations. The one exception to this was scFv26-10, which showed greater immobilization with the AviTag, but this could be due to the higher level of biotinylated scFv26-10-AviTag protein than biotinylated

scFv26-10-BCCP protein present in the lysate (Figure 4.2B). Alternatively, the higher signal for scFv26-10-AviTag may be due to the degradation products, which are biotinylated and contain the FLAG tag, increasing the signal for immobilized protein. The level of immobilization of scFv13R4, scFvD10, and scFv26-10 was higher than the level of immobilization of scFv3, scFv5, and scFv12. The low expression of scFv3, scFv5, and scFv12 (Figure 4.2A) and lesser amount of biotinylated protein present in the cell lysate was likely the main reason for this difference. Because the biotin-streptavidin interaction is very specific, only biotinylated protein is immobilized onto the streptavidin-coated surface; the biotinylated products are being purified from the cell lysate during immobilization, eliminating the need for purification prior to immobilization. Although biotinylated degradation products will also be immobilized, the abundance of the undesired products for most constructs (the scFv26-10 constructs being the exceptions) was low compared to the desired full-length protein.

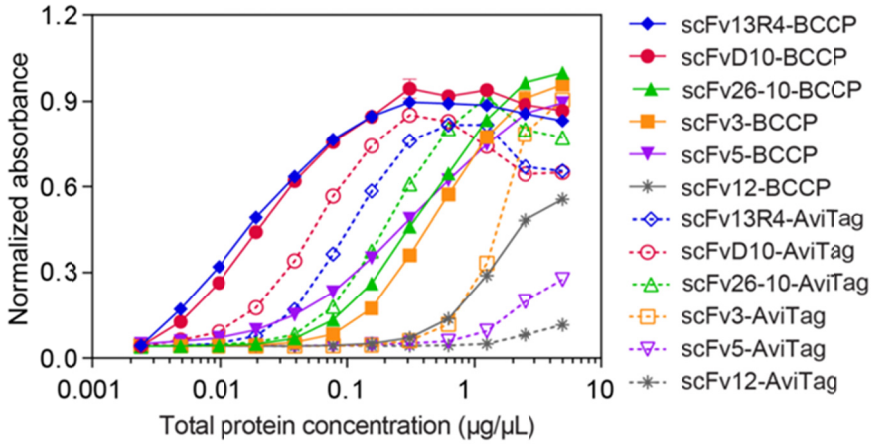

Figure 4.3. Immobilization of scFv constructs from cell lysate. *E. coli* cell lysates were serially diluted, and biotinylated scFvs from the cell lysates were immobilized onto streptavidin-coated 96-well plates. Immobilized scFvs were detected with an anti-FLAG antibody. Data are normalized to the highest absorbance reading. Error bars, most of which are smaller than the svmbol size. indicate the standard error of the mean.

4.3.3. Immobilization of purified scFvs confirms differences in biotinylation tags

To investigate the difference in immobilization observed for the BCCP and AviTag constructs, we purified both biotinylation tag constructs of scFv13R4 and scFvD10. The proteins were purified using FLAG tag affinity purification, and Coomassie staining of the purified products on an SDS-PAGE gel showed that scFvs were the most abundant products in the purified protein samples (Figure 4.4). The purified proteins also contained a small amount of impurities, likely the FLAG-tagged and biotinylated degradation products visible in the Western blot results in Figure 4.2. However, the quantity of the impurities was considerably lower than the quantity of the desired scFv products and unlikely to significantly affect the immobilization results.

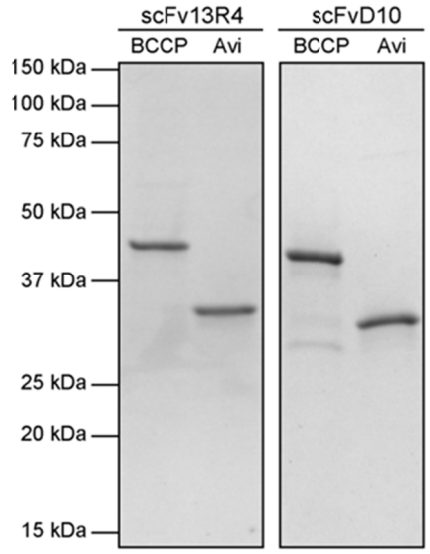

Figure 4.4. Purification of scFv constructs. Biotinylated scFv constructs containing BCCP or the AviTag were purified from *E. coli* cell lysate using FLAG immunoprecipitation. The purified scFv samples were normalized by total protein concentration, run on an SDS-PAGE gel, and visualized with Coomassie stain.

The purified biotinylated proteins were immobilized on streptavidin-coated plates (Figure 4.5). For a given concentration of the purified proteins, the BCCP constructs

immobilized at a higher level than the AviTag constructs, until a maximum level of immobilization was approached (Figure 4.5), which is similar to the data for immobilization from cell lysates (Figure 4.3). The maximum level of immobilization that is approached by the scFv constructs indicates the point at which all of the available binding sites of streptavidin are saturated. These results suggests that the difference in immobilization of the constructs is related to the differences in the biotinylation tags or biotinylation level and that the disparity between the immobilization levels of AviTag and BCCP constructs in Figure 4.3 is not simply a result of the unequal expression levels of the constructs. The results for immobilization of the purified constructs also show that the BCCP constructs of scFv13R4 and scFvD10 immobilize at similar levels, confirming the results observed in the immobilization from cell lysates (Figure 4.3).

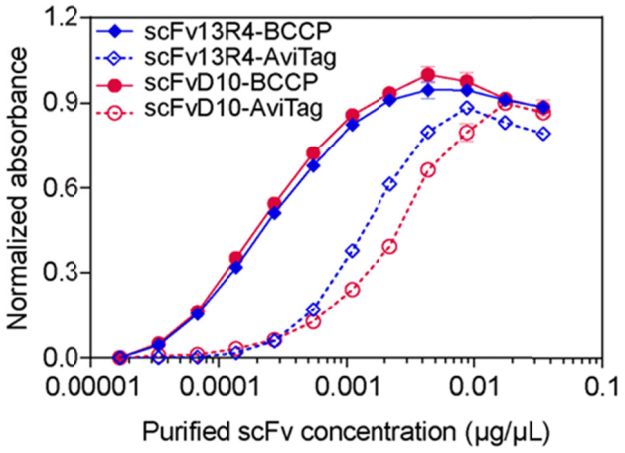

Figure 4.5. Immobilization of purified scFv constructs. Purified biotinylated scFv constructs were serially diluted and immobilized onto streptavidin-coated 96-well plates. Immobilized scFvs were detected with an anti-FLAG antibody. Data are normalized to the highest absorbance reading. Error bars indicate the standard error of the mean.

4.3.4. BirA enhances the biotinylation of AviTag constructs

Once we confirmed that difference in biotinylation tag plays a role in the

immobilization, we tested whether the biotinylation efficiency explains the difference. The scFvs were co-expressed with the BirA biotin ligase to increase the level of biotinylation. Biotinylation efficiency was estimated using a streptavidin gel-retardation assay. Cell lysates containing BCCP and AviTag constructs of scFv13R4 and scFvD10 were boiled, incubated with or without streptavidin at 4 °C for 1 hour, and then detected by Western blot with an anti-FLAG antibody. Biotinylated scFvs bind to the streptavidin and travel slower on SDS-PAGE gels, appearing at a higher molecular weight (Figure 4.6). The level of biotinylation was determined by analyzing the difference in the intensity of the bands for the unbound scFvs with and without exposure to streptavidin. The results show that BCCP constructs were highly biotinylated even in the absence of

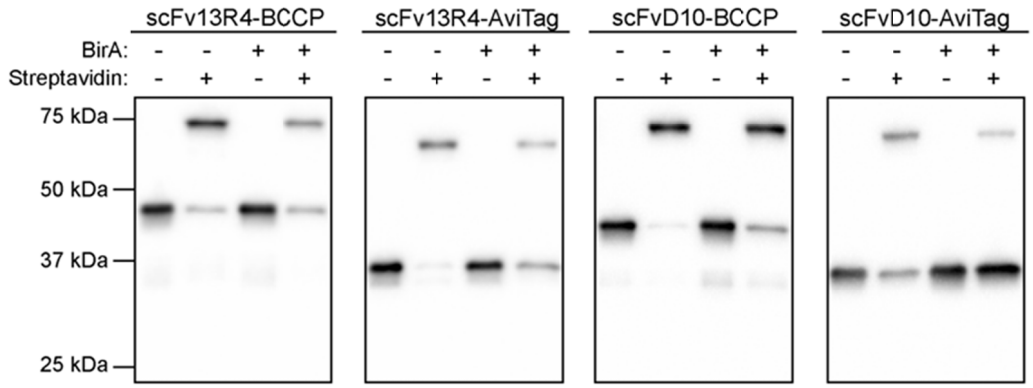

% Biotinylation

	scFv13R4-BCCP	scFv13R4-AviTag	scFvD10-BCCP	scFvD10-AviTag
With BirA:	90.2 ± 1.01	95.6 ± 0.91	102 ± 1.18	52.0 ± 4.28
Without BirA:	88.4 ± 1.78	49.2 ± 7.67	88.3 ± 3.37	2.79 ± 4.47

Figure 4.6. Biotinylation efficiency of scFv constructs with and without overexpressed BirA. Cell lysates of BCCP and AviTag constructs of scFv13R4 and scFvD10 were incubated with or without streptavidin and then separated and detected by Western blot with an anti-FLAG antibody. The scFvs were co-expressed with BirA or a control empty plasmid. The biotinylation efficiency was determined based on a decrease in intensity of the scFv band after incubation with streptavidin. A representative Western blot is shown, and biotinylation efficiency values represent the average and standard error of multiple replicates.

overexpressed BirA. AviTag constructs, on the other hand, showed a significant increase in biotinylation level with co-expressed BirA, more than doubling the biotinylation efficiency in the case of scFvD10. The increase in AviTag biotinylation in the presence of overexpressed BirA is expected, since AviTag was engineered to be used with plasmid-expressed BirA [61].

As the presence of BirA enzyme affected the biotinylation level of AviTag constructs, we examined whether the increased level also affected the immobilization of the scFvs. In most cases, the increase in biotinylation also increases the immobilization of BCCP and AviTag fusions of scFv13R4 and scFvD10 (Figure 4.7). The improvement in

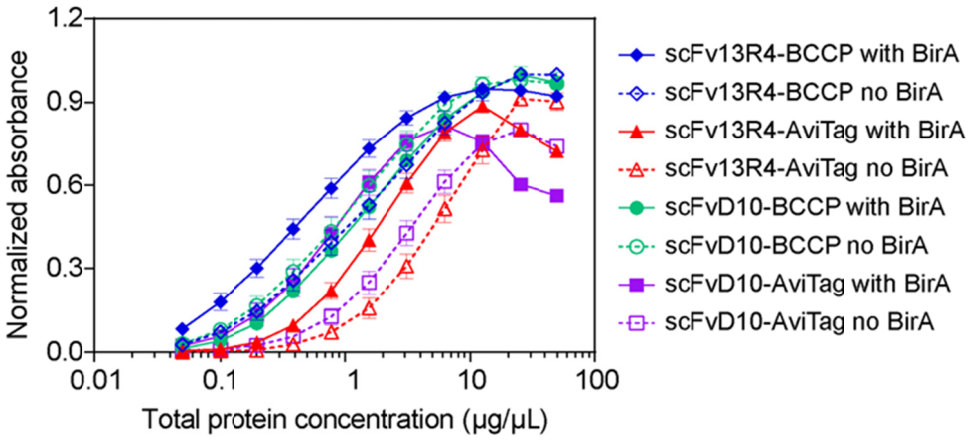

Figure 4.7. Immobilization of scFv constructs with or without co-expressed BirA. *E. coli* cell lysates containing scFvs produced with or without overexpression of BirA were serially diluted, and biotinylated scFvs from the cell lysates were immobilized onto streptavidin-coated 96-well plates. Immobilized scFvs were detected with an anti-FLAG antibody. Data are normalized to the highest absorbance reading. Error bars indicate the standard error of the mean.

immobilization is more evident in AviTag constructs, particularly scFvD10, which shows an immobilization level similar to its equivalent BCCP fusion. For BCCP constructs, the enhanced biotinylation improves scFv13R4 immobilization but has minimal effect on scFvD10. Furthermore, the immobilization of scFv13R4 still shows a significant

difference between BCCP and AviTag tags, despite almost complete biotinylation with BirA. This suggests that the variation in immobilization level between constructs with different biotinylation tags is not fully explained by differences in biotinylation of the tags, and difference in the biotinylation tags may still play a role.

4.3.5. Immobilized scFvs maintain the ability to bind antigen

Unlike non-oriented immobilization where the antigen-binding site may be disrupted by the immobilization process [48], we predicted that the oriented immobilization with biotin-streptavidin via site-specific biotinylation would not diminish the ability of an scFv to bind to its target. To ensure that immobilized scFvs retain functionality, we tested the ability of immobilized scFv13R4 (with the BCCP and AviTag biotinylation fusions) to bind to its antigen β-galactosidase, which is commercially available, and the ability of immobilized scFvD10 (with BCCP biotinylation tag) to bind gpD protein, which we produced recombinantly. scFvD10-AviTag was not included in this experiment, because the anti-6XHis antibody we used to detect gpD cross reacts with the AviTag in this construct. Using data from Figure 4.3 and Figure 4.5, scFv constructs in cell lysate and purified scFv constructs were immobilized at a concentration leading to saturation of the surface with scFvs (0.0125 μg purified protein/μL for purified constructs and 1 μg total protein/μL for cell lysates). We observed an increase in binding to the antigens with an increasing amount of antigen (Figure 4.8), which shows that the scFvs maintained their ability to bind to their target. For scFv13R4, both the BCCP and AviTag constructs showed similar levels of signal at all β-galactosidase concentrations, indicating that the tag does not affect the binding of the scFv to its target. A comparable level of binding to

gpD is also observed between purified and unpurified scFvD10-BCCP. These results support use of our simplified protocol that eliminates the purification step.

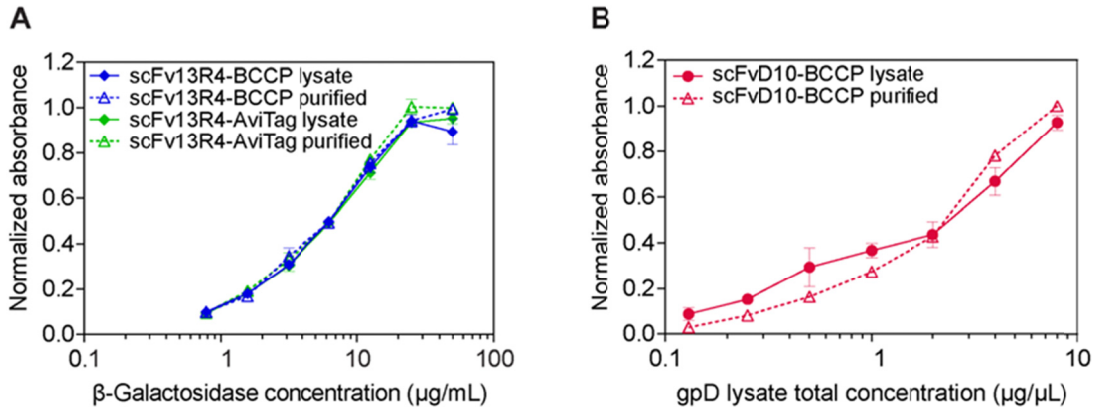

Figure 4.8. Antigen-binding of immobilized scFv constructs. Biotinylated scFv13R4-BCCP, scFv13R4-AviTag, and scFvD10-BCCP were immobilized onto streptavidin-coated plates from cell lysate and from purified samples using concentrations leading to surface saturation. Serial dilutions of β-galactosidase (the target antigen for scFv13R4) and gpD (the target antigen for scFvD10) were incubated with the immobilized scFvs, and the bound β-galactosidase and gpD were detected with an anti-β-galactosidase antibody and an anti-6XHis antibody, respectively. Negative control experiments were also performed to show β-galactosidase and gpD did not bind to other components in the system or to an irrelevant scFv. Data are normalized to the highest absorbance reading. Error bars indicate the standard error of the mean.

4.3.6. Immobilized scFvs are stable for at least 100 days

Once we confirmed that immobilized scFvs maintain their ability to bind their targets, we assessed how long the scFvs retain their functionality after immobilization. Long-term stability of immobilized scFvs would enable bulk preparation of immobilized scFvs for use in future assays or for use in devices requiring storage. We immobilized scFv13R4-BCCP, scFv13R4-AviTag, and scFvD10-BCCP from cell lysate and added PBST containing 0.5% milk or 50% glycerol in water to the wells. Separate plates were stored at 4 °C and -20 °C, and binding of the immobilized scFv constructs to β-galactosidase or gpD was measured (Figure 4.9, Figure C.1). After 100 days, immobilized scFv13R4-

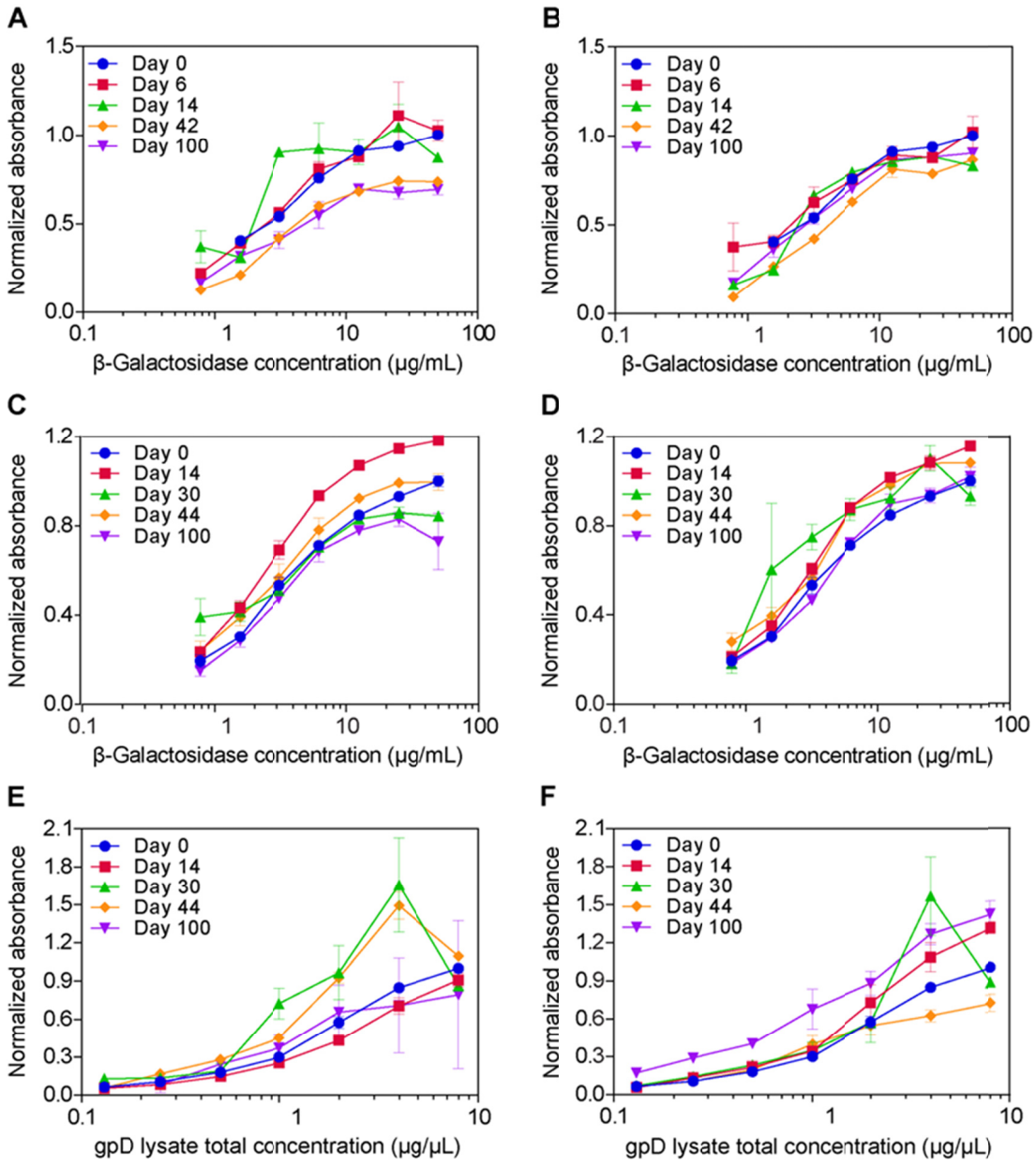

Figure 4.9. Antigen-binding of immobilized scFv constructs after storage. Biotinylated scFv13R4-BCCP (A & B), scFv13R4-AviTag (C & D), and scFvD10-BCCP (E & F) were immobilized onto streptavidin-coated plates from cell lysates and stored in 50% glycerol at 4 °C (A, C, E) and -20 °C (B, D, F). Serial dilutions of β-galactosidase or gpD were incubated with the scFvs, and the bound antigens were detected with an anti-β-galactosidase antibody and anti-6XHis antibody, respectively. Absorbance readings were normalized to the highest signal on Day 0. Normalized absorbance for a given scFv construct at different temperatures and storage solutions can be compared, but the levels at different time points cannot be strictly compared (see Section 4.3.6). Error bars indicate the standard error of the mean.

BCCP, scFv13R4-AviTag, and scFvD10-BCCP stored at both temperatures and in both storage buffers were still able to bind their respective targets. Based on the strong absorbance signal at 100 days, we expect that the immobilized scFvs would maintain their functionality beyond this time point. It must be noted that although the absorbance levels at different temperatures and different storage solutions at each time point can be compared, the levels at different time points cannot be strictly compared due to inconsistencies in the HRP substrate between time points. However, the antigen-dependent binding signal clearly shows that the immobilized scFvs maintain antigen-binding after prolonged storage.

4.4. Discussion

We studied the versatility of using the biotin-streptavidin interaction to immobilize multiple scFvs onto a surface directly from *E. coli* cell lysates. No purification of the scFvs is needed in this process, because the immobilization step acts as a purification step. Only biotinylated proteins bind to the streptavidin-coated surface, while other proteins in the cell lysate are washed off. Our approach to scFv immobilization is further simplified by using *in vivo* biotinylation in our protein production host, *E. coli*. We fused biotinylation tags to the scFvs and took advantage of the native biotinylation machinery of *E. coli*, eliminating the need for additional steps and reagents involved with *in vitro* biotinylation methods [62]. The *in vivo* biotinylation of BCCP and the AviTag allows immobilization that is also site-specific, in contrast to the random immobilization site that is typical for immobilization via *in vitro* biotinylation. Our results extend prior work [77, 80] by showing that immobilization of multiple scFvs with varied framework sequences

and target antigens can be achieved using a single, straightforward protocol and by evaluating the suitability of different biotinylation sequences for scFv immobilization.

We tested two different biotinylation sequences, BCCP and the AviTag, to determine whether one allows for better expression and immobilization of the scFvs when used with endogenous levels of biotin ligases. We initially predicted the AviTag to lead to better immobilization, because we expected its smaller size would cause less steric hindrance. We did see better expression for the AviTag constructs of scFv13R4, scFvD10, and scFv26-10 (Figure 4.2), consistent with our expectation. However, scFvs constructs from both cell lysates and purified samples showed more immobilization with BCCP when the same concentration (below surface saturation) was used for immobilization (Figure 4.3 and Figure 4.5).

The possible role of biotinylation efficiency of the tags was explored by overexpressing the biotin ligase BirA. While enhanced biotinylation did improve immobilization of scFvD10-AviTag to the level of its BCCP analog, scFv13R4 still showed a difference in immobilization level between the biotinylation tags (Figure 4.7), indicating that biotinylation efficiency is only partially responsible for differences in immobilization. The difference in the size of the biotinylation tags may also contribute to the difference. Although the smaller AviTag allows some constructs to be expressed better, the biotin attached to the AviTag may not be as accessible for streptavidin binding in some scFv constructs as the biotin attached to the BCCP constructs. The larger BCCP protein may function as a linker between the biotin and the scFv to improve the accessibility of the biotin to the streptavidin on the surface. Previous studies on linkers between antibody domains and between proteins and affinity tags have shown that the

length of a linker can affect the binding affinity of a protein. For example, longer linker between two scFv variable chains increased affinity [95] and addition of glycyl linker between target and FLAG tag improved immunoprecipitation efficiency [96] . These examples support the possibility that the larger BCCP tag could improve the interaction of biotin with streptavidin in our results. The difference in the tag does not appear to affect the functionality of the scFvs, however, as both constructs of purified scFv13R4 showed similar binding to β-galactosidase when the surface was saturated with scFv (Figure 4.8).

Our results show that, while BirA overexpression is advantageous in improving the biotinylation level of AviTag constructs, BirA overexpression for BCCP constructs unnecessarily complicates the system without providing a significant advantage in immobilization. Using BCCP as the biotinylation tag without overexpressing BirA allows the system to be simpler, by reducing the number of plasmids required and eliminating the need for a second antibiotic.

4.5. Conclusion

Our method for immobilizing scFvs is a simple, robust, and versatile method based on the high-affinity biotin-streptavidin interaction. Few reagents are required beyond typical bacterial culture reagents, and no specialized techniques are required for immobilizing the scFvs or detecting immobilization. Elimination of purification steps reduces the time and cost of sample preparation for immobilization without compromising antigen-binding. The method is adaptable to a variety of scFvs, as we successfully immobilized six different scFvs, and the immobilization is stable, with

immobilized scFvs still binding to targets for at least 100 days after immobilization. The simplicity and ease of our approach make it appealing for many applications involving immobilization of scFvs, such as screening interactions of scFvs with various targets or screening for off-target interactions. For example, it could be used to immobilize scFvs for surface plasmon resonance assays without undertaking a separate purification step, since the scFvs would be purified during binding of the biotinylated scFvs to a streptavidin-coated surface. The versatility of the method will also make it a widely applicable tool for future research and development involving antibody fragment immobilization, such as in microfluidic device development, pathogen or toxin detection, and medical diagnostics.

Chapter 5: Effect of linkers on immobilization of scFvs with biotin-streptavidin interaction

5.1. Introduction

Fusion of proteins can lead to enhancement in functionality, solubility, and binding affinity [95, 97, 98]. A common method to create a fusion protein is with peptide linkers. Furthermore, the linker length has been shown to affect the activity and expression of the fused proteins [99-101]. The three main types of commonly used peptide linkers are flexible, rigid, and cleavable linkers. Flexible linkers such as $(G_4S)_n$, where *n* denotes the number of repeats of the sequence, are typically used to connect the V_H and V_L domains of single-chain variable fragments (scFvs). The flexibility allows the linker to be applied as a method to separate domains [97] or improve their interaction [102]. While the distance between two fusion partners may fluctuate with the flexible linkers, more fixed distance can be maintained with rigid linkers such as the α-helix forming $(EA_3K)_n$ linker [103]. Finally, unlike the flexible and rigid linkers that are generally designed to have proteolytic stability, cleavable linkers instead take advantage of *in vivo* processes, such as reduction of disulfide bonds, to release functional domains [102]. The type of linker that is used depends on the desired role of the linker in the fusion protein design.

Another possible application of a linker is to improve binding of an immobilized protein to its target by expanding the distance between the binding site and the point of immobilization. Previous work in Chapter 4 developed a simple, purification-free scFv immobilization method that uses the biotin-streptavidin interaction and biotinylation

tags—the biotin carboxyl carrier protein (BCCP) or AviTag—that are directly fused to scFvs for *in vivo* biotinylation [75]. In most of the cases, the BCCP fusion of the tested scFvs immobilized better than the corresponding AviTag fusion of the scFvs. Co-expression of the biotin ligase BirA with the scFvs enhanced the biotinylation efficiency of the AviTag constructs and improved their immobilization, but the effect was scFv-dependent. For example, the constructs of scFv13R4 still showed significant difference in immobilization between the biotinylation tags, despite enhanced biotinylation efficiency of the AviTag construct [75]. One theory for the difference is that the FLAG tag used to detect the immobilization is not as easily accessible in the AviTag constructs as in the BCCP constructs, because the larger BCCP biotinylation tag acts as a linker that distances the FLAG tag further from the immobilization surface and enhance its accessibility. To test this theory, flexible peptide linkers of various lengths and a rigid linker were inserted between scFv13R4 and the biotinylation tags, and the effect on immobilization and expression of the scFvs was evaluated. scFv5, which previously showed poor expression and immobilization of its AviTag construct [75] was also tested to determine if the effect of linkers is scFv- or expression-dependent. The study found that while the linkers had a limited effect on the scFv constructs that were able to reach saturated immobilization levels in the work in Chapter 4 (both of scFv13R4 constructs and the BCCP construct of scFv5), the linkers improved the immobilization of the AviTag-fusion of scFv5 that previously showed a low immobilization level. Linkers can be used effectively to enhance immobilization of a protein if initial immobilization is poor.

5.2. Materials and Methods

5.2.1. Linker plasmid construction

To test the effect of linkers on expression and immobilization, flexible $(G_4S)_n$ linkers—with variable lengths of n = 1, 3, and 5—and one rigid linker $(EA_3K)_3$ were incorporated into the fusion of scFv13R4 to the BCCP or AviTag biotinylation tag between the scFv and the tag. Pairs of complementary primers that encode for each linker were designed and inserted between the *Sal*I and *Eco*RI cut-sites of pSPI02B and pSPI02A plasmid backbones to create new backbones with linkers N-terminal to the BCCP and AviTag, respectively (Table 5.1). DNA encoding for scFv13R4 was amplified by polymerase chain reaction (PCR) with a C-terminal FLAG tag and inserted between

Table 5.1. Constructs of scFv13R4 and scFv5 with and without linkers used in this study.

scFv	Linker	Biotinylation Tag	Plasmid backbone	Construct
scFv13R4	None	BCCP	pSPI02B	scFv13R4-BCCP
	$(G_4S)_1$	BCCP	pSPI03B	scFv13R4-$(G_4S)_1$-BCCP
	$(G_4S)_3$	BCCP	pSPI04B	scFv13R4-$(G_4S)_3$-BCCP
	$(G_4S)_5$	BCCP	pSPI05B	scFv13R4-$(G_4S)_5$-BCCP
	$(EA_3K)_3$	BCCP	pSPI07B	scFv13R4-$(EA_3K)_3$-BCCP
	None	AviTag	pSPI02A	scFv13R4-AviTag
	$(G_4S)_1$	AviTag	pSPI03A	scFv13R4-$(G_4S)_1$-AviTag
	$(G_4S)_3$	AviTag	pSPI04A	scFv13R4-$(G_4S)_3$-AviTag
	$(G_4S)_5$	AviTag	pSPI05A	scFv13R4-$(G_4S)_5$-AviTag
	$(EA_3K)_3$	AviTag	pSPI07A	scFv13R4-$(EA_3K)_3$-AviTag
scFv5	None	BCCP	pSPI02B	scFv5-BCCP
	$(G_4S)_3$	BCCP	pSPI04B	scFv5-$(G_4S)_3$-BCCP
	$(EA_3K)_3$	BCCP	pSPI07B	scFv5-$(EA_3K)_3$-BCCP
	None	AviTag	pSPI02A	scFv5-AviTag
	$(G_4S)_3$	AviTag	pSPI04A	scFv5-$(G_4S)_3$-AviTag
	$(EA_3K)_3$	AviTag	pSPI07A	scFv5-$(EA_3K)_3$-AviTag

the *Nde*I and *Sal*I cut-sites N-terminal to the linker or, if no linker was present, N-terminal to the biotinylation tag. To test whether the effect of linkers is scFv specific, scFv5, whose AviTag construct previously showed low immobilization [75], was amplified and inserted into the backbones with $(G_4S)_3$ and $(EA_3K)_3$ linkers. scFv5 has an N-terminal FLAG tag, as it was present in the original source plasmid.

5.2.2. scFv expression

The scFv constructs with or without linkers were produced in *E. coli* BL21 cells. Overnight cultures were subcultured and grown at 37 °C with 20 μg/mL chloramphenicol for plasmid maintenance. Once the cultures reached mid-log phase, isopropyl β-D-1-thiogalactopyranoside (to 100 μM) and biotin (to 5μM) were added [59, 62] to induce expression and allow biotinylation. Cultures were grown overnight at 20 °C. Cells were then harvested at 4 °C, and the cell pellets were frozen at -20 °C until needed. To extract the biotinylated scFvs, cell pellets were thawed and lysed with BugBuster Master Mix, following the manufacturer's protocol. To remove excess biotin and exchange the buffer to phosphate-buffered saline (PBS), each lysate was put in a 5 kDa molecular weight cut-off column (GE). The total protein concentrations in the cell lysates before and after buffer exchange were quantified with the A280 method on the Nanodrop 2000 (Thermo Scientific), with the assumption of 1 absorbance unit = 1 mg total protein/mL.

5.2.3. Western blot for expression analysis

Western blot analysis was used to quantify the effect of the linkers on the expression of the scFvs. After cell lysis with the BugBuster Master Mix, the lysates were mixed with equal volumes of 2X SDS gel-loading buffer (with β-mercaptoethanol, following Cold

Spring Harbor protocol) and boiled for 5 min at 98 °C. Samples were then run on Any kD Mini-PROTEAN TGX gels (Bio-Rad) to separate the proteins by sodium dodecyl sulfate polyacrylamide gel electrophoresis (SDS-PAGE). The separated scFvs were detected using standard Western blotting protocols. After SDS-PAGE, the proteins were transferred onto polyvinyl difluoride (PVDF) membranes, and the membranes were blocked in Tris-buffered saline with 0.1% Tween 20 (TBST) and 5% milk. To detect the expression level of the scFvs, the membranes were washed and stained with horse radish peroxidase (HRP)-conjugated anti-FLAG antibody (Sigma). Antibody-stained PVDF membranes were developed with the Clarity Western ECL substrate (Bio-Rad), and the resulting chemiluminescence was detected on a ChemiDoc MP imaging system. The level of expression was quantified through densitometric analysis on ImageLab software (Bio-Rad).

5.2.4. Enzyme-linked immunosorbent assay for immobilization analysis

The effectiveness of immobilization of the biotinylated scFvs was quantified using an enzyme-linked immunosorbent assay (ELISA). High-binding 96-well polystyrene plates (Corning) were coated with streptavidin, as previously described [75]. PBS buffer-exchanged cell lysates were serially diluted in PBS with 0.1% Tween 20 (PBST) with 0.5% milk and loaded onto streptavidin-coated plates (50 μL/well), which were washed with PBST prior to loading of the samples. After 45 min of incubation, unbound scFvs were washed off with PBST, and the immobilized scFvs were incubated for 1 h with an anti-FLAG antibody (HRP-conjugated). Unbound antibody was washed off and 200 μL of *o*-phenylenediamine dihydrochloride HRP substrate (Sigma) was added to each well to react with the HRP on the antibody. After 30 min of reaction in the dark, 3 M H_2SO_4 was

added to quench the reaction. The level of immobilization was quantified using absorbance at 492 nm, measured on a plate reader (Epoch, Bio-Tek).

5.3. Results

This study investigated whether the distance between the antibody fragment and the point of immobilization affects the immobilization of biotinylated scFvs to a streptavidin-coated surface. The distance between the scFv and the biotinylation site was lengthened through addition of flexible linkers of various length—$(G_4S)_1$, $(G_4S)_3$, and $(G_4S)_5$—and a rigid linker $(EA_3K)_3$ between the scFv and the biotinylation tags, BCCP and AviTag, that are C-terminal to the scFv. scFv13R4 was chosen as the first test candidate, as the BCCP fusion and the AviTag fusion of the antibody fragment previously showed a difference in immobilization [75]. The difference was present even after the biotinylation efficiency of the AviTag construct was enhanced with BirA enzyme. To determine if the effects of the linkers extend to other scFvs or are scFv specific, one of the flexible linkers $(G_4S)_3$ and the rigid linker $(EA_3K)_3$ were also tested with another scFv, scFv5 [89].

5.3.1. scFv13R4 constructs are robust and unaffected by linkers

The effect of the linkers on the immobilization of scFv13R4 was assessed on streptavidin coated 96-well plates using ELISAs. The extent of immobilization was quantified by detection of the FLAG tag at the C-terminal end of the scFv13R4. In agreement with the previous study [75], the BCCP constructs immobilized better than the AviTag constructs (Figure 5.1), approaching higher absorbance signals at lower total

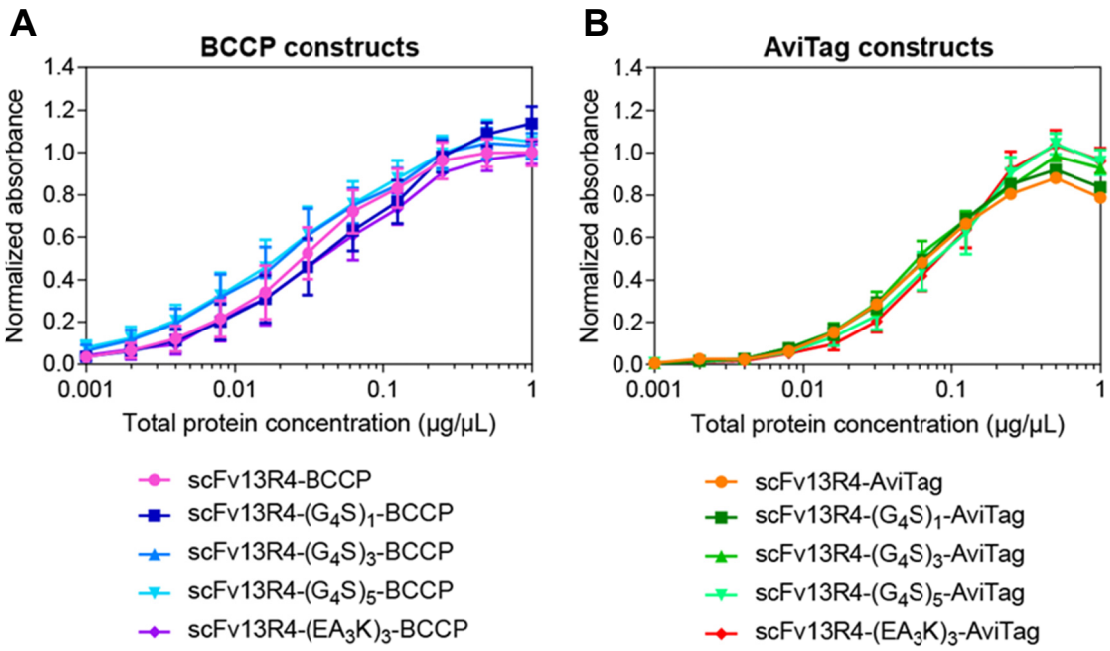

Figure 5.1. Immobilization of (A) scFv13R4- linker-BCCP constructs and (B) scFv13R4-linker-AviTag constructs onto streptavidin coated plates. Serial dilutions of cell lysates in PBST were loaded onto the coated 96-well plates, and the immobilization was detected with an anti-FLAG antibody. Data are normalized to the signal from the highest concentration of scFv13R4-BCCP with no linker for each biological replicate. The error bars represent the standard error of mean (n =4).

protein concentrations than the AviTag constructs. The immobilization of neither the BCCP fusions nor the AviTag fusions of the scFv13R4 was significantly affected by the addition of any of the linkers. As more cell lysate was loaded per well, the absorbance signals of constructs without linkers and with linkers were at comparable levels. The AviTag constructs were particularly robust, with most of the signals of the tested concentrations closely overlapping one another, making it difficult to distinguish the individual curves (Figure 5.1B). Therefore, the length and the flexibility of the linker have no influence on the immobilization of scFv13R4.

5.3.2. Linkers enhance immobilization of the AviTag fusion of scFv5

To determine the effect of the linkers on immobilization of scFv5, the flexible $(G_4S)_3$ linker and the rigid $(EA_3K)_3$ linker were inserted into the BCCP and AviTag fusions of scFv5. scFv5 was selected since, in the previous study, the immobilization levels of its constructs were lower than both of the scFv13R4 constructs (Figure 4.3) [75]. As with the scFv13R4 constructs, the level of immobilization was quantified by detection of the FLAG tag fused to the scFv5, which is N-terminal to the scFv in the scFv5 constructs. Similarly to the scFv13R4 fusions, the insertion of the linkers led to no significant difference in immobilization of the BCCP constructs of scFv5 (Figure 5.2). Interestingly,

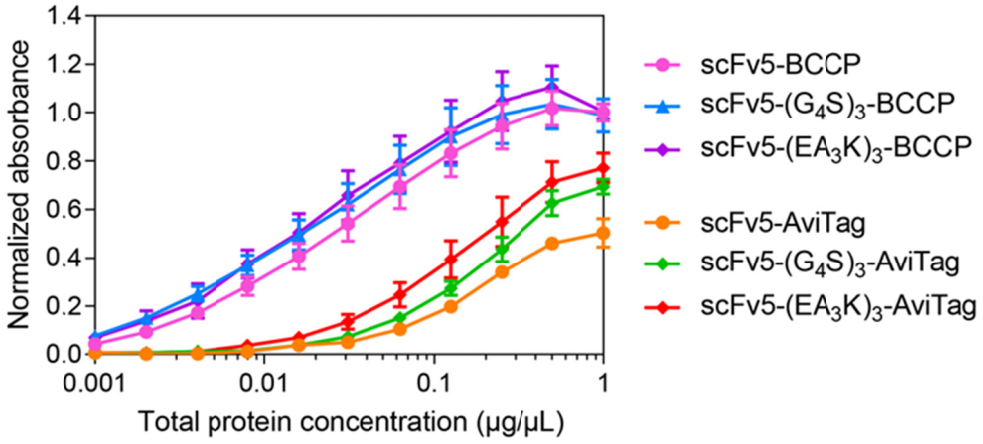

Figure 5.2. Immobilization of (A) scFv5- linker-BCCP constructs and (B) scFv5-linker-AviTag constructs onto streptavidin coated plates. Serial dilutions of cell lysates in PBST were loaded onto the coated 96-well plates, and the immobilization was detected with an anti-FLAG antibody. Data are normalized to the signal from the highest concentration of scFv5-BCCP with no linker for each biological replicate. The error bars represent the standard error of mean (n =4).

the AviTag constructs with linkers showed higher levels of immobilization than the construct with no linker. Both the flexible and rigid linker led to a similar level of enhanced immobilization, which suggests that the flexibility of the linker may not play a significant role in immobilization. This result shows that linkers can be used to improve

immobilization of some scFvs, particularly those that initially have low levels of immobilization.

5.3.3. Linkers do not enhance expression of the scFvs

Once the immobilization assay indicated that linkers could modify immobilization level, the expression level of the constructs was studied to assess whether it played a role in the improvement. The expression was detected by Western blotting with an anti-FLAG antibody and quantified by densitometric analysis on the developed membranes (Figure 5.3). The analysis showed no significant enhancement in the expression level of the

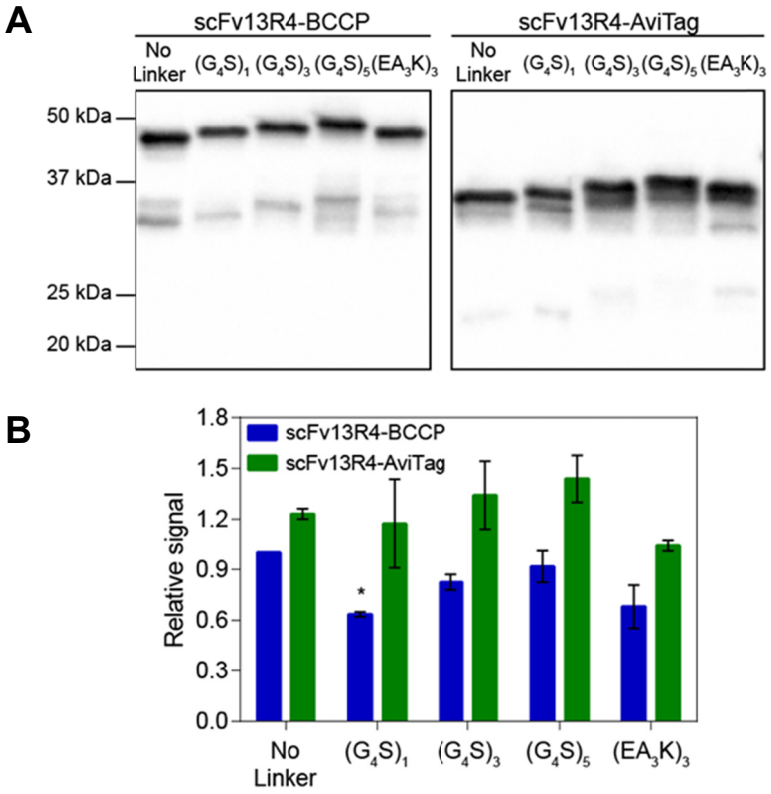

Figure 5.3. The expression of scFv13R4 constructs by (A) Western blotting and (B) densitometric analysis. The constructs were expressed in BL21 *E. coli* cells, and Western blotting was performed on the soluble cell lysates. The level of expression of each scFv13R4 construct was detected with an anti-FLAG antibody. For densitometric analysis, the signals were normalized to the scFv13R4-BCCP construct with no linker. Error bars are standard error of the mean (n =2). The asterisk indicates statistical significance with $p < 0.05$.

scFv13R4 constructs due to presence of the linkers. In fact, insertion of the $(G_4S)_1$ linker led to a decrease in expression. The AviTag constructs showed greater expression than the BCCP constructs, as previously observed (Figure 4.2A) [75], and, unlike the BCCP construct, the $(G_4S)_1$ linker did not cause a decrease in expression level. This is in line with the robustness observed with the AviTag constructs in the immobilization assay (Figure 5.1).

Similarly to the scFv13R4 constructs, the insertion of a linker did not improve the expressions of the scFv5 constructs (Figure 5.4). Unlike the scFv13R4 constructs, however, the expression levels between the two biotinylation tags were comparable. The Western blot analysis indicates that the expression of the scFv constructs fused to BCCP or the AviTag are not enhanced by the addition of peptide linkers between the scFv and the biotinylation tags.

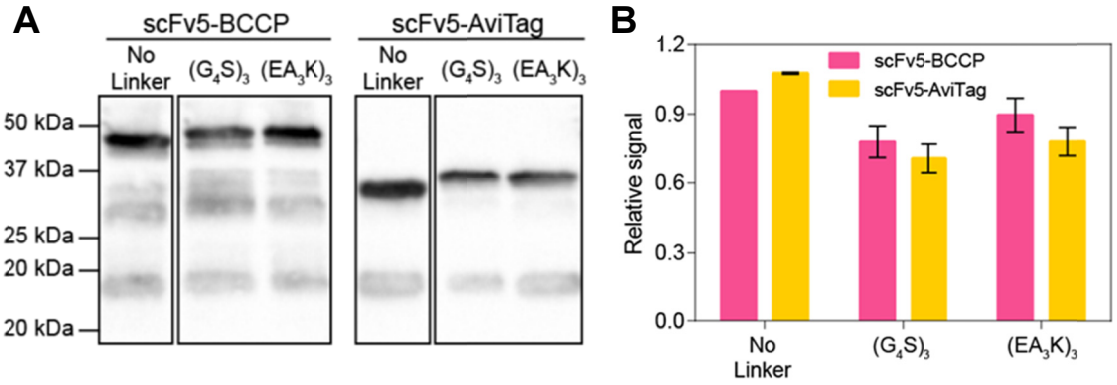

Figure 5.4. The expression of scFv5 constructs by (A) Western blotting and (B) densitometric analysis. The constructs were expressed in BL21 *E. coli* cells, and Western blotting was performed on the soluble cell lysates. The level of expression of each scFv5 construct was detected with an anti-FLAG antibody. For densitometric analysis, the signals were normalized to the scFv5-BCCP construct with no linker. Error bars are standard error of the mean (n =2).

5.4. Discussion

A number of previous studies have used peptide linkers to enhance activity and expression of fusion proteins [102]; however, limited studies have used them as a tool to enhance binding onto a surface [104] or to functionalized beads [96, 99]. This study investigated the effect of flexible and rigid linkers on immobilization of scFvs using the biotin-streptavidin interaction. Flexible linkers $(G_4S)_n$, with n = 1, 3, or 5, or a rigid linker $(EA_3K)_3$ were evaluated with scFv13R4, and the $(G_4S)_3$ linker and the $(EA_3K)_3$ linker were also tested in scFv5. The immobilization of the AviTag fusion of scFv5 was significantly enhanced by the introduction of the linkers (Figure 5.2). At the same time, the linkers had no effect on the immobilization of the scFv13R4 constructs with either biotinylation tag (Figure 5.1) or the BCCP constructs of scFv5 (Figure 5.2), so the influence of the linker is not universal to all scFv constructs. The addition of linker has no negative influence on immobilization, therefore, it could be included as a default part of a construct without a potential to decrease immobilization.

Initially, the improved immobilization signal was hypothesized to be due to enhanced expression of the scFv5-AviTag constructs with a linker, as previous studies have demonstrated enhanced expression of protein fusions due to linkers [101, 105]. However, Western blot analysis with an anti-FLAG antibody showed that the linkers did not increase the expression of either scFv (Figure 5.3 and Figure 5.4). The lack of greater expression due to linkers indicates the immobilization improvements observed with scFv5 constructs are not due simply having a higher level of soluble scFv-biotinylation tag in the cell lysate.

The size of the fused components may explain the significant shift in immobilization of scFv5 fused to the AviTag compared to BCCP. With 15 residues, the AviTag biotinylation tag [62] is much smaller than the 87 residues of BCCP [63]. Therefore, the addition of 15 residues from the three repeats of the linker sequence likely has a larger impact on the AviTag constructs by greatly increasing the distance between the surface and the scFv. However, the immobilization of scFv13R4 does not follow this trend, and, in fact, the AviTag-fusions showed very little variability among the linkers tested. Alternatively, the linkers may simply affect various scFvs fusions differently, improving the immobilization of one yet having no effect on the other.

5.5. Conclusion

This study demonstrated that peptide linkers have neutral to positive effect on immobilization. The linkers can enhance immobilization of scFv that show poor immobilization without a linker while having no adverse effect on a scFv that show high immobilization. Insertion of an even longer linker could lead to an AviTag construct of scFv5 that immobilizes at similar level to the BCCP construct. Study with other types of linkers on more scFvs could give more insight on whether these observations can be extended to a broader set of scFvs and linkers.

Chapter 6: Recommendations for future work

This dissertation demonstrated the use of protein engineering approaches to study topics related to a *Candida* fungal pathogen. Chapter 2 and Chapter 3 looked at improvements toward treatment of *C. albicans* infections through study of the antifungal peptide histatin 5 (Hst-5). The chapters explored the interactions between Hst-5 and the Saps produced by *C. albicans* by designing amino acid modifications that alter the proteolytic susceptibility to the Saps as well as the antifungal activity of the peptide. The effect of modification on both of these properties was explored unlike the previous studies, which mainly focused on effect on antifungal activity. The findings led to designing of a modified peptide with not only enhanced resistance to Saps (K17R, K17L) or improved antifungal activity (K11R), but with both of the properties improved (K11R-K17R). Additionally, during the course of the study, an optical density-based method to test the antifungal activity the peptides was developed. The method allows quicker and easier comparisons of the antifungal activity of multiple peptides simultaneously, at broad concentration ranges, compared the typically used colony-counting method and the results of the two methods are comparable (Figure A.3) Chapter 4 and Chapter 5 used protein engineering approaches to work towards improvements in diagnostics. The simple and versatile scFv immobilization method developed in these chapters could be used to create a diagnostic antibody array not only for *Candida*, but to other pathogens as well.

Based on the work in this thesis, a number of additional experiments could be done. This recommended future work is focused on further characterizing the modified Hst-5 peptides and improving their potential as a therapeutic to treat *Candida* infections.

6.1. Further characterization of the Hst-5 variants

6.1.1. Additional modifications to Hst-5

The single amino acid substitution studies on Hst-5 in Chapter 2 and Chapter 3 discovered modifications that increase the resistance to proteolysis by Saps and *C. albicans* (K17R, K17L) or improve the antifungal activity (K11R, E16R, E16L). Combination of modifications from each improved property led to a variant of Hst-5 with both of the enhanced properties (K11R-K17R). The effect seen with K11R-K17R opens the possibility of exploring other combinations of the peptide modifications with enhanced properties. One recommended modification is the K11R-E16R-K17R (Table 6.1). While E16R modification was more susceptible to proteolysis by Sap9, it showed enhanced resistance to Sap2. Furthermore, it showed improved antifungal activity despite the degradation. By adding this substation to the K11R-K17R peptide, the modified peptide could have even more augmented antifungal activity against *C. albicans*. If the triple-modified peptide successfully shows further improvement in activity, a study with E16R-K17R modified peptide could give more insight into how each modification affects the properties of the peptide as a whole.

Table 6.1. The amino acid sequence of Hst-5 and variants for future studies. The modified residues are highlighted in blue.

Name	Sequence																							
	1	2	3	4	5	6	7	8	9	10	11	12	13	14	15	16	17	18	19	20	21	22	23	24
Hst-5	D	S	H	A	K	R	H	H	G	Y	K	R	K	F	H	E	K	H	H	S	H	R	G	Y
K11R-E16R-K17R	D	S	H	A	K	R	H	H	G	Y	R	R	K	F	H	R	R	H	H	S	H	R	G	Y
E16R-K17R	D	S	H	A	K	R	H	H	G	Y	K	R	K	F	H	R	R	H	H	S	H	R	G	Y

6.1.2. Proteolysis resistance in saliva

Hst-5 and the rest of the family of histatins are secreted by the parotid and submandibular glands [27] and help fight *C. albicans* infection in the mouth. However, saliva is composed of various other proteins that contribute to innate immunity [23, 24] and have a synergetic effect among them [106]. The enzymes in saliva can also cleave histatins, as demonstrated by kinetic studies on proteolysis of Hst-5 by whole saliva [76, 107]. Therefore, it is important to investigate the stability of the Hst-5 variants in whole saliva. Inspired by the work of Sun et al. [76], the modified peptides could be added to pooled samples of whole saliva and the decrease in the intact peptide monitored through mass spectrometry. Isotopically labeling multiple carbons in the peptides to ^{13}C can give a better quantification with mass spectrometry for the intact peptide remaining. The modifications that increased resistance to proteolysis by Saps could also increase resistance to the other proteolytic enzymes, or, alternatively, make them more susceptible. Gaining such understanding can aid in improving methods to introduce the modified peptides to the oral cavity so that the activity of the peptide is not immediately lost due to other salivary proteins.

6.1.3. Cytotoxicity to oral epithelial cells

In addition to ensuring that the variants of Hst-5 remain functional in saliva, it is also important to verify that the modifications do not cause toxicity to oral epithelial cells. Natural antifungal peptides do not have significant toxicity to host cells [68]. While hemolytic activities of Hst-5 variants have been reported [35, 42, 108], the ratio of the concentration at which 50% hemolysis is observed (HC_{50}) to MIC_{50} were higher for all Hst-5 variants than Hst-5 [42]. This suggests that the peptides are more selective for *C. albicans*. However, the hemolysis assay is not enough to evaluate the potential toxicity of antimicrobial peptides. A recent study on the anti-*Candida* activity of uperin 3.6 and its variants found that, while the peptides had no hemolytic activity to erythrocytes, they were highly toxic to human vaginal and esophagial epithelial cells [109]. Therefore, in addition to the hemolysis assay, the potential cytotoxicity of the Hst-5 variants to oral epithelial cells should be evaluated.

6.1.4. *In vivo* efficacy with murine oral candidiasis model

Once the cytotoxicity of the peptides to epithelial cells has been evaluated, the *in vivo* efficacies of the peptides need to be examined to determine whether the improvements observed in *in vitro* assays are translated to *in vivo* results. While numerous studies have looked at the antifungal activity of Hst-5, its fragments, or their variants through *in vitro* assays [33-39], limited *ex vivo* or *in vivo* studies have been done [110, 111]. Kong et al. recently demonstrated that Hst-5 can be delivered to mice with oral candidiasis by formulating the peptide into a bioadhesive hydrogel [71]. Dr. Mary Ann Jabra-Rizk (University of Maryland Dental School) used this hydrogel formulation to test the efficacy of the lysine-substituted Hst-5 variant K17L in her murine oral candidiasis

model (Figure 6.1). The greater decrease in average number of colony forming units (CFUs) per gram of tongue tissue in the K17L treatment group than the Hst-5 group shows a promising result for the Hst-5 variant. In fact, one of the mice in K17L treatment group had essentially no detectable fungal load. The *in vivo* antifungal activity of the other promising Hst-5 variants from Chapter 2 and Chapter 3 could be assessed using the hydrogels and the mouse oral candidiasis model.

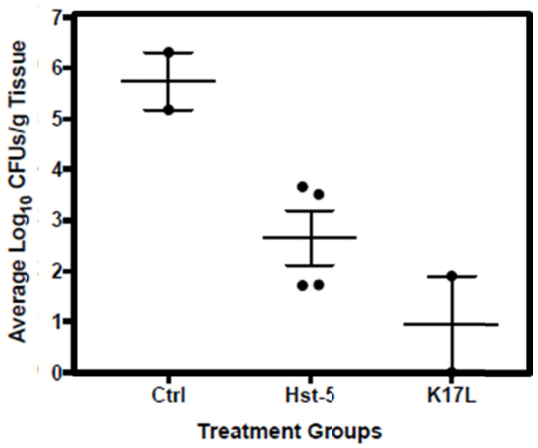

Figure 6.1. Antifungal activity of Hst-5 and K17L in a murine model of oral candidiasis. Mice were orally infected with *C. albicans* and, for three days post-infection, received no treatment (Ctrl) or one daily treatment of hydrogel formulated with Hst-5 or K17L peptide. Four days after infection, mice were euthanized, and the tongues were harvested and processed to determine the number of colony forming units (CFUs) per gram of tongue tissue. (Data from Dr. Mary Ann Jabra-Rizk)

6.2. Structural studies of Hst-5 and Saps

6.2.1. Molecular dynamic simulation of Hst-5

Although structural studies on Hst-5 have been previously done, they were done using either circular dichroism [33] or NMR [41]. Both of the methods have limitations on what solvents can be used during the measurements, which make it difficult to simulate the behavior of the peptide near a cell. The structure of Hst-5 near a cell

membrane could give insight into how the peptide interacts with the cell surface before being transported into the cell. Molecular dynamics (MD) simulations can be used to determine the likely conformation the peptide takes near phospholipids mimicking the cell membrane.

To be able to do MD simulations, the starting structure of Hst-5 is needed. However, no entry was available for Hst-5 in the Protein Data Bank [112]. Therefore, to begin a structural study with MD simulation, the steady-state structure of Hst-5 in water was determined. The starting structure of Hst-5 was predicted from the residue sequence using the Iterative Threading ASSEmbly Refinement (I-TASSAR) online structural prediction server [113-116]. The first two structures predicted by I-TASSAR sever (Figure 6.2) were then used in the CHARMM-GUI Solvator to solvate the peptide and

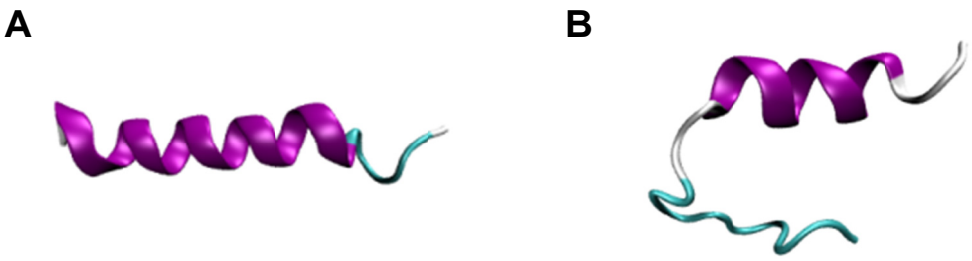

Figure 6.2. Structures of Hst-5 predicted by I-TASSAR server: (A) Model 1 and (B) Model 2. The magenta colored region indicates residues that are in α-helical structure.

create an aqueous environment that will simulate the peptide being far from cell surface [117]. The solvated peptide structure was equilibrated and then simulated for 200 ns on NAMD to determine the steady-state structure of the peptide [118]. Each of the models was run twice and the root-mean-square deviation (RMSD) of the structural changes to the backbone and the changes in the helical characteristics were determined (Table 6.2).

Table 6.2. The RSMD and the average number of residues of the peptide in helical structure in the full peptide after 200 ns of simulations.

		Averaged RMSD	Averaged number of helical residues
Model 1	Run 1	7.270 ± 2.585	9.102 ± 2.065
	Run 2	14.664 ± 1.892	11.368 ± 1.818
Model 2	Run 1	7.614 ± 2.080	7.734 ± 1.143
	Run 2	6.923 ± 1.195	3.860 ± 1.935

High RSMD values were observed for all of the simulations, indicating the structure shifted around quite a bit. The first run of Model 1 started with higher number of residues in helical confirmation than Model 2. However, over the course of 200 ns simulation, the number generally decreased while the number for Model1 2 stayed at similar level (Figure 6.3). The decrease in helical content could be simulating the peptide's tendency to be unstructured in aqueous environments [41].

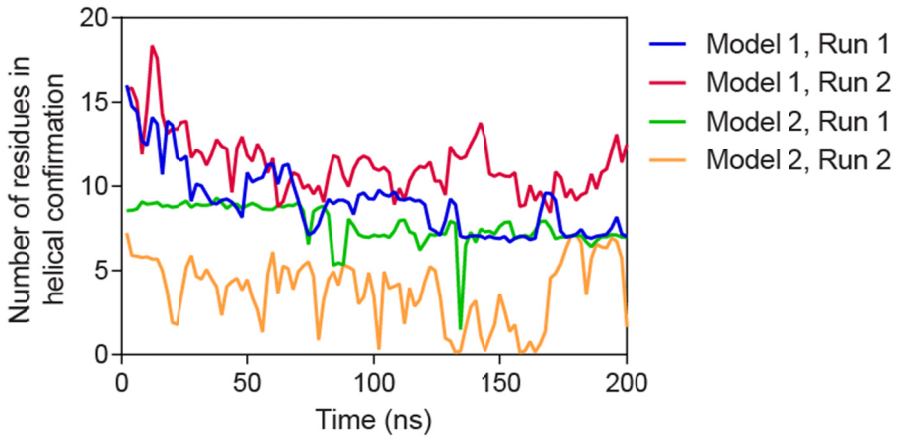

Figure 6.3. Number of residues of Hst-5 sequence in helical formation during the course of the simulation. Each residue with helical characteristic is counted as one and the total number are summed at particular step in the simulation.

With the steady-state structure in an aqueous environment determined, the peptide can now be placed a short distance above a bilayer of phospholipids emulating the cell membrane. Changes in its structural characteristics can be monitored as it approaches the phospholipid bilayer to gain a structural understanding of the peptide near the cell membrane.

6.2.2. Structural determination with NMR

Previous studies have determined the structures of Sap1 [13], Sap2 [15, 119], Sap3 [120], and Sap5 [13]. However, structures on the rest of the Saps, including Sap9, have not yet been elucidated. Furthermore, most of the available Saps structures are in a complex with an inhibitor, most commonly pepstatin A, and no structural determination of a Sap bound to an antifungal peptide like Hst-5 has been done. The structure of free Sap9 and Sap9 in complex with Hst-5 could be determined through NMR or X-ray diffraction of a crystalized sample. If the structural determination of the Sap-peptide complex is successful with Hst-5, the study can be expanded to include the variants of Hst-5 and evaluate how the peptide modifications may affect binding.

6.2.3. Peptide and Sap docking simulation

While the structural determination of Sap9 with NMR or X-ray diffraction should be feasible, the structure of Sap in complex with Hst-5 may be difficult to discern if the time the peptide is in the binding pocket of the Sap is too short. Alternatively, once the structure of Sap9 has been determined, a docking simulation study could be done instead. Lum et al. have successfully demonstrated docking of their synthetic peptides with Sap1 and Sap5 using Autodock Vina software [109, 121]. The docking study could give

information on how the peptide aligns within the binding pocket of Sap9 and could provide insight into why some variants of Hst-5 are more susceptible to proteolysis by Saps than the others.

The recommended further characterization of Hst-5 variants and structural studies of Hst-5 will provide a more comprehensive understanding of the peptide's interaction with cells and gain information that will aid in enhancing the potential of the peptide as a therapeutic.

Appendices

Appendix A. Additional data of lysine substituted Hst-5

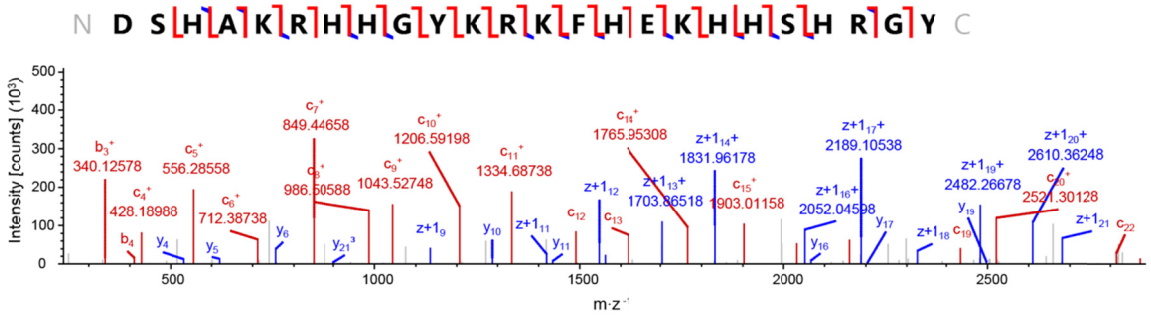

Figure A.1. Annotated electron-transfer and higher-energy collision dissociation (EThCD) spectrum of intact Hst-5.

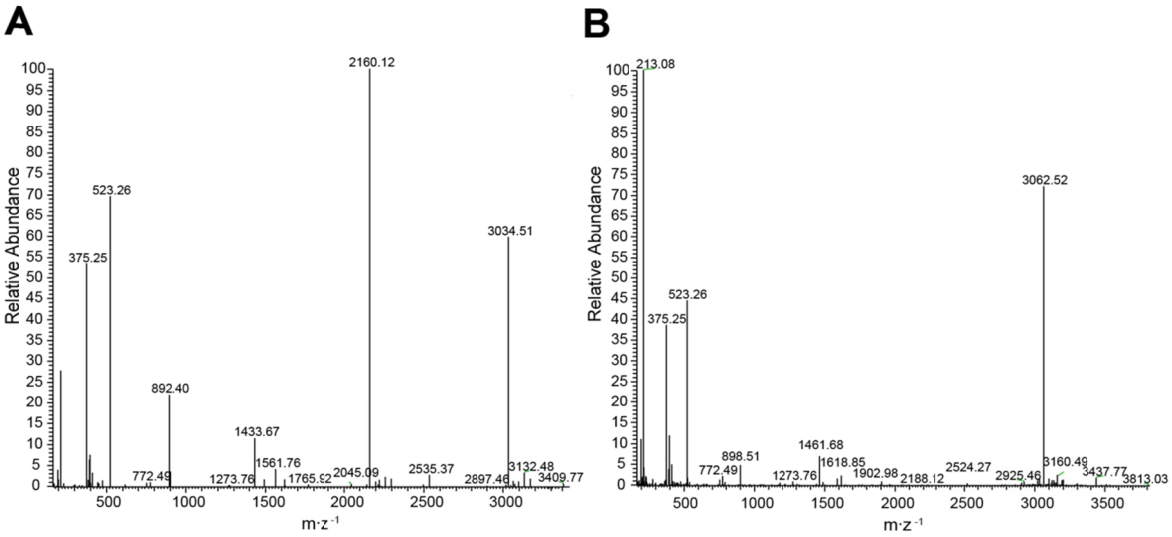

Figure A.2. Representative deconvoluted full scan mass spectra of (A) Hst-5 and (B) K17R after incubation with 3.13 µg/mL Sap9.

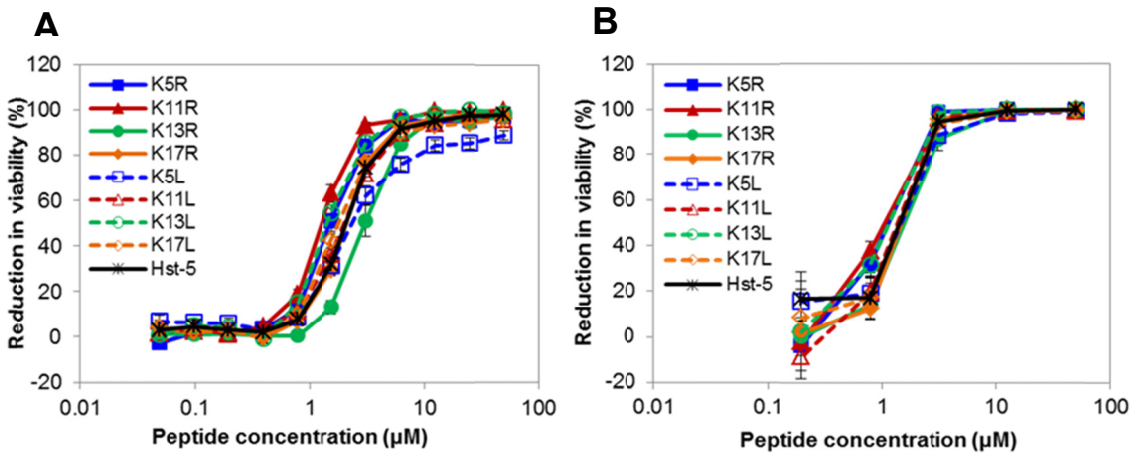

Figure A.3. Comparison of the antifungal activity (2.5×10^5 cells/mL) assay using (A) OD-based and (B) cell-count methods. The OD-method is as described in Chapter 2 and Chapter 3. For cell-count based method, ~500 cells were plated on YPD plates and grown for 24 h. The number of colony forming units (CFUs) on each plate was counted and calculated reduction in viability (%) = (# CFUs in plate with peptide) / (# CFUs in plate with no peptide).

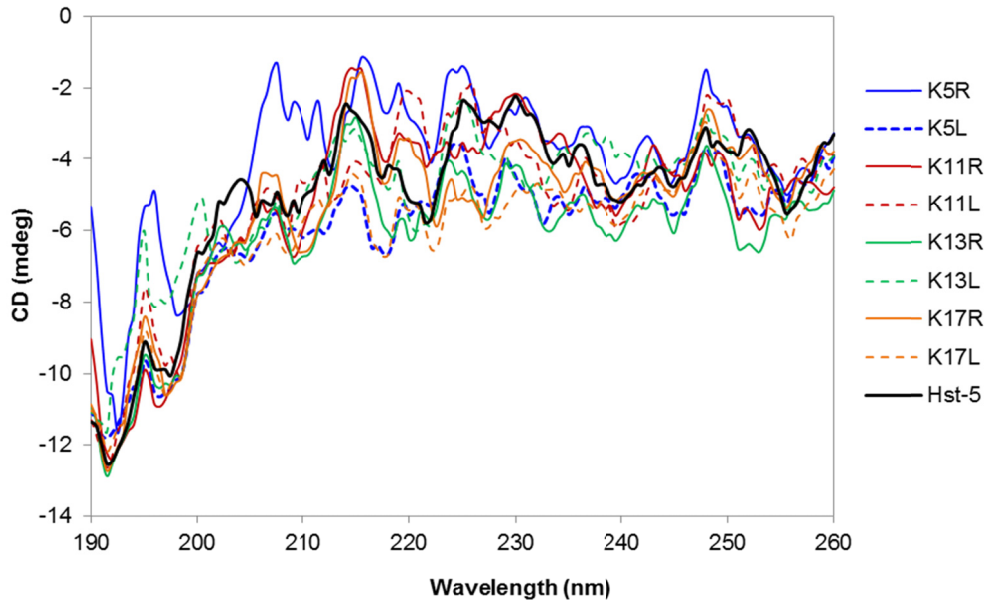

Figure A.4. Circular dichroism data of 5 μM of Hst-5 and lysine-substituted variants in 0.1 mM NaPB.

Appendix B. CE-MS analysis.

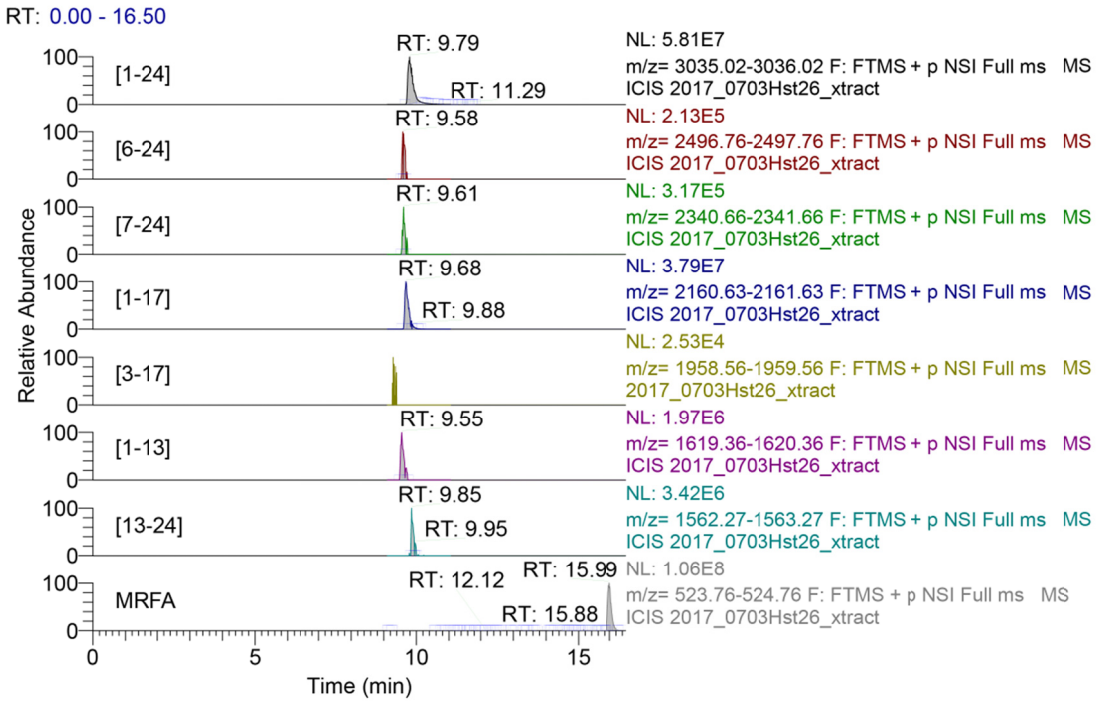

Figure B.1. Deconvoluted ion profile of Hst-5 and degradation fragments after 30 min incubation with Sap9 as well as internal standard MRFA. Deconvolution was done by performing Xtract RAW File on Thermo Xcalibur Qual Browser with "AveragineNoSulture" setting with Max Charge of 10. The relative peak area of intact peptide or degradation fragments was determined by obtaining the signal of area under the peak in the chromatogram of the peptide relative to signal of the area under the peak of MRFA.

Appendix C. Supplementary information for Chapter 4.

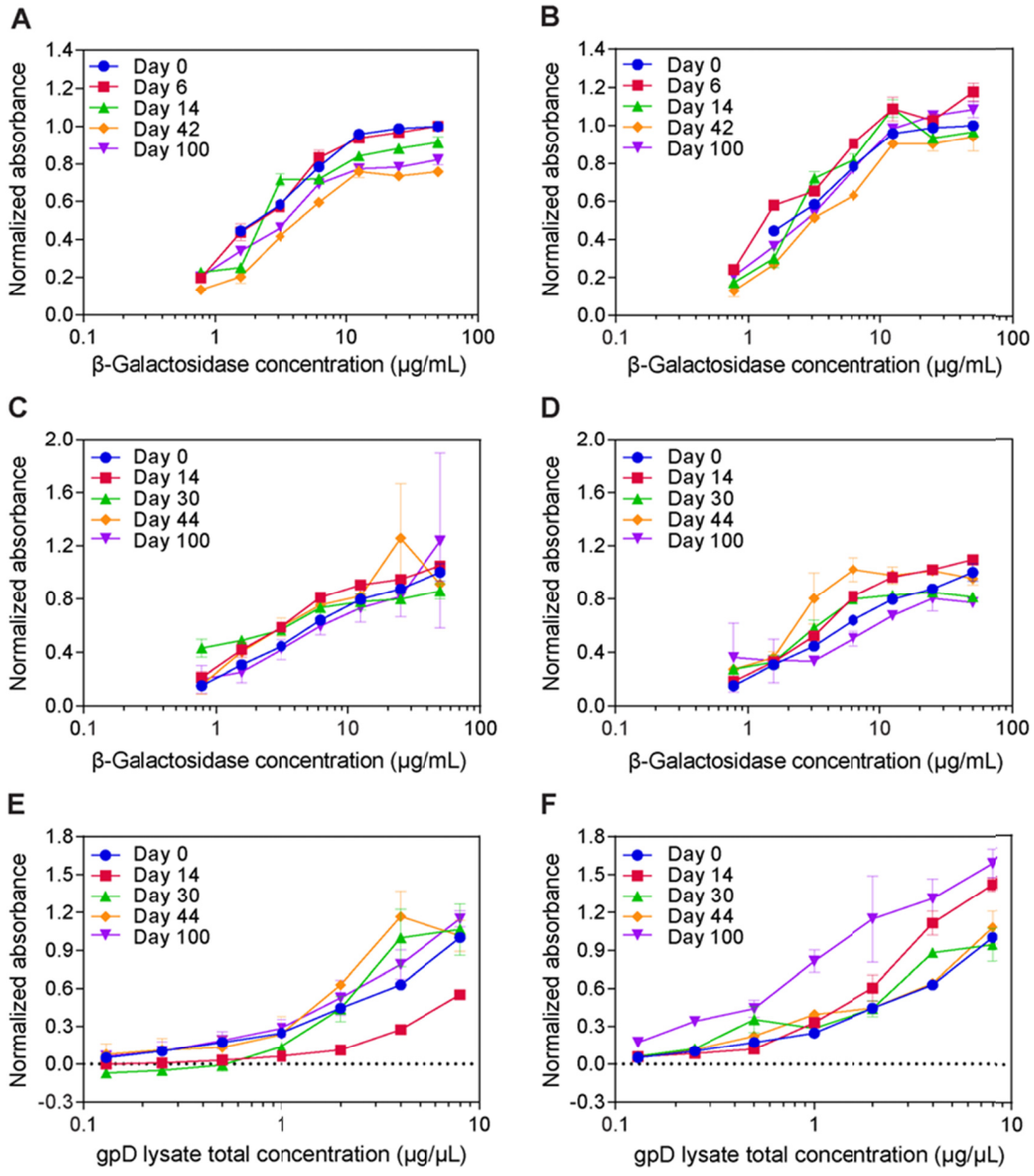

Figure C.1. Antigen-binding of immobilized scFv constructs after storage in 0.5% milk PBST. Biotinylated scFv13R4-BCCP (A & B), scFv13R4-AviTag (C & D), and scFvD10-BCCP (E & F) were immobilized onto streptavidin-coated plates from cell lysates and stored in 0.5% milk in PBST at 4 °C (A, C, E) and -20 °C (B, D, F). Serial dilutions of β-galactosidase or gpD were incubated with the scFvs, and the bound antigens were detected with an anti-β-galactosidase antibody and anti-6XHis antibody, respectively. Absorbance readings were normalized to the highest signal on Day 0. Normalized absorbance for a given scFv construct at different temperatures and storage solutions can be compared, but the levels at different time points cannot be strictly compared. Error bars indicate the standard error of the mean.

Publications and Presentations

Accepted publications

1. **Ikonomova, S. P.**, He, Z. & Karlsson, A. J. (2016) A simple and robust approach to immobilization of antibody fragments, *J Immunol Methods.* **435**, 7-16. DOI: 10.1016/j.jim.2016.04.012.

2. Moghaddam-Taaheri, P., **Ikonomova, S. P.**, Gong, Z., Wisniewski, J. Q. & Karlsson, A. J. (2016) Bacterial inner membrane display for screening antibody fragment libraries. *J Vi Exp* **116**, 54583. DOI: 10.3791/54583.

Submitted publications

1. **Ikonomova, S. P.**, Wang, Y., Jabra-Rizk, M. A., Karlsson, A. J. Designing histatin 5 variants for reduced susceptibility to secreted aspartic proteases.

Publications under preparation

1. **Ikonomova, S. P.**, Wang, Y. & Karlsson, A. J. Effects of residue modifications of histatin 5 on kinetics of its proteolysis and antifungal activity.

2. **Ikonomova, S. P.**, Le, M. T., Kalla, N. & Karlsson, A. J. Effect of linkers on immobilization of scFvs with biotin-streptavidin interaction.

3. Lamp, J., **Ikonomova, S. P.**, Karlsson, A. J., Xia, Q. & Wang, Y. Capillary electrophoresis – mass spectrometry analysis of Histatin-5 and its analogs.

Intellectual property filed

Jabra-Rizk, M. A, Karlsson, A. J. & **Ikonomova, S. P.** "Histatin-5 based synthetic peptides and uses thereof," U.S. Patent Application (No. 62/320,675) filed April 11, 2017.

Delivered Presentations (presenting author underlined)

1. Wang, Y., **Ikonomova, S. P.**, Karlsson, A. J., Zarrin, F. C. & Xia, J. Capillary electrophoresis – mass spectrometry analysis of Histatin 5 and its analogs. American Society for Mass Spectrometry Annual Conference, Indianapolis, IN. June 2017. (Poster)

2. **Ikonomova, S. P.**, Wang, Y. & Karlsson, A. J. Engineering histatin 5 for improved resistance to secreted aspartic proteases. American Chemical Society National Meeting, San Francisco, CA. April 2017. (Oral presentation)

3. **Ikonomova, S. P.**, Wang, Y. & Karlsson, A. J. Enhancing resistance of histatin 5 to proteolytic degradation. International Conference on Biomolecular Engineering, San Diego, CA. January 2017. (Poster)

4. **Ikonomova, S. P.**, He, Z. & Karlsson, A. J. Purification-free antibody fragment immobilization using *in vivo* biotinylation. American Institute of Chemical Engineers Annual Meeting, San Francisco, CA. November 2016. (Oral presentation)

5. **Ikonomova, S. P.** & Karlsson, A. J. Modifying histatin 5 for enhanced resistance to *Candida albicans* secreted aspartic proteases. American Institute of Chemical Engineers Annual Meeting, San Francisco, CA. November 2016. (Oral presentation)

6. **Ikonomova, S. P.** & Karlsson, A. J. Designing histatin 5 variants for reduced susceptibility to secreted aspartic proteases. American Society for Microbiology Conference on Candida and Candidiasis, Seattle, WA. April 2016. (Poster)

7. **Ikonomova, S. P.** & Karlsson, A. J. Effect of histatin-5 mutations on proteolytic degradation by *Candida albicans* secreted aspartic proteases. American Chemical Society National Meeting, San Diego, CA. March 2016. (Oral presentation)

8. **Ikonomova, S. P.** & Karlsson, A. J. Effect of lysine substitution on degradation of histatin-5 by *Candida albicans* secreted aspartic proteases. Gordon Research Seminar: Peptides, Chemistry & Biology of, Ventura, CA. February 2016. (Oral presentation)

9. **Ikonomova, S. P.** & Karlsson, A. J. Effect of lysine substitution on degradation of histatin-5 by *Candida albicans* secreted aspartic proteases. Gordon Research Conference: Peptides, Chemistry & Biology of, Ventura, CA. February 2016. (Poster)

10. **Ikonomova, S. P.**, He, Z. & Karlsson, A. J. Simple and robust antibody fragment immobilization for detection of antigens. American Institute of Chemical Engineers Annual Meeting, Salt Lake City, UT. November 2015. (Oral presentation)

11. **Ikonomova, S. P**, He. Z., Karlsson, A. J. Antibody immobilization by biochemical affinity for developing a diagnostic array. American Institute of Chemical Engineers Annual Meeting, Atlanta, GA. November 2014. (Poster)

References

1. Xu, J. & Mitchell, T. G. (2003) Geographical differences in human oral yeast flora, *Clin Infect Dis.* **36**, 221-4.

2. Pfaller, M. A. & Diekema, D. J. (2007) Epidemiology of invasive candidiasis: a persistent public health problem, *Clin Microbiol Rev.* **20**, 133-63.

3. Calderone, R. A. & Clancy, C. J. (2012) *Candida and Candidiasis, Second Edition*, American Society of Microbiology.

4. Mayer, F. L., Wilson, D. & Hube, B. (2013) *Candida albicans* pathogenicity mechanisms, *Virulence.* **4**, 119-28.

5. Chaffin, W. L. (2008) *Candida albicans* cell wall proteins, *Microbiol Mol Biol Rev.* **72**, 495-544.

6. da Silva Dantas, A., Lee, K. K., Raziunaite, I., Schaefer, K., Wagener, J., Yadav, B. & Gow, N. A. (2016) Cell biology of *Candida albicans*-host interactions, *Curr Opin Microbiol.* **34**, 111-118.

7. Pappas, P. G., Kauffman, C. A., Andes, D. R., Clancy, C. J., Marr, K. A., Ostrosky-Zeichner, L., Reboli, A. C., Schuster, M. G., Vazquez, J. A., Walsh, T. J., Zaoutis, T. E. & Sobel, J. D. (2016) Clinical practice guideline for the management of candidiasis: 2016 update by the Infectious Diseases Society of America, *Clin Infect Dis.* **62**, e1-50.

8. CDC (2013) Antibiotic resistance threats in the United States, 2013.

9. Albrecht, A., Felk, A., Pichova, I., Naglik, J. R., Schaller, M., de Groot, P., Maccallum, D., Odds, F. C., Schafer, W., Klis, F., Monod, M. & Hube, B. (2006) Glycosylphosphatidylinositol-anchored proteases of *Candida albicans* target proteins necessary for both cellular processes and host-pathogen interactions, *J Biol Chem.* **281**, 688-94.

10. Naglik, J. R., Challacombe, S. J. & Hube, B. (2003) *Candida albicans* secreted aspartyl proteinases in virulence and pathogenesis, *Microbiol Mol Biol Rev.* **67**, 400-28, table of contents.

11. Naglik, J. R., Moyes, D., Makwana, J., Kanzaria, P., Tsichlaki, E., Weindl, G., Tappuni, A. R., Rodgers, C. A., Woodman, A. J., Challacombe, S. J., Schaller, M. & Hube, B. (2008) Quantitative expression of the *Candida albicans* secreted aspartyl proteinase gene family in human oral and vaginal candidiasis, *Microbiology.* **154**, 3266-80.

12. Dash, C., Kulkarni, A., Dunn, B. & Rao, M. (2003) Aspartic peptidase inhibitors: implications in drug development, *Crit Rev Biochem Mol Biol.* **38**, 89-119.

13. Borelli, C., Ruge, E., Lee, J. H., Schaller, M., Vogelsang, A., Monod, M., Korting, H. C., Huber, R. & Maskos, K. (2008) X-ray structures of Sap1 and Sap5: structural comparison of the secreted aspartic proteinases from *Candida albicans*, *Proteins.* **72**, 1308-19.

14. Monod, M., Capoccia, S., Lechenne, B., Zaugg, C., Holdom, M. & Jousson, O. (2002) Secreted proteases from pathogenic fungi, *Int J Med Microbiol.* **292**, 405-19.

15. Cutfield, S. M., Dodson, E. J., Anderson, B. F., Moody, P. C., Marshall, C. J., Sullivan, P. A. & Cutfield, J. F. (1995) The crystal structure of a major secreted aspartic proteinase from *Candida albicans* in complexes with two inhibitors, *Structure.* **3**, 1261-71.

16. Borg-von Zepelin, M., Beggah, S., Boggian, K., Sanglard, D. & Monod, M. (1998) The expression of the secreted aspartyl proteinases Sap4 to Sap6 from *Candida albicans* in murine macrophages, *Mol Microbiol.* **28**, 543-54.

17. Aoki, W., Kitahara, N., Miura, N., Morisaka, H., Yamamoto, Y., Kuroda, K. & Ueda, M. (2011) Comprehensive characterization of secreted aspartic proteases encoded by a virulence gene family in *Candida albicans*, *J Biochem.* **150**, 431-8.

18. Schild, L., Heyken, A., de Groot, P. W., Hiller, E., Mock, M., de Koster, C., Horn, U., Rupp, S. & Hube, B. (2011) Proteolytic cleavage of covalently linked cell wall proteins by *Candida albicans* Sap9 and Sap10, *Eukaryot Cell.* **10**, 98-109.

19. Rapala-Kozik, M., Bochenska, O., Zawrotniak, M., Wolak, N., Trebacz, G., Gogol, M., Ostrowska, D., Aoki, W., Ueda, M. & Kozik, A. (2015) Inactivation of the antifungal and immunomodulatory properties of human cathelicidin LL-37 by aspartic proteases produced by the pathogenic yeast *Candida albicans*, *Infect Immun.* **83**, 2518-30.

20. Meiller, T. F., Hube, B., Schild, L., Shirtliff, M. E., Scheper, M. A., Winkler, R., Ton, A. & Jabra-Rizk, M. A. (2009) A novel immune evasion strategy of candida albicans: proteolytic cleavage of a salivary antimicrobial peptide, *PLoS One.* **4**, e5039.

21. Bochenska, O., Rapala-Kozik, M., Wolak, N., Kamysz, W., Grzywacz, D., Aoki, W., Ueda, M. & Kozik, A. (2015) Inactivation of human kininogen-derived antimicrobial peptides by secreted aspartic proteases produced by the pathogenic yeast *Candida albicans*, *Biol Chem.* **396**, 1369-75.

22. Koelsch, G., Tang, J., Loy, J. A., Monod, M., Jackson, K., Foundling, S. I. & Lin, X. (2000) Enzymic characteristics of secreted aspartic proteases of *Candida albicans*, *Biochimica et biophysica acta.* **1480**, 117-31.

23. Salvatori, O., Puri, S., Tati, S. & Edgerton, M. (2016) Innate immunity and saliva in *Candida albicans*-mediated oral diseases, *J Dent Res.* **95**, 365-71.

24. Amerongen, A. V. & Veerman, E. C. (2002) Saliva--the defender of the oral cavity, *Oral Dis.* **8**, 12-22.

25. Bochenska, O., Rapala-Kozik, M., Wolak, N., Aoki, W., Ueda, M. & Kozik, A. (2016) The action of ten secreted aspartic proteases of pathogenic yeast C*andida* a*lbicans* on major human salivary antimicrobial peptide, histatin 5, *Acta Biochim Pol.* **63**, 403-410.

26. Oppenheim, F. G., Xu, T., McMillian, F. M., Levitz, S. M., Diamond, R. D., Offner, G. D. & Troxler, R. F. (1988) Histatins, a novel family of histidine-rich proteins in human parotid secretion. Isolation, characterization, primary structure, and fungistatic effects on *Candida albicans*, *J Biol Chem.* **263**, 7472-7.

27. Xu, T., Levitz, S. M., Diamond, R. D. & Oppenheim, F. G. (1991) Anticandidal activity of major human salivary histatins, *Infect Immun.* **59**, 2549-54.

28. Edgerton, M., Koshlukova, S. E., Lo, T. E., Chrzan, B. G., Straubinger, R. M. & Raj, P. A. (1998) Candidacidal activity of salivary histatins. Identification of a histatin 5-binding protein on *Candida albicans*, *J Biol Chem.* **273**, 20438-47.

29. Puri, S. & Edgerton, M. (2014) How does it kill?: understanding the candidacidal mechanism of salivary histatin 5, *Eukaryot Cell.* **13**, 958-64.

30. Khan, S. A., Fidel, P. L., Jr., Thunayyan, A. A., Varlotta, S., Meiller, T. F. & Jabra-Rizk, M. A. (2013) Impaired histatin-5 levels and salivary antimicrobial activity against *C. albicans* in HIV infected individuals, *Journal of AIDS & clinical research.* **4**, 193.

31. Helmerhorst, E. J., van't Hof, W., Breeuwer, P., Veerman, E. C., Abee, T., Troxler, R. F., Amerongen, A. V. & Oppenheim, F. G. (2001) Characterization of histatin 5 with respect to amphipathicity, hydrophobicity, and effects on cell and mitochondrial membrane integrity excludes a candidacidal mechanism of pore formation, *J Biol Chem.* **276**, 5643-9.

32. Li, X. S., Sun, J. N., Okamoto-Shibayama, K. & Edgerton, M. (2006) *Candida albicans* cell wall ssa proteins bind and facilitate import of salivary histatin 5 required for toxicity, *J Biol Chem.* **281**, 22453-63.

33. Raj, P. A., Edgerton, M. & Levine, M. J. (1990) Salivary histatin 5: dependence of sequence, chain length, and helical conformation for candidacidal activity, *J Biol Chem.* **265**, 3898-905.

34. Rothstein, D. M., Spacciapoli, P., Tran, L. T., Xu, T., Roberts, F. D., Dalla Serra, M., Buxton, D. K., Oppenheim, F. G. & Friden, P. (2001) Anticandida activity is retained in

P-113, a 12-amino-acid fragment of histatin 5, *Antimicrob Agents Chemother.* **45**, 1367-73.

35. Helmerhorst, E. J., Van't Hof, W., Veerman, E. C., Simoons-Smit, I. & Nieuw Amerongen, A. V. (1997) Synthetic histatin analogues with broad-spectrum antimicrobial activity, *Biochem J.* **326 (Pt 1)**, 39-45.

36. Driscoll, J., Duan, C., Zuo, Y., Xu, T., Troxler, R. & Oppenheim, F. G. (1996) Candidacidal activity of human salivary histatin recombinant variants produced by site-directed mutagenesis, *Gene.* **177**, 29-34.

37. Tsai, H. & Bobek, L. A. (1997) Studies of the mechanism of human salivary histatin-5 candidacidal activity with histatin-5 variants and azole-sensitive and -resistant Candida species, *Antimicrob Agents Chemother.* **41**, 2224-8.

38. Tsai, H., Raj, P. A. & Bobek, L. A. (1996) Candidacidal activity of recombinant human salivary histatin-5 and variants, *Infect Immun.* **64**, 5000-7.

39. Situ, H., Balasubramanian, S. V. & Bobek, L. A. (2000) Role of alpha-helical conformation of histatin-5 in candidacidal activity examined by proline variants, *Biochimica et biophysica acta.* **1475**, 377-82.

40. Raj, P. A., Soni, S. D. & Levine, M. J. (1994) Membrane-induced helical conformation of an active candidacidal fragment of salivary histatins, *J Biol Chem.* **269**, 9610-9.

41. Raj, P. A., Marcus, E. & Sukumaran, D. K. (1998) Structure of human salivary histatin 5 in aqueous and nonaqueous solutions, *Biopolymers.* **45**, 51-67.

42. Helmerhorst, E. J., Reijnders, I. M., van 't Hof, W., Veerman, E. C. & Nieuw Amerongen, A. V. (1999) A critical comparison of the hemolytic and fungicidal activities of cationic antimicrobial peptides, *FEBS Lett.* **449**, 105-10.

43. Kozel, T. R. & Wickes, B. (2014) Fungal diagnostics, *Cold Spring Harb Perspect Med.* **4**, a019299.

44. Weisser, N. E. & Hall, J. C. (2009) Applications of single-chain variable fragment antibodies in therapeutics and diagnostics, *Biotechnol Adv.* **27**, 502-20.

45. Holliger, P. & Hudson, P. J. (2005) Engineered antibody fragments and the rise of single domains, *Nat Biotechnol.* **23**, 1126-36.

46. Leong, S. S. J. & Chen, W. N. (2008) Preparing recombinant single chain antibodies, *Chem Eng Sci.* **63**, 1401-1414.

47. Rabe, M., Verdes, D. & Seeger, S. (2011) Understanding protein adsorption phenomena at solid surfaces, *Adv Colloid Interface Sci.* **162**, 87-106.

48. Rusmini, F., Zhong, Z. & Feijen, J. (2007) Protein immobilization strategies for protein biochips, *Biomacromolecules.* **8**, 1775-89.

49. Kumada, Y. (2014) Site-specific immobilization of recombinant antibody fragments through material-binding peptides for the sensitive detection of antigens in enzyme immunoassays, *Biochimica et biophysica acta.* **1844**, 1960-1969.

50. Yuan, Y., He, H. & Lee, L. J. (2009) Protein A-based antibody immobilization onto polymeric microdevices for enhanced sensitivity of enzyme-linked immunosorbent assay, *Biotechnol Bioeng.* **102**, 891-901.

51. Wang, Z. & Jin, G. (2003) Feasibility of protein A for the oriented immobilization of immunoglobulin on silicon surface for a biosensor with imaging ellipsometry, *J Biochem Biophys Methods.* **57**, 203-11.

52. Lo, Y. S., Nam, D. H., So, H. M., Chang, H., Kim, J. J., Kim, Y. H. & Lee, J. O. (2009) Oriented immobilization of antibody fragments on Ni-decorated single-walled carbon nanotube devices, *ACS Nano.* **3**, 3649-55.

53. Zhen, G., Falconnet, D., Kuennemann, E., Vörös, J., Spencer, N. D., Textor, M. & Zürcher, S. (2006) Nitrilotriacetic Acid Functionalized Graft Copolymers: A Polymeric Interface for Selective and Reversible Binding of Histidine-Tagged Proteins, *Adv Funct Mater.* **16**, 243-251.

54. Schmid, E. L., Keller, T. A., Dienes, Z. & Vogel, H. (1997) Reversible oriented surface immobilization of functional proteins on oxide surfaces, *Anal Chem.* **69**, 1979-85.

55. Michael Green, N. & Meir Wilchek and Edward, A. B. (1990) Avidin and streptavidin in *Methods in Enzymology* pp. 51-67, Academic Press.

56. Walper, S. A., Brozozog Lee, P. A., Goldman, E. R. & Anderson, G. P. (2013) Comparison of single domain antibody immobilization strategies evaluated by surface plasmon resonance, *J Immunol Methods.* **388**, 68-77.

57. Cronan, J. E., Jr. (1990) Biotination of proteins *in vivo*. A post-translational modification to label, purify, and study proteins, *J Biol Chem.* **265**, 10327-33.

58. Chapman-Smith, A., Turner, D. L., Cronan, J. E., Jr., Morris, T. W. & Wallace, J. C. (1994) Expression, biotinylation and purification of a biotin-domain peptide from the biotin carboxy carrier protein of *Escherichia coli* acetyl-CoA carboxylase, *Biochem J.* **302 (Pt 3)**, 881-7.

59. Tayapiwatana, C., Chotpadiwetkul, R. & Kasinrerk, W. (2006) A novel approach using streptavidin magnetic bead-sorted *in vivo* biotinylated survivin for monoclonal antibody production, *J Immunol Methods.* **317**, 1-11.

60. Winkler, I. G., Lochelt, M., Levesque, J. P., Bodem, J., Flugel, R. M. & Flower, R. L. (1997) A rapid streptavidin-capture ELISA specific for the detection of antibodies to feline foamy virus, *J Immunol Methods.* **207**, 69-77.

61. Beckett, D., Kovaleva, E. & Schatz, P. J. (1999) A minimal peptide substrate in biotin holoenzyme synthetase-catalyzed biotinylation, *Protein Sci.* **8**, 921-9.

62. Cull, M. G. & Schatz, P. J. (2000) Biotinylation of proteins *in vivo* and *in vitro* using small peptide tags in *Methods Enzymol* pp. 430-440, Academic Press.

63. Yao, X., Wei, D., Soden, C., Jr., Summers, M. F. & Beckett, D. (1997) Structure of the carboxy-terminal fragment of the apo-biotin carboxyl carrier subunit of *Escherichia coli* acetyl-CoA carboxylase, *Biochemistry.* **36**, 15089-100.

64. Laskay, U. A., Srzentic, K., Monod, M. & Tsybin, Y. O. (2014) Extended bottom-up proteomics with secreted aspartic protease Sap9, *J Proteomics.* **110**, 20-31.

65. Ruissen, A. L., Groenink, J., Helmerhorst, E. J., Walgreen-Weterings, E., Van't Hof, W., Veerman, E. C. & Nieuw Amerongen, A. V. (2001) Effects of histatin 5 and derived peptides on *Candida albicans*, *Biochem J.* **356**, 361-8.

66. Li, X. S., Reddy, M. S., Baev, D. & Edgerton, M. (2003) *Candida albicans* Ssa1/2p is the cell envelope binding protein for human salivary histatin 5, *J Biol Chem.* **278**, 28553-61.

67. Karlsson, A. J., Pomerantz, W. C., Neilsen, K. J., Gellman, S. H. & Palecek, S. P. (2009) Effect of sequence and structural properties on 14-helical beta-peptide activity against Candida albicans planktonic cells and biofilms, *ACS Chem Biol.* **4**, 567-79.

68. Matejuk, A., Leng, Q., Begum, M. D., Woodle, M. C., Scaria, P., Chou, S. T. & Mixson, A. J. (2010) Peptide-based antifungal therapies against emerging infections, *Drugs Future.* **35**, 197.

69. Jang, W. S., Li, X. S., Sun, J. N. & Edgerton, M. (2008) The P-113 fragment of histatin 5 requires a specific peptide sequence for intracellular translocation in *Candida albicans*, which is independent of cell wall binding, *Antimicrob Agents Chemother.* **52**, 497-504.

70. Ruissen, A. L., Groenink, J., Krijtenberg, P., Walgreen-Weterings, E., Hof, W. v. t., Veerman, E. C. I. & Amerongen, A. V. N. (2003) Internalisation and degradation of histatin 5 by *Candida albicans* in *Biological Chemistry* pp. 183

71. Kong, E. F., Tsui, C., Boyce, H., Ibrahim, A., Hoag, S. W., Karlsson, A. J., Meiller, T. F. & Jabra-Rizk, M. A. (2016) Development and *in vivo* evaluation of a novel histatin-5 bioadhesive hydrogel formulation against oral candidiasis, *Antimicrob Agents Chemother.* **60**, 881-9.

72. Shukla, A., Fleming, K. E., Chuang, H. F., Chau, T. M., Loose, C. R., Stephanopoulos, G. N. & Hammond, P. T. (2010) Controlling the release of peptide antimicrobial agents from surfaces, *Biomaterials.* **31**, 2348-57.

73. Shi, J., Liu, Y., Wang, Y., Zhang, J., Zhao, S. & Yang, G. (2015) Biological and immunotoxicity evaluation of antimicrobial peptide-loaded coatings using a layer-by-layer process on titanium, *Scientific reports.* **5**, 16336.

74. Karlsson, A. J., Flessner, R. M., Gellman, S. H., Lynn, D. M. & Palecek, S. P. (2010) Polyelectrolyte multilayers fabricated from antifungal beta-peptides: design of surfaces that exhibit antifungal activity against Candida albicans, *Biomacromolecules.* **11**, 2321-8.

75. Ikonomova, S. P., He, Z. & Karlsson, A. J. (2016) A simple and robust approach to immobilization of antibody fragments, *J Immunol Methods.* **435**, 7-16.

76. Sun, X., Salih, E., Oppenheim, F. G. & Helmerhorst, E. J. (2009) Kinetics of histatin proteolysis in whole saliva and the effect on bioactive domains with metal-binding, antifungal, and wound-healing properties, *FASEB J.* **23**, 2691-701.

77. Santala, V. & Lamminmaki, U. (2004) Production of a biotinylated single-chain antibody fragment in the cytoplasm of *Escherichia coli*, *J Immunol Methods.* **284**, 165-75.

78. Seurynck-Servoss, S. L., Baird, C. L., Miller, K. D., Pefaur, N. B., Gonzalez, R. M., Apiyo, D. O., Engelmann, H. E., Srivastava, S., Kagan, J., Rodland, K. D. & Zangar, R. C. (2008) Immobilization strategies for single-chain antibody microarrays, *Proteomics.* **8**, 2199-210.

79. Torrance, L., Ziegler, A., Pittman, H., Paterson, M., Toth, R. & Eggleston, I. (2006) Oriented immobilisation of engineered single-chain antibodies to develop biosensors for virus detection, *J Virol Methods.* **134**, 164-70.

80. Hu, X., Hortigüela, M. J., Robin, S., Lin, H., Li, Y., Moran, A. P., Wang, W. & Wall, J. G. (2013) Covalent and oriented immobilization of scFv antibody fragments via an engineered glycan moiety, *Biomacromolecules.* **14**, 153-159.

81. Mustafaoglu, N., Alves, N. J. & Bilgicer, B. (2015) Oriented immobilization of Fab fragments by site-specific biotinylation at the conserved nucleotide binding site for enhanced antigen detection, *Langmuir.* **31**, 9728-36.

82. Lichty, J. J., Malecki, J. L., Agnew, H. D., Michelson-Horowitz, D. J. & Tan, S. (2005) Comparison of affinity tags for protein purification, *Protein Expr Purif.* **41**, 98-105.

83. Martineau, P., Jones, P. & Winter, G. (1998) Expression of an antibody fragment at high levels in the bacterial cytoplasm, *J Mol Biol.* **280**, 117-27.

84. Koch, H., Grafe, N., Schiess, R. & Pluckthun, A. (2006) Direct selection of antibodies from complex libraries with the protein fragment complementation assay, *J Mol Biol.* **357**, 427-41.

85. Mossner, E., Koch, H. & Pluckthun, A. (2001) Fast selection of antibodies without antigen purification: adaptation of the protein fragment complementation assay to select antigen-antibody pairs, *J Mol Biol.* **308**, 115-22.

86. Jermutus, L., Honegger, A., Schwesinger, F., Hanes, J. & Pluckthun, A. (2001) Tailoring *in vitro* evolution for protein affinity or stability, *Proc Natl Acad Sci U S A.* **98**, 75-80.

87. Jermutus, L., Kolly, R., Foldes-Papp, Z., Hanes, J., Rigler, R. & Pluckthun, A. (2002) Ligand binding of a ribosome-displayed protein detected in solution at the single molecule level by fluorescence correlation spectroscopy, *Eur Biophys J.* **31**, 179-84.

88. Laforce-Nesbitt, S. S., Sullivan, M. A., Hoyer, L. L. & Bliss, J. M. (2008) Inhibition of *Candida albicans* adhesion by recombinant human antibody single-chain variable fragment specific for Als3p, *FEMS Immunol Med Microbiol.* **54**, 195-202.

89. Bliss, J. M., Sullivan, M. A., Malone, J. & Haidaris, C. G. (2003) Differentiation of *Candida albicans* and *Candida dubliniensis* by using recombinant human antibody single-chain variable fragments specific for hyphae, *J Clin Microbiol.* **41**, 1152-60.

90. DeLisa, M. P., Tullman, D. & Georgiou, G. (2003) Folding quality control in the export of proteins by the bacterial twin-arginine translocation pathway, *Proc Natl Acad Sci U S A.* **100**, 6115-20.

91. Binz, H. K., Amstutz, P., Kohl, A., Stumpp, M. T., Briand, C., Forrer, P., Grutter, M. G. & Pluckthun, A. (2004) High-affinity binders selected from designed ankyrin repeat protein libraries, *Nat Biotechnol.* **22**, 575-82.

92. Forrer, P. & Jaussi, R. (1998) High-level expression of soluble heterologous proteins in the cytoplasm of Escherichia coli by fusion to the bacteriophage lambda head protein D, *Gene.* **224**, 45-52.

93. Predonzani, A., Arnoldi, F., Lopez-Requena, A. & Burrone, O. R. (2008) *In vivo* site-specific biotinylation of proteins within the secretory pathway using a single vector system, *BMC Biotechnol.* **8**, 41.

94. Gasteiger, E., Hoogland, C., Gattiker, A., Duvaud, S., Wilkins, M. R., Appel, R. D. & Bairoch, A. (2005) Protein identification and analysis tools on the ExPASy server in *The proteomics protocols handbook* (Walker, J. M., ed) pp. 571-607, Humana Press Inc., Totowa, NJ.

95. Whitlow, M., Bell, B. A., Feng, S. L., Filpula, D., Hardman, K. D., Hubert, S. L., Rollence, M. L., Wood, J. F., Schott, M. E., Milenic, D. E. & et al. (1993) An improved linker for single-chain Fv with reduced aggregation and enhanced proteolytic stability, *Protein Eng.* **6**, 989-95.

96. Ueda, M., Manabe, Y. & Mukai, M. (2011) The high performance of 3XFLAG for target purification of a bioactive metabolite: a tag combined with a highly effective linker structure, *Bioorg Med Chem Lett.* **21**, 1359-62.

97. Dong, J., Kojima, T., Ohashi, H. & Ueda, H. (2015) Optimal fusion of antibody binding domains resulted in higher affinity and wider specificity, *J Biosci Bioeng.* **120**, 504-9.

98. Raran-Kurussi, S., Keefe, K. & Waugh, D. S. (2015) Positional effects of fusion partners on the yield and solubility of MBP fusion proteins, *Protein Expr Purif.* **110**, 159-64.

99. Bergeron, L. M., Gomez, L., Whitehead, T. A. & Clark, D. S. (2009) Self-renaturing enzymes: design of an enzyme-chaperone chimera as a new approach to enzyme stabilization, *Biotechnol Bioeng.* **102**, 1316-22.

100. Bai, Y. & Shen, W. C. (2006) Improving the oral efficacy of recombinant granulocyte colony-stimulating factor and transferrin fusion protein by spacer optimization, *Pharm Res.* **23**, 2116-21.

101. Amet, N., Lee, H. F. & Shen, W. C. (2009) Insertion of the designed helical linker led to increased expression of tf-based fusion proteins, *Pharm Res.* **26**, 523-8.

102. Chen, X., Zaro, J. L. & Shen, W. C. (2013) Fusion protein linkers: property, design and functionality, *Adv Drug Delivery Rev.* **65**, 1357-69.

103. Klein, J. S., Jiang, S., Galimidi, R. P., Keeffe, J. R. & Bjorkman, P. J. (2014) Design and characterization of structured protein linkers with differing flexibilities, *Protein Eng Des Sel.* **27**, 325-30.

104. Shen, Z., Yan, H., Zhang, Y., Mernaugh, R. L. & Zeng, X. (2008) Engineering peptide linkers for scFv immunosensors, *Anal Chem.* **80**, 1910-7.

105. Gong, Z., Walls, M. T., Karley, A. N. & Karlsson, A. J. (2016) Effect of a flexible linker on recombinant expression of cell-penetrating peptide fusion proteins and their translocation into fungal cells, *Mol Biotechnol.* **58**, 838-849.

106. Fabian, T. K., Hermann, P., Beck, A., Fejerdy, P. & Fabian, G. (2012) Salivary defense proteins: their network and role in innate and acquired oral immunity, *Int J Mol Sci.* **13**, 4295-320.

107. Helmerhorst, E. J., Alagl, A. S., Siqueira, W. L. & Oppenheim, F. G. (2006) Oral fluid proteolytic effects on histatin 5 structure and function, *Arch Oral Biol.* **51**, 1061-70.

108. Stallmann, H. P., Faber, C., Bronckers, A. L., de Blieck-Hogervorst, J. M., Brouwer, C. P., Amerongen, A. V. & Wuisman, P. I. (2005) Histatin and lactoferrin derived peptides: antimicrobial properties and effects on mammalian cells, *Peptides.* **26**, 2355-9.

109. Lum, K. Y., Tay, S. T., Le, C. F., Lee, V. S., Sabri, N. H., Velayuthan, R. D., Hassan, H. & Sekaran, S. D. (2015) Activity of novel synthetic peptides against *Candida albicans*, *Scientific reports.* **5**, 9657.

110. Peters, B. M., Zhu, J., Fidel, P. L., Jr., Scheper, M. A., Hackett, W., El Shaye, S. & Jabra-Rizk, M. A. (2010) Protection of the oral mucosa by salivary histatin-5 against *Candida albicans* in an ex vivo murine model of oral infection, *FEMS Yeast Res.* **10**, 597-604.

111. Tati, S., Li, R., Puri, S., Kumar, R., Davidow, P. & Edgerton, M. (2014) Histatin 5-spermidine conjugates have enhanced fungicidal activity and efficacy as a topical therapeutic for oral candidiasis, *Antimicrob Agents Chemother.* **58**, 756-66.

112. Berman, H. M., Westbrook, J., Feng, Z., Gilliland, G., Bhat, T. N., Weissig, H., Shindyalov, I. N. & Bourne, P. E. (2000) The Protein Data Bank, *Nucleic Acids Res.* **28**, 235-42.

113. Yang, J., Yan, R., Roy, A., Xu, D., Poisson, J. & Zhang, Y. (2015) The I-TASSER Suite: protein structure and function prediction, *Nat Methods.* **12**, 7-8.

114. Yang, J. & Zhang, Y. (2015) I-TASSER server: new development for protein structure and function predictions, *Nucleic Acids Res.* **43**, W174-81.

115. Roy, A., Kucukural, A. & Zhang, Y. (2010) I-TASSER: a unified platform for automated protein structure and function prediction, *Nat Protoc.* **5**, 725-38.

116. Zhang, Y. (2008) I-TASSER server for protein 3D structure prediction, *BMC Bioinformatics.* **9**, 40.

117. Jo, S., Kim, T., Iyer, V. G. & Im, W. (2008) CHARMM-GUI: a web-based graphical user interface for CHARMM, *J Comput Chem.* **29**, 1859-65.

118. Phillips, J. C., Braun, R., Wang, W., Gumbart, J., Tajkhorshid, E., Villa, E., Chipot, C., Skeel, R. D., Kale, L. & Schulten, K. (2005) Scalable molecular dynamics with NAMD, *J Comput Chem.* **26**, 1781-802.

119. Abad-Zapatero, C., Goldman, R., Muchmore, S. W., Hutchins, C., Stewart, K., Navaza, J., Payne, C. D. & Ray, T. L. (1996) Structure of a secreted aspartic protease from C. albicans complexed with a potent inhibitor: implications for the design of antifungal agents, *Protein Sci.* **5**, 640-52.

120. Borelli, C., Ruge, E., Schaller, M., Monod, M., Korting, H. C., Huber, R. & Maskos, K. (2007) The crystal structure of the secreted aspartic proteinase 3 from *Candida albicans* and its complex with pepstatin A, *Proteins.* **68**, 738-48.

121. Trott, O. & Olson, A. J. (2010) AutoDock Vina: improving the speed and accuracy of docking with a new scoring function, efficient optimization, and multithreading, *J Comput Chem.* **31**, 455-61.